



SOUTHERN CALIFORNIA EARTHQUAKE CENTER



UNIVERSITY
OF SOUTHERN
CALIFORNIA

1999 SCEC Annual Meeting

September 26-29, 1999



CALIFORNIA
INSTITUTE OF
TECHNOLOGY



LAMONT-DOHERTY
EARTH OBSERVATORY
OF COLUMBIA
UNIVERSITY

US/China GPS Workshop

September 29-30, 1999



UCLA



UC SAN DIEGO
SCRIPPS INSTITUTION
OF OCEANOGRAPHY

Proceedings and Abstracts



UNIVERSITY OF
CALIFORNIA
SANTA BARBARA

Riviera Resort and Racquet Club

Palm Springs, CA



UNITED STATES
GEOLOGICAL
SURVEY

Table of Contents

SCEC Annual Meeting Agenda	2
US/China GPS Workshop Agenda	6
1999 Annual Meeting Participants	8
China Participants in the US/China GPS Workshop	12
US Participants in the US/China GPS Workshop	13
SCEC Organization	14
1999 SCEC Advisory Council	17
SCEC Senior Research Investigators	18
Message from the Directors	22
Legacy Matrix	24
Legacy Document Outline	25
EarthScope	32
SCEC Outreach Program Overview	41
1999 SCEC Science Abstracts	45
US/China GPS Workshop Abstracts	98

1999 SCEC ANNUAL MEETING

“The SCEC Legacy Workshop”

Sunday, September 26 to Wednesday, September 29, 1999

Riviera Resort and Racquet Club

Palm Springs, CA

Sunday, September 26, 1999

Visit trenches in San Bernardino (Sally McGill) and San Gorgonio Pass/Burro Flats (Kerry Sieh/Doug Yule) en route

12:00 to 2:00	Group F Pre-Meeting Workshop - Steve Day
2:00 to 6:00	Group B Pre-Meeting Workshop – Ralph Archuleta
6:00 to 9:00	Group C Pre-Meeting Workshop – Tom Rockwell
6:00 to 9:00	GEM Meeting – John Rundle
	Poster Session Set-Up

Note: Computational demos are invited. There will be internet access at the hotel.

Monday, September 27, 1999

8:00 SCEC Steering Committee Meeting

SCEC Plenary Session I

8:00 – 9:00 Continental Breakfast

9:00 Introduction - Tom Henyey (including comments on EarthScope)

9:30 Remarks by Jim Whitcomb and John Unger

10:00 Education and Outreach Report - Jill Andrews

10:30 Break

11:00 The SCEC “Legacy Document” - Bernard Minster

12:00 Lunch

Breakouts I

12:30 – 1:30 1. Seismotectonics Chapter Tom Henyey

1:30 – 2:30 2. Crustal Deformation Chapter Duncan Agnew

2:30- 3:30 3. Earthquake History Chapter Kerry Sieh

3:30 – 4:30 4. Velocity Model Chapter Rob Clayton

4:30 – 6:30 Caucus Period for Chapters 1-4

4:30 – 7:00 SCEC Advisory Council Meeting with SCEC Steering Committee
Final set-up for poster session

6:45 Dinner
SCEC Advisory Council Executive Session
Special Ceremony

7:30 Icebreaker and Poster Session I

Tuesday, September 28, 1999

SCEC Plenary Session II

8:00 – 8:30

Continental Breakfast

8:30

SCEC Response to Turkey Earthquake by
Simon McClusky for Geodesy
Tom Rockwell for Geology
Nano Seeber for Seismology

9:30

SCEC Working Group 2000 Report by Ned Field

10:00

Break

Note:

SCIGN Coordinating Board Meeting at 10:15

10:15-11:15

5. Wave Propagation Chapter

Ralph Archuleta

11:15 – 12:15

6. Source Physics Chapter

Steve Day

12:15

Lunch

1:00 – 2:00

7. SCEC Earthquakes Chapter

Lucy Jones/Egill Hauksson

2:00 - 3:00

8. Stress Transfer Chapter

Ruth Harris/Ross Stein

3:00 – 4:00

9. Earthquake Potential Chapter

Dave Jackson

4:00 – 6:00

Caucus Period for Chapters 5-9

5:00 – 7:00

SCIGN Advisory Council Meeting

6:45

Dinner

7:30

Poster Session II

Wednesday, September 29, 1999

SCEC Plenary Session III

8:00 – 8:30

Continental Breakfast

8:30 – noon

Reports from Legacy Document Chapter Authors (15 minutes) and Discussion on SCEC Legacy and Future – Bernard Minster and Tom Henyey

- | | |
|-------------------------|---------------------------|
| 1. Seismotectonics | Tom Henyey |
| 2. Crustal Deformation | Duncan Agnew |
| 3. Earthquake History | Kerry Sieh |
| 4. Velocity Model | Rob Clayton |
| 5. Wave Propagation | Ralph Archuleta |
| 6. Source Physics | Steve Day |
| 7. SCEC Earthquakes | Lucy Jones/Egill Hauksson |
| 8. Stress Transfer | Ruth Harris |
| 9. Earthquake Potential | Dave Jackson |

End of SCEC Meeting

**1999 US/China GPS Workshop
Wednesday, September 29, 1999**

1:00 Introductory Remarks - Walter Mooney, Leonard Johnson

Network and Data Analysis

1:15 Ruth Neilan - International GPS Service and Cooperation

1:35 Chen Xinlian et al. - Crustal Movement Observation Network of China

1:55 Zhang Zusheng - Arrangement and Observation of Regional Net of Crustal Movement Observation Network of China

2:15 Ken Hudnut et al. – The Southern California Integrated GPS Network (SCIGN)

2:45 Break

3:15 Gu et al. – Data Processing of the First Observation in the Crustal Movement Observation Network of China

3:35 Luo Zhiguang – A Method on the Establishment of the Atmospheric Distribution Model and its Application in GPS Data Processing

Beginning and Proposed Collaborations

3:55 Zheng-kang Shen et al – Collaborative Research: GPS Crustal Deformation Monitoring in China

4:15 - 5:00 Discussion of Concrete Plans for this NSF Grant - What needs to be done this year? What is the strategy for ongoing support?

6:00 **Icebreaker and Dinner**

Evening Posters/Informal Discussion

R. Bendick et al. - New Constraints on Asian Deformation from Geodesy Across the Altyn Tagh Fault

Andrea Donnellan - Mongolia

Z. Chen et al. - GPS Measurement of Crustal Motion in Southwest China

D. Dong – Extracting Tectonic Information from the Quasi-Observation Approach

Lanbo Liu – Fault-Block Deformation Model in Northern China

Walter D. Mooney – Continental Evolution: Ideas from Seismology and GPS Data

Zheng-Kang Shen et al. - GPS-Derived Deformation Along the Northern Rim of the Tibetan Plateau and the Southern Tarim Basin

Frank Webb - Reservoir Loading and Rheology

Thursday, September 30

Large-Scale Deformation - Results and Models

- 8:30 J. Ren et al – The Anticlockwise Rotation of Southeast Asia
- 8:45 Robert King et al. – Reference Frames for East Asian Studies
- 9:00 Li-ren Huang and Min Wang - Recent Crustal Horizontal Movement in Mainland China
- 9:15 Wenyao Zhu et al – Crustal Motion of Chinese Mainland Monitored by GPS
- 9:30 William Holt et al. – Joint Modeling of the Kinematics and Dynamics of Asia
- 9:45 Peter Molnar and Philip England – The Use of GPS Measurements in Quantifying the Kinematics of Asian Deformation for Study of its Dynamics, and the Dynamics of Continental Deformation in General
- 10:00 Wang Qing-Liang et al – Dynamic Correlation between LOD Variations and Site Deformations: Implication to Geodynamics
- 10:15 - 10:45 Break

Regional Deformation - Results and Models

- 10:45 Linbo Ma – The Observation and Result Analysis for the Geodynamical GPS Networking in Xinjiang
- 11:00 Qiao Xuejun et al. – The Initial Study on Present-Day Tectonic Activity and Crustal Deformation Monitored by GPS in the Area of Jiashi and Northeast Pamir Region
- 11:15 Brad Hager et al – Comparison of Geologic and Geodetic Rates of Shortening Across the Tien Shan of Kyrgyzstan, Central Asia
- 11:30 Jeffrey T. Freymueller et al. – Present-Day Kinematics of the India-Eurasia Plate Collision Zone
- 11:45 Yang Guohua et al – Introduction of the Present Crustal Horizontal Movement in Shanxi Fault Belt Shown by GPS
- 12:00 Lunch
- 1:00 - 4:45 Panel discussion - What concrete steps should we take?
- 4:45 - Closing Remarks

1999 SCEC ANNUAL MEETING PARTICIPANTS

Marie Herrera Adsetts	UCSB
Duncan Agnew	UC-San Diego
Yin An	UCLA
John Anderson	Nevada-Reno
Jill Andrews	SCEC Outreach
Rasool Anooshehpour	Nevada-Reno
Ralph Archuleta	UC-Santa Barbara
Donald Argus	JPL
Ramon Arrowsmith	Arizona State
Aris Aspiotes	USGS-Pasadena
Shirley Baher	UCLA
Rebecca Bendick	Colorado
Mark Benthien	SCEC Outreach
Yehuda Ben-Zion	USC
Tom Bjorklund	Houston
Natanya Black	UCSB
Ann Blythe	USC
Yehuda Bock	UC-San Diego
Fabian Bonilla	UC-Santa Barbara
David Bowman	USC
Jim Brune	Nevada-Reno
Roland Burgmann	UC-Berkeley
Gary Cahn	Landers Search Lab
Maurice Cahn	Landers Search Lab
Natalie Cahn	Landers Search Lab
Youlin Chen	USC
Shari Christofferson	USC
Rob Clayton	Caltech
Lloyd Cluff	PG&E
C.B. Crouse	Dames and Moore
Paul Davis	UC-Los Angeles
Tim Dawson	San Diego State
Steve Day	San Diego State
Robert de Groot	SCEC Outreach
Safaa Dergham	CSU-Long Beach
James Dolan	USC
Danan Dong	JPL
Andrea Donnellan	JPL
Herb Dragert	Geological Survey of Canada
Debra Einstein	UC-Irvine
Leo Eisner	Caltech
Geoff Ely	SDSU
Peng Fang	UCSD
Javier Favela	Caltech
Ned Field	USC
Geoffrey Fox	Syracuse
Jeff Freymueller	Alaska
Gary Fuis	USGS-Menlo Park
John Galetzka	USC
Weijun Gang	USGS/CSB
Tania Gonzalez	ECI
Lisa Grant	UC-Irvine

Robert Graves
Larry Gurrola
Katrin Hafner
Brad Hager
Jeanne Hardebeck
Ruth Harris
Ross Hartleb
Egill Hauksson
Tomasz Haupt
Mike Heflin
John Helly
Ed Hensley
Sally Henyey
Tom Henyey
Jenn Holsten
Bill Holt
Susan Hough
Martha House
Yue-quiang Huang
Ken Hudnut
Ken Hurst
Charles Hutt
Dave Jackson
Leonard Johnson
Peg Johnson
Lucy Jones
Tom Jordan
Yan Kagan
Marc Kamerling
Ed Keller
Louise Kellogg
Katherine Kendrick
Cameron Kennedy
Grant Kier
Nancy King
Robert King
Bill Klein
Monica Kohler
Robert Langridge
Nadia Lapusta
Daniel Lavalley
Mark Legg
Shoshana Levin
Jennifer Lewis
Yong-Gang Li
Grant Lindley
Scott Lindvall
Lanbo Liu
Peng-Cheng Liu
Yun-Feng Liu
Bruce Luyendyk
Christopher Lynch
Harold Magistrale
Carey Marcinkovich

URS/Woodward-Clyde
UC-Santa Barbara
Caltech
MIT
Caltech
USGS-Menlo Park
USC
Caltech
Syracuse
JPL
UCSD/NPACI
SCEC Outreach
USC
USC
USC
SUNY-Stony Brook
USGS-Pasadena
Caltech
USC
USGS-Pasadena
JPL
USGS-Albuquerque
UC-Los Angeles
NSF
USGS-Pasadena
USGS-Pasadena
MIT
UC-Los Angeles
UC-Santa Barbara
UC-Santa Barbara
UC-Davis
USGS-Pasadena
CSU-Northridge
Colorado
USGS-Pasadena
MIT
Boston College
UC-Los Angeles
USGS-Menlo Park
Harvard
UC-Santa Barbara
Legg Geophysical
USC
San Diego State
USC
UCSB
William Lettis Assoc.
Connecticut
UC-Santa Barbara
USC
UC-Santa Barbara
SDSU
San Diego State
UCSB

Chris Marone
John Marquis
Aaron Martin
Simon McClusky
Sally McGill
Patrick McNamara
John McRaney
Dennis Mileti
Bernard Minster
Jack Moehle
Peter Molnar
Walter Mooney
Angie Moore
Lalliana Mualchin
Karl Mueller
Julie Nazareth
Ruth Neilan
Craig Nicholson
David Oglesby
David Okaya
Kim Olsen
Altangeral Orgin
Susan Owen
Jay Parker
Zhi-Gang Peng
Taylor Perron
Mark Petersen
Arben Pitarka
Will Prescott
Daniel Ragona
Robin Reichlin
Luke Reusser
Jim Rice
Eliza Richardson
Carlos Rivero
Nathan Robison
Tom Rockwell
Barbara Romanowicz
Yufong Rong
Mousumi Roy
Charlie Rubin
John Rundle
Jonathan Saben
Charlie Sammis
Jim Savage
David Schwartz
Nano Seeber
Gordon Seitz
John Shaw
Peter Shearer
Kaye Shedlock
Zheng-Kang Shen
Bingming Shen-tu
Kerry Sieh

MIT
Caltech
UC-Santa Barbara
MIT
Cal State-San Bernardino
Shamrock Geologic
SCEC
Colorado
UC-San Diego
PEER
MIT
USGS-Menlo Park
JPL
Caltrans
Colorado
Caltech
JPL
UC-Santa Barbara
UC-Santa Barbara
USC
UC-Santa Barbara
SDSU
USC
JPL
USC
USGS-Menlo Park
CDMG
URS/Woodward-Clyde
USGS-Menlo Park
SDSU
NSF
USC
Harvard
MIT
Harvard
Nevada-Reno
San Diego State
UC-Berkeley
UCLA
New Mexico
Central Washington
Colorado
USC
USC
USGS-Menlo Park
USGS-Menlo Park
Lamont
LLNL
Harvard
UC-San Diego
USGS-Denver
UC-Los Angeles
SUNY-Stony Brook
Caltech

Mark Simons
Bob Smith
Chris Sorlien
Keith Stark
Jamie Steidl
Heidi Stenner
Elizabeth Stone
Ashley Streig
Feng Su
Tammy Surko
Lynn Sykes
Leon Teng
Tim Tierney
Allan Tucker
Terry Tullis
Alexei Tumarkin
Don Turcotte
John Unger
Matt van Domselaar
Kathryn van Rosendaal
Shannon VanWyk
Jan Vermilye
Frank Vernon
Paul Vincent
Dave Wald
Lisa Wald
Chris Walls
Hanbiao Wang
Min Wang
Steve Ward
Alex Weaver
Kris Weaver
Frank Webb
Shelly Werner
Steve Wesnousky
Jim Whitcomb
Cecily Wolfe
Francis Wu
Frank Wyatt
Zhiqiang Yang
Mark Yashinsky
Bob Yeats
Alan Yong
Jeri Young
Bill Young
Doug Yule
Yuehua Zeng
Lupei Zhu
Mary Lou Zoback

Caltech
Utah
UCSB
USGS-Pasadena
UC-Santa Barbara
USGS-Menlo Park
Arizona State
Occidental College
Nevada-Reno
CSU-Northridge
Lamont
USC
UC-Santa Barbara
USC
Brown
UC-Santa Barbara
Cornell
USGS-Reston
UCSD
CSU-Northridge
USC
Whittier
UCSD
LLNL
USGS-Pasadena
USGS-Pasadena
Earth Consultants International
UCLA
UCLA
UC-Santa Cruz
Colorado
Lettis and Associates
JPL
SCEC
Nevada-Reno
NSF
NSF
SUNY-Binghamton
UC-San Diego
Alaska
Caltrans
Oregon State
USGS/Pasadena
Arizona State
SCIGN
CSU-Northridge
Nevada-Reno
USC
USGS-Menlo Park

China Participants in the US/China GPS Workshop

Zhang Peizhen, Deputy Director, Institute of Geology, CSB

Bao Dongjian, Deputy Director, Inner Mongolia Autonomous Region Seismological Bureau, CSB

Chen Xinlian, Center of Earthquake Analysis and Prediction, CSB

Ding Ping, Director, Second Center of Deformation Monitoring, CSB

Gu Guohua, Center of Earthquake Analysis and Prediction

Huang Liren, First center for Deformation Monitoring, CSB

Luo Zhiguang, Technique Center of the Network of Crust

Ma Linbo, Deputy Director, Second Brigade of Crust Deformation Survey, State Bureau of Surveying and Mapping Monitoring of China

Niu Zhijun, Deputy Director, Dept. of Earthquake Monitoring and Prediction, CSB

Qiao Xuejun, Institute of Earthquakes in Wuhan, CSB

Ren Jinwei, Institute of Geology, CSB

Wang Qingliang, Second Center of Deformation Monitoring, CSB

Wang Yongxiang, Senior Engineer, Department of Fundamental Sciences, Chinese Academy of Sciences

Yang Guohua, First Center of Deformation Monitoring, CSB

Yin Jin, Deputy Division Director, Department of International Cooperation, Ministry of Science and Technology of China

You Xinzhao, Institute of Earthquakes in Wuhan, CSB

Zhang Zusheng, First Center of Deformation Monitoring, CSB

Zhao Ming, Deputy Division Director, Dept. International Cooperation, CSB

Zhu Wenyao, Research Institute of Shanghai Astronomical Observatory

US Participants in the US/China GPS Workshop

Yin An	UCLA
Rebecca Bendick	Colorado
Yehuda Bock	UC-San Diego
Danan Dong	JPL
Andrea Donnellan	JPL
Peng Fang	UCSD
Jeff Freymueller	Alaska
Weijun Gang	USGS/CSB
Brad Hager	MIT
Bill Holt	SUNY-Stony Brook
Ken Hudnut	USGS-Pasadena
Charles Hutt	USGS-Albuquerque
Dave Jackson	UC-Los Angeles
Leonard Johnson	NSF
Robert King	MIT
Lanbo Liu	Connecticut
John McRaney	SCEC
Peter Molnar	MIT
Walter Mooney	USGS-Menlo Park
Angelyn Moore	JPL
Ruth Neilan	JPL
Will Prescott	USGS-Menlo Park
Zheng-Kang Shen	UC-Los Angeles
Bingming Shen-tu	SUNY-Stony Brook
Min Wang	UCLA
Frank Webb	JPL
Francis Wu	SUNY-Binghamton
Zhiqiang Yang	Alaska

SCEC ORGANIZATION - 1999

Management

Center Director: Thomas L. Henyey
University of Southern California

Acting Science Director: J. Bernard Minster
University of California, San Diego

Director for Administration: John K. McRaney
University of Southern California

Director for Outreach: Jill H. Andrews
University of Southern California

Assistant Director for Outreach: Mark Benthien
University of Southern California

Board of Directors

Chair: J. Bernard Minster
University of California, San Diego

Vice-Chair: Ralph Archuleta
University of California, Santa Barbara

Members: John Anderson
University of Nevada, Reno

Robert Clayton
California Institute of Technology

James F. Dolan
University of Southern California

Kenneth Hudnut*
United States Geological Survey

David D. Jackson
University of California, Los Angeles

Thomas Rockwell
San Diego State University

Leonardo Seeber
Columbia University

Ex-officio: Thomas Henyey
University of Southern California

* represents Lucy Jones on Board.

Research Group Leaders

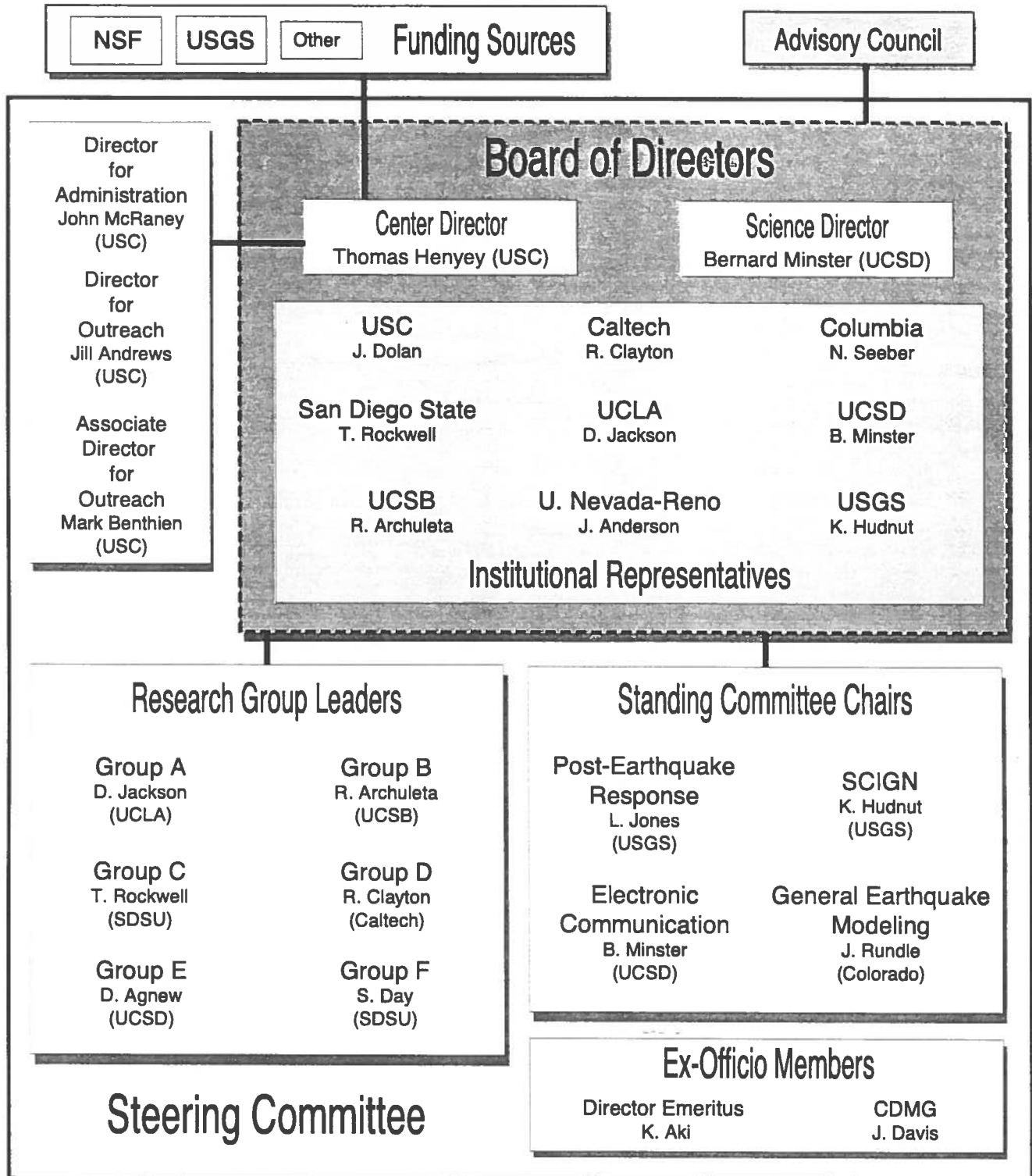
A: Master Model:	David D. Jackson University of California, Los Angeles
B: Strong Motion Prediction:	Ralph Archuleta University of California, Santa Barbara
C: Earthquake Geology:	Thomas Rockwell San Diego State University
D/F: Subsurface Imaging and Tectonics and Seismicity and Source Parameters:	Robert Clayton California Institute of Technology
E: Crustal Deformation:	Duncan Agnew University of California, San Diego
G: Earthquake Source Physics:	Steve Day San Diego State University

Steering Committee Members (ex-officio)

Director Emeritus	Keiiti Aki University of Southern California
State of California Representative	James Davis California State Geologist
SCIGN Board Chairman	Ken Hudnut United States Geological Survey



Southern California Earthquake Center



1999 SCEC ADVISORY COUNCIL

Robert SMITH (Chair), University of Utah, Department of Geology and Geophysics, Salt Lake City, UT 84112-1183

Lloyd S. CLUFF, Pacific Gas and Electric Co., Geosciences Department, P.O. Box 770000, Mail Code N4C, San Francisco, CA 94177

C. B. CROUSE, Dames and Moore, 2025 First Avenue, Suite 500, Seattle, WA 98121

George DAVIS, Department of Geosciences, University of Arizona, Tucson, AZ 85721

James DIETERICH, United States Geological Survey, 345 Middlefield Road, MS 977, Menlo Park, CA 94025

Robert HAMILTON, NRC/National Academy of Sciences, 2101 Constitution Ave., NW, Washington, DC 20418

Thomas JORDAN, Massachusetts Institute of Technology, Department of Earth, Atmospheric and Planetary Sciences, Cambridge, MA 02139

Dennis MILETI, University of Colorado, Natural Hazards Research and Applications Information Center, Campus Box 482, Boulder, CO 80309-0482

Jack MOEHLE, Pacific Earthquake Engineering Center, University of California, 1301 South 46th Street, Richmond, CA 94804-4698

Barbara ROMANOWICZ, University of California, Berkeley, Department of Geology and Geophysics, Berkeley, CA 94720

Kaye SHEDLOCK, United States Geological Survey, Denver Federal Center, MS 966, Denver, CO 80225

Susan TUBBESING, EERI, 499 14th St., Suite 320, Oakland, CA 94612-1902

Southern California Earthquake Center
Senior Research Investigators (1999)

Principal Investigator and Center Director:

Thomas L. Henyey
Department of Earth Sciences
University of Southern California
Los Angeles, California 90089

Acting Science Director:

J. Bernard Minster
Scripps Institution of Oceanography
University of California
San Diego, California 92093

Principal Institutions

University of Southern California
Department of Earth Sciences
Los Angeles, California 90089

Scientists

Keiiti Aki
Yehuda Ben-Zion
James F. Dolan
Edward Field
Nikki Godfrey
Yong-Gang Li
David Okaya
Charles G. Sammis
Ta-liang Teng
Lupei Zhu

University of Southern California
Department of Civil Engineering
Los Angeles, California 90089

Geoffrey R. Martin

California Institute of Technology
Seismological Laboratory
Pasadena, California 91125

Robert Clayton
Jishu Deng
Michael Gurnis
Egill Hauksson
Thomas Heaton
Donald Helmberger
Martha House
Hiroo Kanamori
Kerry Sieh
Mark Simons
Joann Stock

Columbia University
Lamont-Doherty Earth Observatory
Palisades, New York 10964

John Armbruster
Leonardo Seeber
Bruce Shaw
Lynn Sykes

University of California
Department of Earth and Space Sciences
Los Angeles, California 90024

Mark Abinante
Paul Davis
Monica Kohler
Zheng-kang Shen
Li-Yu Sung
John Vidale

University of California
Institute of Geophysics and Planetary Physics
Los Angeles, California 90024

Yan Kagan
Leon Knopoff

University of California
Department of Civil Engineering
Los Angeles, California 90024

Mladen Vucetic

University of California
Scripps Institution of Oceanography
LaJolla, California 92093

Duncan Agnew
Yehuda Bock
Hadley Johnson
Peter Shearer
Frank Vernon
Nadya Williams
Frank Wyatt

University of California
Department of Geological Sciences
Santa Barbara, California 93106

Ralph Archuleta
Marc Kamerling
Edward Keller
Bruce Luyendyk
Craig Nicholson
Kim Olsen
Peter Rodgers
Jamie Steidl
Alexei Tumarkin

University of Nevada
Department of Geological Sciences
Reno, Nevada 89557

John Anderson
Rasool Anooshepoor
James Brune
Raj Siddharthan
Feng Su
Steven Wesnousky
Yue-hua Zeng

San Diego State University
Department of Geological Sciences
San Diego, California 92182

Steven Day
Harold Magistrale
Thomas Rockwell

United States Geological Survey

Gary Fuis
Tom Hanks
Ruth Harris
Susan Hough
Ken Hudnut
Peggy Johnson
Lucy Jones
Nancy King
Daniel Ponti
Ross Stein
David Wald
Lisa Wald

Member Institutions

Arizona State University
Tempe, Arizona

University of California
Davis, California

University of California
Irvine, California

University of California
Department of Earth Sciences
Riverside, California 90024

University of California
Earth Sciences Board of Studies
Santa Cruz, California 95064

California Division of Mines and Geology

California State University
Department of Geology
San Bernardino, California 92407

Carnegie Mellon University
Pittsburgh, Pennsylvania

Central Washington University
Department of Geology
Ellensburg, Washington 98926

University of Colorado
Department of Geological Sciences
Boulder, CO 80309

Harvard University
Department of Earth and Planetary Sciences
Cambridge, Massachusetts 02138

Jet Propulsion Laboratory
Pasadena, California

Lawrence Livermore National Lab
Livermore, California

Scientists

Ramon Arrowsmith

Louise Kellogg

Lisa Grant

Stephen Park

Steven Ward

James Davis
Mark Petersen
Michael Reichle

Sally McGill

Jacobo Bielak

Charles Rubin

Karl Mueller
John Rundle

James Rice
John Shaw

Danan Dong
Andrea Donnellan
Mike Heflin
Ken Hurst
Michael Watkins
Frank Webb

Bill Foxall

Massachusetts Institute of Technology
Department of Earth, Atmospheric, and
Planetary Sciences
Cambridge, Massachusetts 02139

Brad Hager
Tom Herring
Robert King
Simon McClusky
Robert Reilinger

University of Oregon
Department of Geological Sciences
Eugene, Oregon 97403

Gene Humphreys
Ray Weldon

Oregon State University
Department of Geosciences
Corvallis, Oregon 97331

Robert Yeats

Woods Hole Oceanographic Institute
Department of Geology and Geophysics
Woods Hole, Massachusetts 02543

Jian Lin

Industry Participants
Earth Consultants International
Orange, California

Scientists
Eldon Gath

Maxwell Labs
La Jolla, California

Jeffry Stevens

Willis Lettis and Associates
Walnut Creek

Scott Lindvall

Pacific Gas and Electric
San Francisco, California

Norman Abrahamson

Woodward-Clyde Associates
Pasadena, California

Robert Graves
Arben Pitarka
Chandon Saikia
Paul Somerville

Message from the Directors

To: SCEC Community

From: Bernard Minster, Tom Henyey, Dave Jackson

Subject: 1999 Annual Meeting

As you know, SCEC (as we know it) is approaching the time when budgets will decrease and many activities will be phased out. This does not obviate by any means ongoing efforts to conceive and design a new consortium-like activity to carry on the mission we have collectively embarked upon into the next decade. This year's annual meeting should focus on setting the stage for an effective transition into this next phase.

A basic message that we wish to convey is that this year's meeting should take a slightly different flavor than our meetings of the last few years. In particular, the usual exercises of holding working group meetings to identify priorities for the coming year will have largely taken place before the meeting, either by email or through teleconferences or through actual meetings. Some of our working groups (e.g. WG E) have historically functioned in this fashion, and this has served them quite well.

In Palm Springs, we can then proceed directly to the summary presentations of the consensus achieved in each working group, with concomitantly shorter discussions. For this to work, each WG leader has not only secured input from the WG members, but also sought feedback and input from others who have an abiding interest in the activities of the group. At the same time, any SCEC member who wishes to volunteer input and suggestions should do so by communicating with the appropriate WG leader.

The basic motivation for this strategy is that, after nearly a decade of existence, it is time for SCEC to regroup and summarize its successes and accomplishments, to compare those to the goals we initially set for ourselves when we started, and to identify the challenges ahead, as well as a set of roadmaps we might follow to address these challenges. This process is deliberately retrospective, insofar as it is essential to look back at where we have been in order to make a cogent argument concerning where we intend to go next.

The following pages constitute a preliminary strawman outline for this so-called "legacy" document. (We need a nice title!). It is not cast in concrete, naturally, but we hope it will serve as a first step toward defining the flavor of our discussions. Similarly, the named editors and contributors are only intended as examples of SCEC persons who might be counted upon to contribute.

We would like this document to serve as a basis to organize our discussions at the annual meeting, and a more mature version, which should come out of the meeting, to serve as the means to organize the Center activities over the next two years. Ultimately, the full volume (paper and CD-ROM) will be the final documentation of the SCEC legacy. At the same time, it should help us over the next year to focus our thinking and our directions, so that (1) we fill as many of the gaps as we can, and (2) we define the kind of coordinated community activity that might follow the formal termination of SCEC as an S&T center. Therefore, even though the final document may not be ready for 18 months or so, it would be useful to have preliminary drafts of the various pieces in support of a proposal writing effort, due in late Spring 2000.

The agenda for the annual meeting follows the draft outline fairly closely, and takes into account comments from the Steering Committee. It should be noted that the chapters in the outline do not match the current working groups on a one-to-one basis. This means that there is a need for chapter and working group leaders to coordinate and exchange views and information as part of this process. The attached matrix is an attempt to identify some important connections to be established.

This is a transition year for SCEC. We should look at it as an opportunity to highlight what we have achieved collectively, and to come up with a clear and logical statement of the challenges we would like to tackle over the next decade.

Chapters	WG A: Master model (Jackson)	WG B: Ground Motion (Archuleta)	WG C: Earthquake Geology (Rockwell)	WG D/F: Imaging and seismotectonics (Clayton)	WG E: Crustal deformation (Agnew)	WG G: Earthquake Physics (Day)	WG H: Engineering (Martin)	E&O (Andrews)	SCIGN: Hudnut/Bock /Webb	Data Centers (Clayton, Bock, Archuleta)
Preface/introduction (Minster)	X							X		
Ch1: Seismotectonics (Henvey)			X	X	X					X
Ch2: Crustal Deformation (Agnew)	X				X				X	X
Ch3: Earthquake history (Sieh)	X		X	X						X
Ch4: Velocity/density model (Clayton)		X		X						X
Ch5: Wave propagation (Archuleta)		X		X		X				X
Ch6: Source Physics (Day)				X		X				
Ch7: SCEC Earthquakes (Jones/Hauksson)	X	X	X	X	X	X	X	X	X	X
Ch8: Stress transfer (Stein/Harris)	X		X	X	X					
Ch9: Earthquake potential (Jackson)	X		X	X	X					X
Ch10: E&O (Andrews)	X						X	X		
CH11: PHASE 5 M.M. (Field)	X	X	X	X	X	X	X	X	X	X

The SCEC “Legacy” document

Editorial Committee (tentative):

Bernard Minster, Tom Henyey, Dave Jackson, Jill Andrews, Ralph Archuleta, Jim Brune, Rob Clayton, Tom Jordan, Kerry Sieh, Bob Smith

Issues for discussion:

- Purpose
- Time table: Draft by summer 2000, final by Xmas 2000?
- Organization

Proposed generic Chapter template (5-10 pages of text/chapter, not including figures, boxes, side-bars)

- What is the problem, how does it address the SCEC science goals
- What we have done in the first 10 years of SCEC
 - A.
 - B.
 -
- Include pretty pictures, side-bars or boxes to explain concepts
- Include E&O material if appropriate
- Where we are:
- What role did SCEC play? What progress was accomplished that would not have been without SCEC?
- Challenges for the future and a roadmap to address these challenges.

Miscellaneous items

- Establish an editorial committee
- Poll group leaders about the next couple of years
- Tell people what we have in mind and get feedback/input
- People below are to animate discussion and to organize production and writing of chapters.
- Each chapter has a head honcho, and each subchapter has potential contributors.
- Level is Scientific American. Technical materials may be submitted in Appendices on CD-ROM.
- Color pictures desirable.

➤
1. **Preface (B. Minster, ed.)**

2. **The view from Advisory Council**

Tom Jordan?, Bob Smith

3. **Introduction (B. Minster, ed.)**

3.1. The role and purpose of this document

This is the legacy of the first decade of SCEC research

3.2. A short history of SCEC

Keiiti Aki, Tom Henyey, Dave Jackson, Bernard Minster

3.3. The role of group science in earthquake research

Problem selection

Data collection

Model construction

The role of consensus building

Multi-disciplinary approaches to science

3.4. The place of SCEC within new initiatives such as EarthScope

1. **Seismotectonic Framework of southern California (T. Henyey, ed.)**
 - 1.1. **Background: see e.g. "putting down roots..."**
Kerry Sieh, Tom Henyey, Jill Andrews., Tom Rockwell., Egill Hauksson, Steve Wesnousky
 - 1.2. **Faults**
 - 1.2.1. Various SoCal faulting regimes, active inactive
 - 1.2.2. Blind thrusts
John Shaw
2. **Regional Crustal Deformation Model (Duncan Agnew, ed.)**
 - 2.1. **Using geodesy and strain measurements**
Quick summary of various technologies and techniques.
How this evolved rather quickly over the lifetime of SCEC
 - 2.2. **The southern California velocity model**
Southern California Deformation Model, with time dependence and descriptive paper.
Calculations for version 3 are in progress; no organization yet to write summary paper.
 - 2.3. **New techniques on the horizon**
Ken Hudnut, Duncan Agnew, Dave Jackson, Yehuda Bock, Brad Hager
3. **Earthquake history (Kerry Sieh, ed.)**
 - 3.1. **Southern California paleoseismology**
 - 3.1.1. San Andreas fault:
Kerry Sieh
 - 3.1.2. LA Basin:
Tom Rockwell, J. Dolan, Scott Lindvall, John Shaw, Eldon Gath
 - 3.1.3. Ventura/Santa Barbara Basin;
E. Keller
 - 3.2. **Historical seismicity**
L. Jones/D. Jackson
4. **Crustal Velocity and Density Models (E. Hauksson, ed.)**
 - 4.1. **Southern California Seismic Velocity and Density Model;**
Working group has made good progress and a version will be presented at the annual meeting.
Rob Clayton, Harold Magistrale, Rob Graves, Egill Hauksson
 - 4.2. **LARSE**
Rob Clayton, G. Fuis, Egill Hauksson
5. **Wave propagation simulations in realistic earth structures (R. Archuleta, ed.)**
 - 5.1. **Wave propagation in 3D Basins**
Ralph Archuleta, Kim Olsen, Steve Day
 - 5.2. **Calculating Strong ground motions**
 - 5.2.1. Basin effects
 - 5.2.2. Near source effects
 - 5.2.3. Site effects
 - 5.2.4. Attenuation relation
 - 5.2.5. Use of downhole instrumentation

5.2.6. Nonlinear effects

A report on theoretical and empirical methods to model ground motion from large earthquakes. Group B has included some relevant items in its 1999 plan, and Steve Day is interested in pursuing this, but it has not reached "Working Group" status at present.

Steve Day, John Anderson

5.3. Earthquake scenarios

Kim Olsen, Ralph Archuleta, Rob Graves

6. Source physics (S. Day, ed.)

6.1. Sources: Imaging studies

6.1.1. Direct Fault imaging

Gary Fuis, Dave Okaya, Tom Henyey

6.1.2. Indirect Fault imaging

John Shaw, Peter Shearer, Nano Seeber

6.1.3. Trapped waves and fault geometry

Yehuda Ben-Zion, Y. Li, John Vidale

6.2. Sources: Constraints from Lab. and field evidence

6.2.1. Rocks and foam rubber

6.2.2. Fault-normal displacements

6.2.3. Precarious rocks

Jim Brune, Jim Dieterich

6.3. Sources: Theoretical studies

6.3.1. Single fault simulations and Rupture dynamics

Jim Rice, Yehuda Ben-Zion, Steve Day, Ruth Harris

6.3.2. Fault segment interactions

Steve Day, Ruth Harris, Steve Ward

6.4. Micro-Macro scale physics:

Leon Knopoff, Charlie Sammis, John Rundle

7. The SCEC earthquakes (Lucille Jones, ed.)

7.1. Background Seismicity

Hauksson, Seeber, Shearer

7.2. Landers:

Tom Rockwell and Sieh (mapping, GPS, aftershocks, fault structure etc)

7.3. Northridge:

Andrea Donnellan, Paul Davis, and Cie

8. Stress modeling and stress transfer (Ross Stein, ed.)

8.1. The basic theory

Source models and Earth structure models

Rheologies

Coulomb stress

8.2. The role of stress transfer simulations

Changes in load conditions

Potential effects on future seismicity

8.3. The tools we now have

Software packages and workshops

Ross Stein, Lynn Sykes, Jishu Deng

9. Estimating earthquake potential (Dave Jackson, ed.)

9.1. Earthquake potential

A report on earthquake potential in southern California (WG2K), multi-models (seismicity, fault slip, strain rate); funded by SCEC in 1999, first workshop to be in September. Should include update on fault slip rate table, self consistent geometries of blind thrusts, and earthquake catalog with uncertainties.

Ned Field, Dave Jackson, Steve Ward, Jim Dolan

9.2. An earthquake deficit in California?

Ned Field, Dave Jackson, Ross Stein, Tom Hanks, L. Jones

9.3. Seismicity simulations

9.4. Intermediate-term prediction

Sammis, Minster, others?

10. Reaching out to the community (Jill Andrews, ed.)

10.1. EOT

Try to highlight activities with fancy graphics and/or photographs.

Jill Andrews

11. THE MASTER MODEL (phase 5) (Ned Field, ed.)

- This is the final phase, at least in the current concept.
- Should this be prospective chapter, since this will not be done by the time we need to use the document
- Do we have a plan?

1. APPENDIX: Contents of CD-ROM

11.1. CD-ROM: Phase1 and Phase 2

Summarize the various phases. Describe process, and describe progression and improvements.

11.2. CD-ROM: Phase 3 (site effects);

nearly done, to be published in BSSA.

Recommendation: continue, of course.

Ned Field

11.3. CD-ROM: Infrastructure/facilities

11.3.1. Seismology:

Data Center

Coordination with UCB

SCSN, Trinet, other networks (ANZA)

Use in EOT

Clayton

11.3.2. Geodesy:

Campaign data sets

PGGA and then SCIGN

Strainmeters (PFO)

Orbits and other data products. EOT aspects

Shen, Jackson, Agnew, Bock

11.4. CD-ROM: SCEC Newsletters

11.5. CD-ROM: SCEC workshops

11.6. CD-ROM: SCEC publications

EXTRAS...EXTRAS...

1. BOXES or side-bars, to be scattered among chapters

Possible Examples....we need input and suggestions!

- Characteristic earthquakes
- Fault segmentation
- Earthquake deficit?
- Trapped waves
- Blind faults
- GPS measurements
- Strain measurements
- Fault trenching
- Nonlinear wave propagation
- Borehole instrumentation
- Focusing and defocusing
- Precarious rocks
- Various EOT boxes
- Fault zone rheology
- Coulomb stress

2. Figures

Possible Examples....we need input and suggestions!

- SCEC Velocity model
- Southern California faults
- Some trench walls?
- SCEC crustal model
- Cross section
- Seismicity
- Landers
- Northridge
- Networks
- Earthquake Hazards (phase x)
- Stress transfer, stress shadows
- LARSE
- Wave propagation (CD-ROM could have an animation!)

Etc....

EarthScope

The following pages are an introduction to EarthScope, a new initiative in the Earth Sciences community. The membership of the EarthScope Working Group is listed below.

EarthScope Working Group

Member	Representing
Jeff Freymueller	UNAVCO
Tom Henyey- Chair	SCEC
Steve Hickman	SAFOD
Tom Jordan	NAS
John McRaney- Secretary	SCEC
Anne Meltzer	USArray/IRIS
Bernard Minster	SCEC/InSAR
Dennis Nielson	DOSECC
Paul Rosen	InSAR
Paul Silver	PBO
Mark Simons	InSAR
David Simpson	USArray/IRIS
Bob Smith	PBO
Seth Stein	UNAVCO
Wayne Thatcher	USGS/Menlo Park
Mark Zoback	SAFOD

Executive Committee: Henyey, McRaney, Meltzer, Minster, Silver and Zoback

Agency Representatives

John Filson	USGS/Reston
Leonard Johnson	NSF
Russell Kelz	NSF
Earnie Paylor	NASA
Robin Reichlin	NSF
Dan Weill	NSF
Cecily Wolfe	NSF
Jim Whitcomb	NSF
Herm Zimmerman	NSF

EarthScope — A Look into Our Continent

A. Overview

Scientific Justification

EarthScope is an integrated research effort designed as a distributed, multi-purpose geophysical instrument array that has the potential for making major advances in our knowledge and understanding of the structure and dynamics of the North American continent. This knowledge is not only important scientifically but is important socially because of its use in mitigating the impact of the infrequent, but increasingly costly, disasters caused by earthquakes and volcanic eruptions.

Advances in theory, computing and the technology of optical and radio telescopes have allowed us to see ever deeper into the universe overhead. Similarly, theoretical, computational, and technological advances in seismology, extraterrestrial geodesy, and drilling provide the tools to make major advances in looking downward into the planet. High-precision geodesy using the Global Positioning System (GPS) is mapping the large-scale deformation field in space and time. Interferometric Synthetic Aperture Radar (InSAR) represents a complementary means of mapping deformation over broad areas with high spatial resolution. A new generation of seismometers can now provide detailed images of crust and mantle structure, as well as our best look ever at the earthquake process. Strainmeters give us nano-strain sensitivity with the ability to measure short-term aseismic deformation transients that provide insight into the processes of earthquake nucleation. Advances in drilling technology made by the petroleum industry have brought new science objectives, previously unattainable because of intractable drilling problems, within our reach. Significant technological advances are taking place in microelectronics, data collection systems and communication, allowing the miniaturization of downhole instrumentation and the efficient real-time handling of vast volumes of data from large arrays of geophysical instrumentation.

Initial results from these new technologies, coupled with multidisciplinary integrative approaches to scientific discovery and management, demonstrate the potential for significant advances. For example:

- The Southern California Earthquake Center (SCEC), a multi-institutional NSF Science and Technology Center, is showing how a multi-disciplinary scientific approach involving seismology, geodesy, and fault zone geology can significantly improve knowledge in areas that impact seismic risk reduction. These include estimating earthquake potential, determining the properties of fault zones and the physics of rupture, predicting ground motions for future earthquakes, and transferring this knowledge to engineers and the public.

SCEC, with two years remaining under the NSF/STC program, has started planning for its future. SCEC intends to expand its focus on the physics of earthquakes (i.e., those processes leading up to and including earthquake nucleation, fault rupture, and the ensuing ground motions) with a practical aim of improving earthquake forecasting and seismic hazard assessment. It will employ a multi-disciplinary, integrative (systems) approach to problem solving similar to that pioneered by SCEC with its "master model" approach to earthquake science and hazard analysis. Numerical modeling and simulations of fault evolution, rupture propagation and ground motions will play an enhanced role in the future. Products will include complete theoretical seismograms for plausible future earthquakes that can be used by engineers for performance-based engineering design.

- Seismological data, collected with NSF support by the Incorporated Research Institutions for Seismology (IRIS) is improving our understanding of the nature of earthquake mainshock/aftershock sequences, as well as providing dramatically better images of seismogenic and other deformational structures within the earth. These results are crucial for understanding plate boundary processes, in that earthquakes reflect ongoing deformation, while both earthquakes and subsurface structures provide crucial clues on the mechanics of boundary zones around the world.
- Global Positioning System (GPS) data, collected, for example, under the auspices of the University Navstar Consortium (UNAVCO), and by the Southern California Integrated GPS Network (SCIGN), are being used by scientists to map motions in plate boundary zones and investigate their relation to earthquake and volcanic processes. These data give our first clear look at how plate boundary zones around the world, including western North America, Japan, New Zealand, the Andes, and the Himalayas, are evolving today. GPS data similarly permit new insight into intraplate deformation, such as the eastern half of the U.S., where the earthquake hazard is high but not well understood.
- Interferometric Synthetic Aperture Radar (InSAR) is providing stunning images and insight of co-seismic and post-seismic ground deformation accompanying major earthquakes. Future advances should allow creation of deformation images along major faults during the strain build-up portion of the earthquake cycle. Coupled with GPS, these data will be crucial for understanding and forecasting earthquakes at intermediate and long-terms.
- Access to high performance computing is opening new opportunities for simulating complex systems such as plate boundary kinematics and dynamics, space-time seismicity patterns, and earthquake ground motions. Until now, we could not contemplate realistic calculations at meaningful spatial/temporal resolutions. Advances in speed, parallel processing, storage, and algorithms, plus the development of new theories in non-linear dynamics have created opportunities to change this. However, in order to produce realistic calculations in space-time, the models need realistic inputs of the rheology and dynamics of the crust and upper mantle. EarthScope is designed to provide this critical input.

Implementation

The implementation strategy of EarthScope is staged as follows:

- Stage I. A) USArray, and B) San Andreas Fault Observatory at Depth
- Stage II. Plate Boundary Observatory
- Stage III. Interferometric Synthetic Aperture Radar (InSAR)

Stage I of EarthScope is composed of two elements. The first element is the USArray, which is a dense array of high-capability seismometers that will be deployed in a step-wise fashion throughout the U.S. to greatly improve our resolution of the subsurface rheology. Figure 1 shows a schematic of the important earthquake processes in space and time along with the observational strategies. Below the cm level, laboratory investigations are effective. Above one-km scale, the observational fields of seismology, fault mapping, and crustal deformation are effective. The USArray will greatly improve the uniform resolution of crust and upper mantle rheology from the current 500-km resolution to about 30-km resolution, and special studies will show even finer detail to the 1-km level.

The second element of Stage I, the San Andreas Observatory at Depth, addresses the remaining uncovered observational gap in Figure 1, between 1 cm and 1km. This zone represents the range of nucleation and rupture processes of earthquakes. The physics of these processes is one of the most challenging

problems in science today. A number of theories and inferences from laboratory and large scale (>km) observations have been proposed to model the dynamics of these critical events. Yet, there has been no observational means of testing these theories because of the difficulty of access, at reasonable cost, to an active fault at seismogenic depths. We are now in a position to do this and the San Andreas Fault Observatory at Depth is the means.

The acquisition, deployment and installation costs of EarthScope — Stage I are requested to be supported through the MRE account starting in FY 2001 and continuing through FY 2004 with a total request of \$74.8 million. Support from the GEO Directorate/Earth Sciences Division for operations, science and management is estimated to total approximately \$62 million over the 10 year period until FY 2010. Funding is planned to start at \$2.5 million in FY 2001 and reach approximately \$8 million per year by FY 2005. For Stage I, it is estimated that more than 160 U.S. scientists and a similar number of students will be involved in the operations and data utilization. We estimate foreign participation of more than 75 scientists and students.

Stage II involves the construction of a Plate Boundary Observatory (PBO) encompassing the western half of the US. The PBO is composed of an array of permanent borehole installations of multiple instruments, including GPS receivers, strainmeters, tiltmeters, and seismometers. The entire region west of the Rocky Mountains is dominated tectonically by the forces related to the movement between the North American and Pacific plates. The concept of the Plate Boundary Observatory was inspired by recent exciting discoveries showing the interconnectedness of fault systems and the non-seismic distortion of the crust and upper mantle that appear to be related to future seismic events.

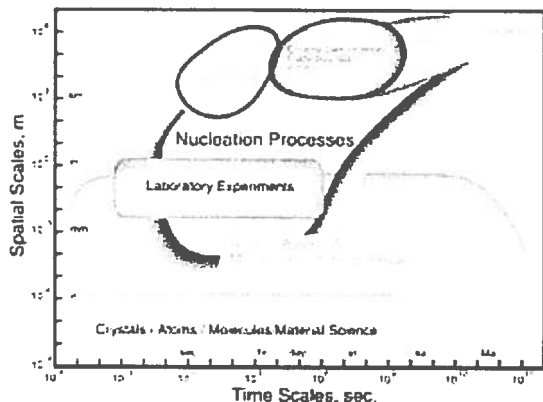


Figure 1. A schematic representation of the Earth's crust and mantle dynamics as a function of space and time. Earthquake nucleation and rupture processes occupy a spatial zone between about 1-cm to 1-km that is not observable without access to active faulting at seismogenic depths. (figure from J.B. Minster, personal communication, 1999)

Stage III involves flying a synthetic aperture radar (SAR) on a satellite. Interferometric SAR (InSAR) has produced spectacular images of crustal distortion of earthquakes, volcanoes, and land subsidence with high precision and spatial resolution. This instrument will address much of the observational gap shown in the space/time plot of Figure 1. Because of the need for a satellite, NASA currently has the main role for InSAR. However, after more than eight years from proof of concept, budget restrictions have delayed NASA commitment even though the need is generally accepted. The current NASA plan, an Announcement of Opportunity named LightSAR, is now open for proposals with a decision on the successful proposal due in July 1999. An NSF partnership with NASA may be desirable to provide support to the data retrieval component of the project and protect the scientific uses of this critical technology.

Management

Operational aspects of EarthScope will be coordinated through a federation of the participating consortia under cooperative agreements with NSF. Oversight for implementation, operation, and data acquisition and archival will be provided by a working group composed of the leaders of the participating consortia, plus representatives from involved government agencies. The consortia - SCEC, IRIS, and UNAVCO - have successfully managed comparable facility construction and operation, and work well together to maximize the value gained from agency funding, and set priorities on the basis of scientific merit and effective implementation of facility goals. The major agencies - NSF, USGS, NASA, and DOE - that will be involved have demonstrated the ability to collaborate effectively with each other and with the scientific community in efforts such as NEHRP (National Earthquake Hazard Reduction Program), SCIGN (Southern California Integrated GPS Network), and the Interagency Coordinating Committee for Continental Drilling. Research based on EarthScope data will be supported through the normal peer-review funding process at NSF, other US agencies, and other international agencies such as the International Continental Drilling Project (ICDP), and the overall effort will be tightly coordinated by a science steering committee. Utilization of the data for practical considerations will be closely coordinated with mission agencies at state and federal levels.

Education and Outreach

A unique feature of the EarthScope is the involvement of students and the general local community in the plans, installation, operation and analysis of results within each region of occupation. Significant benefit will be gained from the already ongoing support structure and concepts of the IRIS Education and Outreach program including the PEPP (Princeton Earth Physics Project), which features a seismic station at 55 participating high schools throughout the country. The high schools connect their seismometer to the Internet and have access to all other PEPP seismograph data for doing educational projects related to earthquakes and the structure of the Earth. EarthScope is envisioned to be the prominent catalyst for an exciting public education program.

Two components will comprise the education and outreach part of EarthScope. The first will be online real-time access to recorded data. The second is an organized, integrated, earth science program designed to go into an area before the USArray arrives and prepare people for the arrival of the array. This will include primers on earth structure, earth dynamics, earthquake hazard and interesting regional geologic features to be investigated by the array and ancillary geologic studies. There will be educational materials addressed to and made available to both the general public and local/state governments as well as for K-12 (as appropriate). While the array is in a region, the program will bring results from the array to the community. Finally, a follow-up program will continue to link communities to the array as it moves across the country and show how the data recorded by the array in their region merges with data from other regions that build a continuous image of lithospheric and mantle structure. One idea still in the conceptual stage is to provide a feed into the weather channel so that "significant event" data can be broadcast.

Milestones

2001: Compete and award contracts for broadband and short-period seismic systems. Community planning on permanent seismic sites and first array deployment. San Andreas Fault Observatory at Depth main hole drilling contract competed and awarded. Drilling begins at end of year. Down-hole monitoring equipment constructed. NSF conducts review of plans and costs.

2002: Delivery and installation of 50 transportable array sites. Delivery and installation of 500 flexible pool short period sites. Delivery and installation of 5 GSN and 10 NSN permanent stations. Main hole completed at San Andreas Fault Observatory. Down-hole monitoring instrumentation installed. NSF conducts review of plans and costs.

2003: Delivery and installation of 200 transportable array sites. Delivery and installation of flexible pool sites: 200 broadband and 1000 short period seismic systems. Delivery and installation of 5 GSN and 10 NSN permanent stations. San Andreas Fault site characterization studies carried out.

2004: Delivery of 50 and installation of 200 transportable array sites. Delivery of flexible pool sites: 150 broadband and 500 short period. Installation of flexible pool sites: 200 broadband and 1000 short period. Delivery and installation of 5 NSN permanent stations. Use site characterization and monitoring data to chose four coring intervals at depth in San Andreas Fault Observatory. Commence coring operations. NSF conducts review of plans and costs.

2005: Redeployment of USArray continues at approximate 1.5 year intervals. Install permanent monitoring instrumentation in four core intervals and main hole of San Andreas Fault Observatory at Depth.

2006: Complete analysis of San Andreas Fault cores, cuttings and logs. Continue monitoring at depth. NSF conducts review of plans and costs.

2007:

2008: NSF conducts review of plans and costs.

2009:

2010: NSF conducts review of plans and costs.

Continue to: [USArray](#)
Return to: [Table of Contents](#)

B. Stage I — USArray and San Andreas Fault Observatory at Depth

USArray

Scientific Justification USArray is a facility for investigating the structure and evolution of the North American continent. It is the next logical step in a sequence of recent dramatic successes imaging the internal structure of the Earth with seismic tomographic techniques using observations gathered by the IRIS Global Seismographic Network. USArray is designed to systematically map the continental lithosphere and upper mantle under the US, with potential extensions into Canada, Mexico, and the continental shelf. The concept is to move across the country with a high-resolution "inverted seismic telescope" probing continental structure. The USArray will also be organized to take advantage of the potential for raising public awareness in the earth sciences during the period that the array is deployed in a particular region of the US

The topography of North America displays a rich variety of landforms as shown in Figure 2a — the ancient mountains of the Appalachians, the rolling plains of the Midwest, the relatively young and rugged Rockies, the ridges and valleys of the Basin and Range Province, and the volcanic Cascades of the Northwest. Each of these landforms is the surface manifestation of deeper-seated geologic processes. Although our knowledge of the continental surface is known in great detail through high-resolution topographic and geological mapping, we have only a sketchy interpretation of the underlying continental structures that produced these landforms and continue to control their evolution.

USArray will be a versatile observational platform designed to produce the first high-resolution synoptic view of the continental crust and lithosphere under North America. The comparative effect of increasing resolution is illustrated in Figure 2. Plates a, b, and c show the nation's topography at different levels of resolution: 1, 30, and 500 km. Our current level of resolution for Earth structure (about 50-500 km wavelength) is shown in Figure 2d and 2e; the 50 km resolution is only possible with piecing together ad hoc studies which cover only small parts of the continent. The USArray will allow an increase in uniform resolution comparable to the 30-km level of topography.

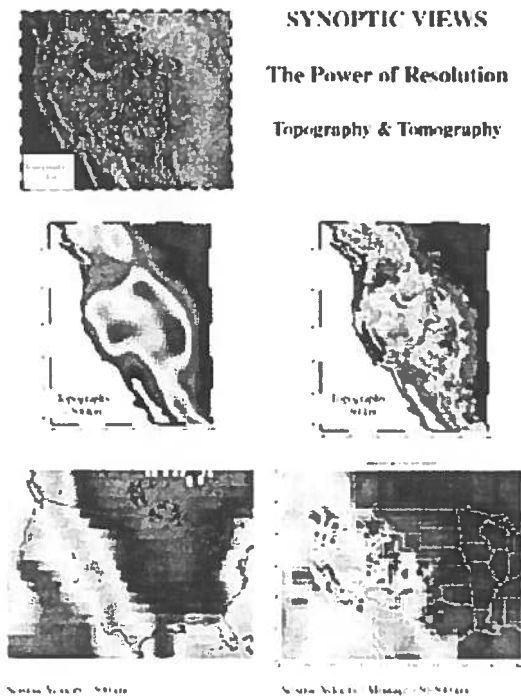


Figure 2. Views of US topography and seismic velocity at 100-km depth. a) Western US topography at 1 km resolution; b) the data of Figure 2a smoothed to a scale-length of 500 km; c) the data of Figure 2a smoothed to a scale-length of 30 km which is the estimated uniform resolution of the USArray in the crust and upper mantle; d) seismic velocity of the US at 100 km depth at the current uniform resolution of about 500 km scale-length; e) seismic velocity at 100 km depth with the best, pieced-together, studies showing non-uniform coverage.(Figure courtesy of Gene Humphreys and David Simpson)

In the Pacific Northwest, the USArray will image the slab of ocean crust descending beneath Cascadia and giving rise to the Northwest's volcanoes and earthquakes. Contrasting structures across the San Andreas Fault system in California reflect the northward motion of the Pacific Plate. Thin hot crust of the Snake River Plain reveals the track of an upwelling mantle hotspot now controlling the thermal activity in Yellowstone. The roots of the Appalachians retain evidence of an ancient mountain chain uplifted by colliding continents similar to today's Himalayas. Hidden beneath the flat expanse of the Great Plains is a piece of ancient oceanic crust, rafted in from the Pacific. From high-resolution imaging of the differences in structure between these diverse tectonic terranes, we will learn much about how continental growth is initiated, how North America evolved, where and how mineral deposits formed, and what controls geologic hazards such as earthquakes and volcanoes.

Project Description

To image the range of structures of different scales and different depths beneath North America will require a wide range of seismological and complementary geophysical techniques. The heart of the USArray facility will consist of two mobile seismic arrays:

(1) A transportable array of broadband seismometers to cover the US with a regular grid of 2000 observation points with 50-70 km spacing between points. A pool of 400 instruments would be able to cover the entire US over an eight-year period; gathering seismic signal from each observation point for durations of 1-2 years as the array migrates over the country. With a spacing of 50-70 km, earthquake waves recorded on this grid at periods of 0.5 to 120 seconds will be able to resolve major features in the crust and upper mantle with resolution on the order of tens of kilometers. At the same time, seismic signals from distant earthquakes will also probe the deepest parts of the Earth, providing increased resolution for imaging structures in the lower mantle and core. In order to complement the imaging capabilities of the seismic array, 50 MT (magnetotelluric) field systems are also incorporated in the transportable array. The MT method depends on measuring natural fluctuations of electromagnetic fields at the Earth's surface. Time variations of magnetic sources that are external to the Earth induce telluric currents in the conducting Earth. These fields diffuse into the Earth and are scattered back from heterogeneities in electrical resistivity. Since resistivity depends strongly on factors such as temperature and fluid content, the MT method is a valuable complement to

seismology for imaging the crust and upper mantle.

(2) A complementary flexible pool of 400 broadband instruments and 2000 short-period (1-50Hz) seismic recording systems will be required to "focus in" on the details of structures of special interest in the continental crust. This flexible pool of instruments will have higher frequency response and can be deployed in tighter arrays configured to fit the imaging requirements of the target of interest. Explosives, in addition to natural earthquakes, can be used to achieve special source configurations as needed.

An example of the interaction between the transportable array and the flexible pool can be illustrated by anticipating the synoptic images from the transportable array as it extends across Wyoming and Idaho, showing a broad arc of low seismic velocities underlying the Snake River Plain and terminating in Yellowstone Park. These low velocities, a signature of heated crust and lithosphere, outline the path of the North American plate as it moved over an upwelling plume of hot mantle (a "hotspot"). Following the analysis of data from the transportable array, instruments from the flexible pool will then be brought in to record both explosive and natural seismic signals in order to probe the structures in much greater detail. It should be possible to track the history of the mantle plume as it has distorted and fractured the crust, producing the volcanic eruptions that flooded the Snake River region and the volcanic and hydrothermal activity in Yellowstone. The flexible pool observations will also provide highly sensitive listening posts that will enable study of the detailed faulting characteristics of the region's numerous earthquakes. Mapping of the earthquake locations and orientations will further refine the structure and dynamics of this unique area of the US and its role in the evolution of the North America continent.

Finally, successful operation of the USArray will depend on the installation of permanent stations to provide fixed reference points for the calibration of the transportable arrays at key locations on the continent. To achieve this, USArray plans to install 25 NSN-quality (National Seismic Network) and 10 GSN-quality (Global Seismographic Network) permanent seismograph installations to form the USArray's reference network. Geodetic-quality GPS (Global Positioning System) receivers will be co-located with the seismic stations at 16 of these installations to provide direct and real-time data on crustal deformation of the continent.

Planning Time Line

Over the past few years, there has been discussion within the geophysics community of the opportunities, scientific and technical, for an initiative to improve the resolution with which the structure of continental lithosphere and mantle can be imaged. The general concepts of USArray were developed in a series of workshops including the 1994 ILIAD Workshop (Investigations of Lithosphere Architecture and Development) and several IRIS (Incorporated Research Institutions for Seismology) sponsored workshops starting in 1994.

More recently, the USArray Workshop of March 15-17, 1999 was attended by 87 participants representing a broad spectrum of earth scientists assembled to discuss the specific scientific, technical, and educational objectives of the USArray facility. A workshop report describing the scientific rationale of USArray, defining its operational components, organizational partnerships, and management structure, and developing timelines for the acquisition of USArray instrumentation and their deployment is due to be submitted to NSF in July 1999. The project descriptions above, as well as the budget estimates given below, are informed by the results of the USArray Workshop.

Estimated Cost Projection

The USArray project can be thought of as a set of two, inward-looking, roving telescopes (the transportable array and the flexible pool) capable of focusing on the continent's internal structure at different acoustic frequencies. Except for installation of stations making up the permanent reference network, the project's budget timeline necessarily differs somewhat from that of the traditional construction projects supported by MRE. The significant investment in instrumentation that is required to reach the steady-state capacity of the transportable array and the flexible pool will dominate costs during the initial stages of USArray. Due to the limited number of enterprises capable of fabricating seismic sensor systems with the stringent specifications required, full instrumentation of USArray will take four years.

Emplacement in the field of the components of USArray requires a number of activities that will start in the first year and continue through the duration of the project. Careful site selection (i.e., choosing the specific locations of individual instruments and/or arrays) and permitting must precede the installation of an instrument array for its operation in a given region of the country. Regional workshops to engage the participation of local scientific, educational and public outreach experts will help the USArray management team in selecting sites and recruiting regional volunteers to help with logistics. The transportable array has been designed so that it can record seismic signals for periods averaging 1.5 years at a total of 2000 sites covering the continent. Limited deployment of field systems begins in year-2 and full deployment capacity is achieved for years 3-10. With the exception of some active source data acquisition for the flexible pool deployments, adequate data accumulation depends on natural earthquake sources. For this reason, an average residence time of 1.5 years per location is desirable.

Continue to: [San Andreas Fault Observatory](#)

Return to: [Table of Contents](#)

Return to: [Overview](#)

B. Stage 1 — USArray and San Andreas Fault Observatory at Depth

San Andreas Fault Observatory at Depth

The San Andreas Fault Observatory at Depth is the second part of Stage I. The objective is to install instrumentation to provide the first at-depth observatory within a major active fault, the San Andreas Fault, at Parkfield, California. A variety of instrumentation types and techniques will be used. The monitoring instrumentation is to be emplaced through a 4.0-km deep drill hole that intersects the San Andreas Fault at the location of the 1966 magnitude 6 Parkfield earthquake shown in Figure 3. At this location, fault slip takes place through a combination of small-to-moderate magnitude earthquakes and aseismic creep. Emplacement of the observatory will be done in two stages. The main hole will be rotary drilled vertically to a depth of ~2.2 km and then deviated through the fault zone at a ~50 degree inclination from the vertical to a final depth of 4.0 km. After two years of monitoring and analysis, four depth intervals will be picked for continuous coring within the fault zone through "windows" cut in the drill casing. A long-term monitoring package will then be re-inserted within the fault zone. The scientific goals are to provide direct observational data on the composition, physical state and mechanical behavior of a major active fault zone at depth as a function of time. Such data will test and constrain a number of hypotheses pertaining to faulting and earthquake generation.

The Need for an Observatory at Depth

An enormous amount of field, laboratory and theoretical work has been directed toward understanding the mechanical and hydrological behavior of faults. But, it is still difficult to differentiate or constrain the broad range of conceptual models for the mechanical behavior of faults at depth. One of the primary causes for this dilemma is the difficulty of either directly observing or accurately inferring physical properties and deformation mechanisms along faults at depth with the relevant rock types, volumes, fluid content, and stresses. We have no direct knowledge of the stress conditions under which earthquakes initiate nor do we know whether, as is often proposed, high pore fluid pressure exists within the San Andreas fault zone at depth or if variations in fluid pressure with time affect fault behavior.

Intensive downhole geophysical measurements and long-term monitoring are planned within and adjacent to the active fault zone. Monitoring experiments will include nearfield, wide-dynamic-range seismological observations of earthquake nucleation and rupture and continuous monitoring of variations in pore pressure, temperature and crustal deformation during the earthquake cycle. We hope to directly evaluate the roles of fluid pressure, intrinsic rock friction, chemical reactions, in situ stress and other parameters in the earthquake generation process. In this way, we can provide earthquake researchers with the opportunity to simulate earthquakes in the laboratory and on the computer using realistic fault zone properties and physical conditions.

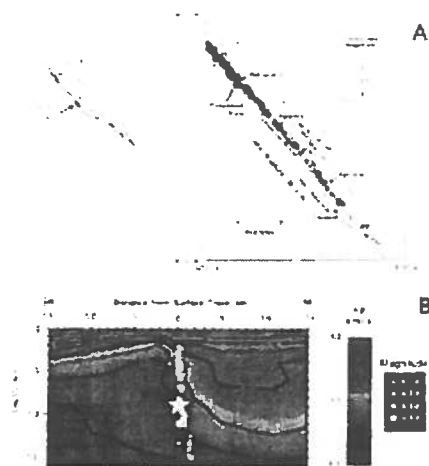


Figure 3. A) Earthquake locations at Parkfield from 1984-1990, together with the location of the proposed drill hole. The 1966 $M=6.0$ earthquake initiated directly beneath the proposed drillsite and ruptured toward the south, stopping near the town of Cholame. B) Southwest-northeast cross section through the proposed drillsite, showing hypocenters of background microearthquakes (circles) and the 1966 $M=6.0$ mainshock (star) together with P-wave velocities from a tomographic inversion by Michael and Eberhart-Phillips (1991). (Figure from M.D. Zoback, S. Hickman and W. Ellsworth, personal communication, 1999.)

Planning and the Diverse Science Team

While the idea of instrumenting the San Andreas Fault has arisen many times over the past several decades, this project had its origin in December of 1992 when a workshop was convened with support from NSF. 113 scientists and engineers from seven countries attended the workshop. Its purpose was to initiate a broad-based scientific discussion of the issues that could be addressed by direct experimentation and monitoring within the fault at depth, to identify potential sites, and to identify technological developments required to make the construction and drilling possible. The fundamental scientific issue addressed in this effort, obtaining an improved understanding of the physical and chemical processes responsible for earthquakes along major fault zones, is clearly of global scientific interest. Throughout the planning process leading to the development of this proposal, the US scientific community has invited participation by scientists from around the world, especially through the International Continental Drilling Consortium.

A proposal was submitted in January 1999 to NSF to accomplish the goals of the San Andreas Fault Observatory at Depth. At the present, the science team includes 33 principal investigators from 19 US universities, about 15 scientists from the US Geological Survey, several scientists from Lawrence Berkeley and Lawrence Livermore National Laboratories of the US Department of Energy and scientists from 12 institutions in 4 foreign countries.

Choice of the Parkfield Site

After consideration of all the candidate sites for this first at-depth fault observatory, the scientific community chose the Parkfield location through a consensus process involving preliminary site-characteristic studies and numerous workshops. The site is intensively studied geologically and geophysically, has shallow seismicity within reach of the projected observatory depth, and is now under permit for at least 20 years of scientific monitoring.

Construction-stage Work Plans

The plan of work during construction is divided into four categories: 1) downhole measurements, 2) measurements on core, cuttings and fluids, 3) geophysical and geological site characterization, and 4) fault zone monitoring.

Downhole measurements include logging while drilling, open hole geophysical logging, cased-hole logging, and stress, pore pressure and permeability measurements coupled with fluid sampling.

Measurements on core, cuttings and fluids include studies on the mineralogy, deformation microstructures, physical properties, and constitutive behavior of

rock samples recovered from the San Andreas zone and country rock at depth. Other studies are aimed at studying the chemical and isotopic composition of fault zone fluids and gases.

Extensive geophysical and geological site characterization studies have already been done during the site selection process. Further studies, with the use of the downhole seismometers and the USArray concentrated network at the surface, will be aimed at providing a high-resolution image of the earthquakes and physical environment of the fault zone and upper crust beneath the drill site. These projects will address two main objectives. The first is to provide technical information that is critical to the siting and drilling of the borehole, including the precise location of earthquake foci that will be intersected and the presence of geological complications to avoid. The second is to create a comprehensive structural and physical model of the fault zone. Detailed knowledge of the physical environment of the fault will be essential to the interpretation of structures and properties observed in the borehole for the ultimate decision of positioning four offshoot core holes and their related monitoring instruments.

The goal of the fault zone monitoring work is twofold: 1) to make in-situ measurements of deformation, pore pressure, seismic wave radiation and other relevant parameters in the nearfield of earthquakes, and 2) to select the optimal intervals for instrumentation and sampling, such as continuous coring through the fault zone. It is expected that the instruments will catch multiple earthquake cycles for repeating earthquakes ($M \sim 2$ or larger) in the target zone at distances of less than a few hundred meters to about 1.5 km over a 20-year lifetime of the experiment. With luck, they may catch the rupture process of the fault in a large-magnitude event over this same time period.

After the first stage of the construction program when the main observatory is completed, a 2-year-long period of intensive monitoring will be done using a re-deployable monitoring array shown schematically in Figure 4. The array will consist of seismometers, accelerometers and a fluid pressure monitor. The removable monitoring array will be pulled out of the borehole after about 1 year to conduct a high precision-borehole directional survey and ultrasonic cement imaging (USI) log. The USI log identifies any changes in casing shape or the cement bond integrity behind the casing. This will determine if the faults crossed by the hole are actively creeping, or if broad-scale deformation is occurring. Repeat measurements of casing ovality and trajectory over time using casing shape logs and gyroscopic directional surveys similar to those proposed here have identified casing offsets as small as 1 cm over a 5-m-wide shear zone. Following the completion of coring, the borehole will be re-instrumented with a modified borehole array that will be augmented with additional pressure transducers, a borehole strainmeter and other sensors.

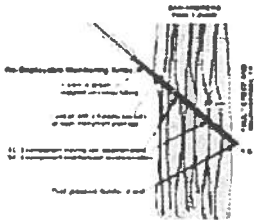


Figure 4. Schematic illustration of the fault zone monitoring string in place in the proposed 4-km-deep San Andreas Fault Observatory at Depth. Although not shown here, additional sensors in the instrument package will monitor borehole deformation and/or tilt. The monitoring string is designed so that it can be removed for instrument repair and maintenance and so that the cased hole can be repeatedly logged for deformation induced by ongoing fault creep and/or earthquakes. (Figure from M.D. Zoback, S. Hickman and W. Ellsworth, personal communication, 1999.)

Technology at High Pressures and Temperatures

The San Andreas Fault Observatory at Depth is intended to stand on its own scientific merits. However, it is also an important step toward conducting a more ambitious program of deeper (~ 10 km) sampling and monitoring that reaches further into the active seismic zone. The seismogenic zone of the San Andreas Fault extends to 20 km in some regions. The technological challenges amplify greatly with depth because of the effects from the high pressures and temperatures encountered. The 4-km monitoring effort will contribute to the development of technology in drilling and instrumentation to extend our capability to deeper depths.

Coordination with USArray

One of the goals of the San Andreas Fault Observatory at Depth is to use the strong geometry of the deep seismometer string in coordination with the surface USArray instruments to construct a very-high-resolution tomographic picture of the San Andreas Fault at Parkfield and the surrounding areas. Even though the San Andreas Fault at Parkfield is one of the most intensively studied fault sites in the world, the site's earthquake locations still have large uncertainties due to the strong lateral velocity contrasts as a result of materials on either side of the fault. The combination of the dense surface spacing of the USArray instruments and the deep emplacement of seismometers in the fault will resolve this question. The array combination will simultaneously be locating small earthquakes with unprecedented accuracy along the fault. The resulting detailed 3-D rheology from the tomographic inversion and earthquake locations will be used in dynamic computer models of faulting and strong motion calculations.

Timetable and Hole Design

Pre-project Site Characterization. A variety of site characterization studies near the proposed observatory have been going on for the past several years under support of NSF and the USGS. For example, Figure 5 shows a resistivity cross-section across the fault along with a schematic of the proposed observatory. The next significant set of studies at the site began in 1998. First, a 7-km long high-resolution seismic reflection profile was shot across the observatory site and fault zone with support of the USGS. Twelve portable reflection seismographs were used with 700 channels of seismometers along a dense, fault crossing profile with 10-m spacing. The main goals of this experiment were to refine the picture of near-surface geology in the observatory area, and to assure that the site is not located directly above small-scale secondary faults which might needlessly complicate drilling at shallow depth. The second site characterization study will be to deploy a number of additional seismographs in the region surrounding the site for earthquake monitoring.

2001/Year 1. Construction, downhole measurements and casing of the main hole are scheduled to commence in late 2001 and end in early 2002. The recently developed capability of the petroleum industry to drill "multi-laterals" — satellite wells which are emplaced from a single "parent" well — has enabled a simplification of the project strategy not previously available. Earlier strategies included the necessity to continuously core an inclined hole across an entire fault zone. As the fault zone is likely to be severely crushed and altered to gouge, as well as potentially over-pressured; this was a formidable challenge. This is especially true with the requirement of maintaining a sufficient hole diameter to conduct the necessary downhole measurements and deploy fault zone monitoring instrumentation after casing the hole. With the new "multi-lateral" strategy, a rotary drilled "main hole" can penetrate the entire fault zone. Geophysical logging, casing and cementing of such deviated holes are now routine procedures in the petroleum industry, even in poorly consolidated and overpressured formations. After appreciable study of the results from the main hole, we will emplace four continuously cored "multi-laterals" off of the main hole at carefully selected locations, as outlined below.

2002/Year 2. Fault zone monitoring begins in 2002 and goes on for 2 years. Measurements on core and cuttings will begin as well as analyses of borehole geophysical data.

2003/Year 3. Fault zone monitoring and measurements on core and cuttings continue. A comprehensive suite of site characterization studies is begun in coordination with the USArray instrumentation.

2004/Year 4. Data from site characterization and fault zone monitoring are analyzed. A comprehensive analysis of all available data will be used to pick intervals for continuous coring. Continuous coring within the fault zone will be carried out at four depth intervals through "windows" cut in the casing. The seismicity rate in the area is such that after 2 years of fault zone monitoring, there should be a sufficient number of shallow earthquakes near the observatory hole to accurately locate the active fault trace(s) using the clamped seismometer array in the borehole. This information, when combined with the geologic data from spot cores and cuttings, geophysical logs, downhole measurements, fluid and gas chemistry data, pore pressure and in situ stress measurements and the results of site characterization studies will enable the science team to determine the optimal intervals for continuous coring. As a result of this strategy, each core will be interpretable in terms of its proximity to active fault traces, the composition and physical properties of the fault zone, pore pressure, and stress, etc. A comprehensive scientific measurement program is planned for the exhumed core. Following core retrieval, the core holes will be lined with uncemented perforated casing and used for monitoring fluid pressure at depth.

2005/Year 5. When coring activities have been completed at the site, a permanent monitoring string will be deployed in the hole so that the hole can be utilized as a continuous fault zone observatory well into the future. Investigations of core samples are underway.

2006/Year 6. Data analysis and measurements on core are completed. Fault zone monitoring continues.

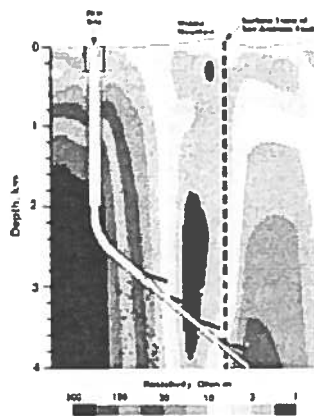


Figure 5. Resistivity structure of the primary drill site based on inversion of continuous magnetotelluric data. (Martyn Unsworth, pers. comm. 1988; see also Unsworth et al., 1997). The proposed drill hole is also shown along with earthquake hypocenters (crosses from Michellini and McEvelly, 1991; circles from Eberhardt-Phillips and Michael, 1991). (Figure from M.D. Zoback, S. Hickman and W. Ellsworth, personal communication, 1999.)

References

- Eberhart-Phillips, D., and A.J. Michael, Three-dimensional velocity structure, seismicity and fault structure in the Parkfield region, central California, *J. Geophys. Res.* , 98, 15737-15758, 1993.
- Michael, A.J., and D. Eberhart-Phillips, Relations among fault behavior, subsurface geology and three-dimensional velocity models, *Science* , 253, 651-653, 1991
- Michellini, A. and T.V. McEvelly, Seismological studies at Parkfield. I. Simultaneous inversion for velocity structure and hypocenters using cubic B-splines parameterization, *Bull. Seis. Soc. America* , 81, 524-552, 1991.

Return to: [Table of Contents](#)
Return to: [Overview](#)
Return to: [USArray](#)

SCEC Outreach Program Overview

Jill H. Andrews and Mark Benthien
SCEC Outreach Office

Mission and Goals

The SCEC Outreach mission is *to promote earthquake loss reduction and lifelong learning by engaging the public at large in activities that focus on earthquake-related education, research-based technology development and transfer, and systemic reform.*

We have divided our efforts into three programmatic categories: *Public Awareness, Formal and Nonformal Education, and Knowledge Transfer.*

A Mutually Influencing Network
to Promote Earthquake Education and Outreach



Figure 1.

PUBLIC AWARENESS

Our public awareness programs target civic groups and professional organizations, media reporters and writers, and the general public.

- The SCEC Web site (www.scec.org)
- EqIP and EQNET (www.eqnet.org)
- The SCEC Quarterly Newsletter

- “Putting Down Roots in Earthquake Country” (3 million copies disseminated throughout southern California)
- Neighborhood Earthquake Watch & Community Guidebook
- Contact with media reporters and writers and the general public (*Earthquake Preparedness Month, LA Underground radio spots / book / game, Teachable Moment Initiative, Earthquake Studies and the Civic Scientist*)
- Video development / Seismic Sleuths with AGU, FEMA, CEA, CA Dept of Insurance, IBHS – Summer Productions / Discovery Channel: Pilot due April, 2000

EDUCATION

Our programs target students and educators, museums, building industry professionals, insurers, urban planners, code officials, public policy makers, and emergency planners and responders.

- SCEC Summer Intern Program
- Resource for Middle Schools and High Schools
- Development of earth science education modules through Development of Earth Science Curricula On line (DESC On-line):
- Investigating Earthquakes through Regional Seismicity
<http://www.scecdc.scec.org/Module>
- Exploring the Use of Space Technology in Earthquake Studies
<http://scign.jpl.nasa.gov/learn>
- Partnerships with professional educators from K-12 Alliance, California Science Implementation Network (CSIN), L.A. Educational Partnership (LAEP), and L.A. County Office of Education (LACOE).

- Science curriculum development / enhancement through LACOE's South East Educational Technology Consortium (covers a student population of about 200,000 or 13% of L.A. County's total student body)
- Field trips to local faults; Museum lectures, exhibit development, patron field excursions (under development).
- Consultation / resource to San Francisco Exploratorium for "Fault Line" Webcasting project, to be aired October 1999
- Civic group presentations, participation at annual conventions and conferences.

KNOWLEDGE TRANSFER

Our Knowledge Transfer programs target technical professionals, geotechnical and structural engineers, engineering geologists and seismologists, and scientists and engineers in academia and government.

- Los Angeles City / SCEC / SEAOSC Ground Motion Joint Task Force: workshops, technical publications on liquefaction, ground motion; public awareness booklets on vulnerable buildings.
- Post-Earthquake Technical Clearinghouse working group.
- SCEC-LANL partnership to provide a set of science- and technology-based computational tools that will include real-time feedback for disaster planning, training, and management in time of crisis and long-term recovery.
- "Real Meaning of Seismic Risk" workshop series in collaboration with LA County Emergency Preparedness Commission, BICEPP.
- Workshops for insurers to address topics such as the California Earthquake Authority; outcomes of the WSSPC Insurance Summit; and how to use new hazard maps and other mapping products (HAZUS, DMG, EPEDAT, ZOD depictions).

- *CUREe / PEER / MCEER / MAE / SCEC Lectures* for earthquake engineering and earth science students and professionals to address joint concerns and issues relating to state-of-the-art practice in both disciplines.
- *Earthquake Hazard Mitigation of Woodframe Construction* - Outreach management for the 3-year FEMA-funded project.
- SCEC Science Seminars and Workshops (8 per year)

1999 SCEC Science Abstracts

Transient Strain Events on the Southern San Andreas Fault

Duncan Carr Agnew and Frank K. Wyatt
University of California, San Diego

The southernmost section of the San Andreas Fault, in the Coachella Valley in southern California, is known to undergo creep at the surface and has produced episodic creep in some locations. We operate two long-base laser strainmeters at Durmid Hill, near the southern end of this section of the fault, where it terminates against the Brawley Seismic Zone. One of these instruments is a fully-anchored system 524 m long, and oriented NS (45 degrees to the local fault strike); the other is a more temporary installation 304 m long, oriented perpendicular to the fault, NE-SW. On days 198 and 199 of 1999 we observed three rapid changes on the two sensors (which share only line power and a datalogger). These events had durations of about 10 minutes, and amplitudes of up to 40 nanostrain, with predominately extensional strain change. Auxiliary recordings show no meteorological disturbances on these days. Several field checks for cracking along the fault trace did not provide clear evidence for surface slip on the fault near the sensors, though slippage of less than a few millimeters would be hard to identify in the unconsolidated surface material. The ratio of strain on the two instruments was not the same for the three events (indeed the smaller second event was not obvious at all in the NE-SW recording); if this reflects the true strain, this complexity implies that the source area(s) must have been on the portion of the fault very close to the strainmeters. This section of the fault has very low reported creep rates. Simple modeling shows that a slip of 1 mm on a 1-by-1 km patch would be sufficient to cause the largest of the signals seen. Two similar strain transients (amplitude 27 nanostrain) were seen on the NS instrument in early 1997, but as this was before the other instrument was running, we could not then be as confident that this reflected true ground deformation.

New Results for Toppling Accelerations and Site Conditions at Precarious Rock Locations in Southern California

Rasool Anooshehpour and James N. Brune
University of Nevada, Reno

Field measurements of the quasi-static toppling accelerations of precariously balanced rocks can provide constraints on the peak ground accelerations experienced during previous earthquakes at those locations. The quasi-static toppling acceleration is determined by the ratio of the maximum of a slowly varying horizontal force through the center of mass and the estimated mass of the rock. Measurements of the quasi-static toppling accelerations for five rocks in the San Gabriel Mountains, at a distance of 15 km from the San Andreas Fault, have been completed. The quasi-static toppling accelerations range from 0.3 g to 0.4 g. As a first order approximation, we use results from previous studies to estimate the dynamic toppling peak ground accelerations for a time history with the same shape as the N-S component of the 1940 El Centro accelerogram by increasing the quasi-static toppling acceleration by 30%. The resulting constraint on peak ground accelerations is about 0.4 g.

As part of our study we have deployed three-component digital stations at Lovejoy Buttes, and at Piute Butte in Mojave Desert, near the San Andreas fault to investigate any anomalous site conditions at the location of precariously balanced rocks. We have recorded numerous local and regional earthquakes in the past year. In particular, we have recorded several small earthquakes on the San Andreas fault near Lovejoy Buttes. Preliminary studies of these small earthquakes recorded at Lovejoy Buttes indicate a simple pulse-like S-waves with relatively low scattering, low attenuation and no evidence of site resonances, thus suggesting no obvious anomalous site conditions at that location.

Continued Improvements to the UCSB Strong Motion Database

Ralph Archuleta, Alexei Tumarkin, and Grant Lindley
University of California, Santa Barbara

Improvements to the UCSB Strong Motion Database (<http://smdb.crustal.ucsb.edu/>) are continuing to be made. Over the last year, the database has been improved in access speed, amount of data available, display of information on Web pages, and in its access methods.

The database now contains 7061 strong motion traces, up 27% from last year. The new data includes records from the Guerrero Gap in Mexico recorded by the University of Nevada, Reno, from the Kyoshin Net in Japan, from the 1985 Valparaiso earthquake and its aftershocks, and from several Alaskan earthquakes. A new map access method has been added to the database, allowing earthquakes and stations to be selected from dynamically created maps. This new method may be accessed from the SMDB home page.

Improvements to the display of information on the Web pages have also been made. Sensor locations are now shown routinely on most query results pages. This is especially important for sites that have multiple instruments such as dams or office buildings. Additional pages have also been added to the database. These pages include pages showing recent changes or additions to the database, a page listing all agencies that have contributed data to the database, and a page describing how to use the Web site.

Finally, improvements to the code used to access the database through the Web site have significantly decreased query times by as much as half. For example, a query returning all of the data in the database for the 1994 Northridge earthquake has been reduced from 15 to 7 seconds.

The database continues to see heavy use. Over the last year there have been 97,000 Web pages downloaded (265/day), 2450 MB of strong motion data downloaded from UCSB (7 MB/day), and 3919 strong motion data files downloaded from outside FTP and Web sites via the Strong Motion Database (11 files/day).

ON ATTRIBUTING THE SHORTENING AND THICKENING OF METROPOLITAN LOS ANGELES OBSERVED AND INFERRED USING GEODESY TO DEEP FAULT SLIP

Donald F. Argus, Michael B. Heflin, Andrea Donnellan, and Frank H. Webb
Jet Propulsion Laboratory

Geodetic observations from the Southern California Integrated GPS Network (SCIGN) are providing information on the buildup of elastic strain in and near metropolitan Los Angeles. Here we determine the velocity field in southern California using permanent and campaign Global Positioning System (GPS), very long baseline interferometry, satellite laser ranging, and trilateration geodesy. Northern metropolitan Los Angeles is observed to shorten from north-northeast to south-southwest at ~ 5 mm/year. The rate of shortening is highest immediately south of the southern front of the San Gabriel mountains in a belt a few km to 40 km wide running from the Ventura Basin across the San Fernando valley to the western San Gabriel valley. The gradient in fault-parallel motion across the Mojave segment of the San Andreas fault indicates the fault is locked to a depth of 20 ± 3 km and has a deep slip rate of 25 ± 3 mm/yr (95% confidence limits).

The lithosphere on either side of the San Andreas comprises two distinct blocks, the west Mojave desert and the San Gabriel mountains, that are rigid aside from the elastic strain due to locking of the San Andreas. Aside from the San Andreas fault elastic strain, metropolitan Los Angeles is observed to be not lengthening from east to west. Therefore the shortening is being taken up by crustal thickening. Here we attempt to use the geodetic observations limit the deep slip rate along known faults in the shortening belt. The motions generated by shallow locking and deep slip along the Sierra Madre, Verdugo Hills, Raymond, Elysian Park, and Puente Hills faults will be calculated and compared with the observed velocity field.

Active Tectonics of South Mountain Anticline and Buried Oak Ridge Fault, Near Ventura, CA

Antonio Azor# and Edward A. Keller, University of California, Santa Barbara
#Permanent address: Universidad de Granada, Granada, Spain

South Mountain is an antiformal ridge, forming above the active, buried Oak Ridge reverse fault. Rocks affected by the fold range in age from the Oligocene (Sespe Formation) to the Upper Pleistocene (Saugus Formation) (Dibblee, 1992). Accordingly, the fold must have formed in the last 0.5-0.6 Ma at an estimated slip rate for the Oak Ridge fault of 5.9-12.5 mm/yr (Yeats, 1988). Geodetic observations suggest a 6 mm/yr rate of north-south shortening for the block located between the Oak Ridge and San Cayetano faults (Argus et al., 1999). Although no historic earthquakes have occurred on the western Oak Ridge fault, it represents a potential serious source of future seismicity in the populated Santa Clara valley area for towns and cities including Santa Paula, Fillmore and Ventura.

We test the hypotheses that 1) there are systematic variations in active tectonics processes along the South Mountain Antiform and that 2) the antiform is propagating laterally to the west.

We interpret the available geomorphic data and observations as supporting the hypotheses that active tectonic processes are systematically variable along the South Mountain - Oak Ridge Antiform; and the antiform is propagating laterally to the west. Assuming lateral propagation is occurring, fold length is about 35 km, and fold growth began after deposition of the Pleistocene Saugus Formation (about 0.5 to 0.6 Ma), then we calculate a rate of lateral propagation of folding at 6 to 7 cm/yr.

LARSE II SANTA MONICA HIGH RESOLUTION SEISMIC SURVEY

Shirley Baher and Paul Davis, University of California, Los Angeles
Gary Fuis, U.S. Geological Survey, Menlo Park
Robert Clayton, California Institute of Technology

Santa Monica sustained concentrated damage from the anomalous amplification of seismic energy during the 1994 Northridge earthquake. Several hypothesis have been developed to explain the high amplitudes of ground motion. These include 1) focusing by a deep geological structure which acted like an acoustic lens, 2) a combination of focusing and shallow basin effects, 3) shallow (less than 1 km) basin edge effects involving constructive interference of surface and body waves.

Part of LARSE (Los Angeles Region Seismic Experiment) involves a high resolution seismic survey, designed to test the deep basin focusing hypothesis against the alternative models. The experiment takes place during October 1999 and includes a refraction and Vibroseis reflection experiment.

The refraction experiment involves recording shots by a total of 225 portable stations, deployed in two linear arrays and a cluster of stations. The first array extends N-S through the high damage zone with an additional cluster at the hypothesized location of the lens. The second array extends N-S through the non-damaged zone. The Vibroseis reflection experiment will consist of a 10 km line along the first array.

Frequency-Size and Temporal Statistics of Earthquakes in a Regional Lithospheric Model for Coupled Evolution of Earthquakes and Faults

Yehuda Ben-Zion, University of Southern California
Vladimir Lyakhovsky, The Hebrew University, Jerusalem, Israel

We study the coupled evolution of earthquakes and faults in a model consisting of a seismogenic upper crust governed by damage rheology over a viscoelastic substrate

[Lyakhovsky et al., sub. to JGR, '99; Ben-Zion et al., EPSL, '99]. The simulated earthquake statistics depend on the space-time window of the observational domain, i.e., the model response is non-ergodic. The results indicate that high ratio of time scale for damage healing τ_H to time scale for tectonic loading τ_L leads to the development of geometrically regular fault systems and the characteristic frequency-size (FS) earthquake distribution. Conversely, low ratio of τ_H/τ_L leads to the development of a network of disordered fault systems and the Gutenberg-Richter FS statistics. For intermediate ratios of τ_H/τ_L the results exhibit alternating overall switching of response, from periods of intense seismic activity and characteristic earthquake statistics to periods of low seismic activity and Gutenberg-Richter statistics. These results are compatible with fault-trace and earthquake statistics data of Wesnousky [BSSA, '94], Stirling et al. [GJI, '96], and Marco et al. [JGR, '96], and with corresponding simpler simulations on heterogeneous planar faults of Ben-Zion and Rice [JGR, '93, '95], Ben-Zion [JGR, '96] and Dahmen et al. [PRE, '98].

In the energy-time domains we attempt to understand properties of accelerated moment release (AMR) and establish connections between AMR and FS statistics. Various observational studies [e.g., Bufe and Varnes, JGR, '93; Bowman et al., JGR, '98; Vere-Jones et al., ms. '98, Yang and Ma, A. S. Sinica, '99] indicate that large earthquakes are sometimes preceded by a phase of AMR. This has been quantified by fitting a power law time-to-failure relation $A + B(t_f - t)^m$ to cumulative Benioff strain in a region. Observed values of m are typically in the range 0.2-0.4. The damage rheology model of Lyakhovsky et al. [JGR, '97] leads with a straightforward analytical derivation to a power law time-to-failure relation with exponent $m = 1/3$. Statistical analyses of synthetic catalogues generated for various realizations of our regional lithospheric model, producing the characteristic FS statistics, Gutenberg-Richter statistics, and mode switching activity, show that AMR exists *only* when the FS statistics of earthquakes before the large event follow the Gutenberg-Richter distribution. In such cases the exponent in the power-law time-to-failure equation is $m = 1/3$, in agreement with the analytical derivation. The AMR is accommodated by increase of both the average rate of events and average earthquake size (compatible with increasing a -value and decreasing b -value of the Gutenberg-Richter relation). The former and latter increases occur in the simulations over 5-10 years and 1-3 years before t_f , respectively. The lack of AMR in portions of seismicity not following the Gutenberg-Richter statistics may explain why some large earthquakes are preceded by AMR and some are not.

Inversion of Seismic Fault Zone Waves in the Rupture Zone of the 1992 Landers Earthquake for Velocity Structure at Depth

Yehuda Ben-Zion and Zhigang Peng, University of Southern California
 Andrew J. Michael, United States Geological Survey/Menlo Park
 Heiner Igel, Ludwig-Maximilian Universitaet, Muenchen

Waveform modeling of seismic fault zone (FZ) trapped waves provides a potentially high resolution means of investigating seismic velocities, seismic attenuation, width of FZ, and structural continuity at depth. The 1992 Landers aftershock sequences generated a wealth of seismic data. From a digital waveform data of 238 Landers aftershocks [William Lee, per. Com., '99], we identified about 30 events with good candidate trapped waves. These are generated for cases when both the event locations and receivers are close to or in the FZ, and the S-P time is smaller than about 3 seconds. Most of the trapped wave energy is in the 3 to 6 Hz frequency range.

The FZ waveforms are modeled with a genetic inversion algorithm that maximizes the correlation between observed and synthetic waveforms [Michael and Ben-Zion, ms. in prep., '99]. The synthetic seismograms are generated with a two-dimensional analytical solution for a scalar wavefield in a layered vertical FZ between two quarter-spaces [Ben-Zion and Aki, BSSA, '90; Ben-Zion, JGR, '98]. Inversion results for a single waveform indicate that it is possible to find a good fit for the structure between the generating source and receiver assuming a single FZ layer in a half space. The model FZ layer is characterized by a width of

150-200 m, shear wave velocity of 1.5-2.0 km/s, and shear wave Q of about 50. The half space has a shear wave velocity and attenuation coefficient of 3.1 km/s and 200, respectively. These results are compatible with those obtained by Li et al. [JGR, '94]. Our study also show, however, that it is possible to get equally good fits for a wide range of parameters, due to significant trade-offs between FZ width, propagation distance along the fault, source offset from the fault, velocity contrast, and attenuation. The problem may be overcome or reduced by modeling many waveforms simultaneously and incorporating in the inversion additional seismic phases. Work in this direction is underway.

Complementary to the genetic inversion analysis, we have been working toward developing an accurate three-dimensional computational ability for modeling seismic fault zone waves in structures with material and geometrical variations along strike and with depth. Following the previous related calculations of Igel et al. [GJI, '97], the method is based on a high-order staggered-grid finite-difference scheme. Work in this direction focused so far on verifying the accuracy of the numerical calculations against analytical solutions for waves generated by a point-dislocation along a material interface [Ben-Zion, GJI, '90, '99]. We have not yet been able to obtain satisfactory numerical solution close the material interface, but we anticipate succeeding in the near future. When this is accomplished, clear remaining features of the Landers FZ waveform data (if any), not accounted for by 2D piece-wise modeling with the genetic inversion, will be modeled with 3D finite-differences simulations.

Acknowledgment: We thank Willie Lee from the U.S.G.S., Menlo-Park, for providing us with the waveforms used in this work.

Reconstruction of Trench Logs as a Test for Interpreted Paleoseismic Events

Natanya Black, University of California, Santa Barbara
SCEC Summer Intern

A trench on the left-lateral Garlock fault has exposed a remarkable section of playa sediments that has provided an extended record of mid-late Holocene earthquakes for the central segment of this fault. This work in progress is a continuation of a study initiated and published by McGill and Rockwell (1998) at the El Paso Peaks site, with the intent of 1) Extending the record of paleoearthquakes at this site, by identifying additional event horizons in deeper parts of the stratigraphic section, and 2) Reevaluating evidence for paleoearthquakes previously identified in the original trench.

In order to reconstruct the paleoseismic history at this site, the stratigraphy and structural relationships must be correctly interpreted. The basis of this study is to test the interpretations made in the field using logs generated at the El Paso Peaks trench site. By reconstructing a cross-section of the trench wall at each event horizon, any misinterpretations of the paleoseismic record can be discovered if mismatches occur in the stratigraphy. This is done through removing the deformation caused by the event by "back slipping" and unfolding the stratigraphy affected by an individual event. If the event horizons have been interpreted correctly, then each reconstruction should produce fairly continuous stratigraphy below the reconstructed event horizon, but above the next older event. If the reconstruction does not produce a reasonable cross-section, then further interpretation is needed to discover whether the discrepancy is due to a change in unit thickness from lateral slip, or from a misinterpretation of the paleoseismic record, possibly the result of an unidentified paleoearthquake.

So far, six well-documented events have been interpreted in the stratigraphic record exposed at this site. Events W, U, Q, R, K, and F (in order of youngest to oldest) were identified in the field through observations of increasing/decreasing displacement, upward terminations, folding, and fissure-fills. These were selected as candidate events to use as a basis for the reconstructions. The first step was to construct a photomosaic of the trench exposure by scanning and rectifying each photograph to remove distortion caused by the camera lens. The images were then assembled in a computer into a larger photomosaic of the entire trench wall .

On the final mosaic units, faults, event horizons, and burrows were drafted on to the log in a separate artwork layer. Key units were highlighted so displacements could be followed easily. The first reconstruction was of the most recent paleoearthquake, event W. The continuous sediment overlying the event horizon was removed and the faulted units below the event were backslipped. The process was repeated for each older event.

By removing vertical deformation and folding from the four most recent events, most of the vertical component of deformation has been removed and no obvious mismatches in stratigraphy exists. This suggests that the events interpreted thus far are correct since no major mismatches have occurred in the stratigraphy. The remaining two events show only minimal displacement and folding which suggests that no additional events can be resolved through this retrodeformation technique.

Activities at the Scripps Orbit and Permanent Array Center

Y. Bock, J. Dean, P. Fang, P. Jamason, H. Johnson, M. Scharber,
M. van Domselaar, and J. Gonzalez¹
Scripps Institution of Oceanography, ¹Visiting from CICESE

The Scripps Orbit and Permanent Array Center (SOPAC) was established to support continuous GPS for the study of crustal deformation in southern California. SOPAC currently maintains and downloads data from 28 of the SCIGN sites, and archives and disseminates raw and RINEX data for the nearly 150 SCIGN sites. In addition, SOPAC archives RINEX data from over 400 other permanent GPS, including the IGS, CORS, BARD, BARGN, and PANGA networks. SOPAC also archives precise ephemerides, navigation, and meteorological data. The capacity of the archive totals over 700 GB allowing all data to be on-line. The total file transfers per month to the GPS community average 200,000 and are increasing steadily. The daily site positions for SCIGN are estimated with the GAMIT/GLOBK software and post-processed to produce time-series for studying the crustal deformation cycle and learning more about GPS error sources. SCIGN related activities at SOPAC highlighted in this poster include:

Data Archiving

- I. Access statistics for SCIGN and other Western U.S. array data
- II. SOPAC's Relational Data Base Management System

Web Page Tools

- (1) SIMpl: Site Information Manager
- (2) Velocity Map Generator
- (3) GPS Positioning Service

Other Activities

- Establishment of SCIGN sites in Baja California (CICESE)
- The California Spatial Reference Center (<http://csrc.ucsd.edu>)

Comparison of Hysteresis Models and Their Effects on Earthquake Strong Ground Motions

L.F. Bonilla, D. Lavallee, and R.J. Archuleta
University of California Santa Barbara

Implementation of hysteretic behavior (also known as the memory effect) in nonlinear soil rheology is often based on a set of empirical rules; common examples include the Masing rules (with or without the extended Masing Rules) or variations of these rules. These rules prescribe when the actual path in the stress-strain space (given by the values of the stress and the strain at a given time in the current cycle) must jump to another path or when it must return to a path visited in a previous cycle. The interplay between these rules ensure that the stress-strain

paths will be constrained on loops of different sizes that intersect one to another. Using the hyperbolic model to describe the anelastic properties of soil, we compared three formulations of hysteretic behavior: a description given by the Masing and extended Masing rules, a description given by the Cundall-Pyke hypothesis, and a description given by a new hysteresis model, the Generalized Masing rules. This new formulation, based on the classical Masing rules, has several features. It has a functional representation; it depends only on one parameter related to the amount of energy dissipated through the nonlinear property of the material; and it includes the Cundall-Pyke hypothesis as a special (or limit) case. The free parameter controls the intersection where the paths intersect in the stress-strain space. The shape and the size of the loops in the stress-strain space vary with the values of this parameter. For each formulation, we analyze the behavior of the strain and stress relationship under simple physical situations corresponding to simple laboratory loading and also for complex situations reproducing earthquake accelerograms. These numerical investigations suggest the following conclusions. The Generalized Masing rules provide a better description of soil behavior. The intermittency behavior and the observation of spiky waveforms in the signals depend on the free parameter characterizing the Generalized Masing rules. Finally, the Cundall-Pyke hypothesis produces the largest modulus reduction and a greater hysteresis damping of the signal.

Gutenberg-Richter Statistics and Accelerating Moment Release During the Seismic Cycle

David D. Bowman and Charles G. Sammis
University of Southern California

Recent years have seen the proliferation of models describing the evolution of the stress field and concurrent seismicity over long time and distance scales using the language of statistical mechanics. These hypotheses which link earthquakes and the stress field to critical phenomena belong to a new class of models called intermittent criticality. In this viewpoint, earthquakes are the result of a process of stress redistribution in which the crust spontaneously evolves towards a critical state (analogous to Self-Organized Criticality). However, in intermittent criticality large earthquakes produce strong perturbations in the stress field which disrupt the self-organization process and move the system away from criticality. A common prediction of these models is a period of accelerating seismic moment release before large earthquakes, an observation which has received considerable attention from a number of workers in recent years. In models of intermittent criticality, the predicted accelerating moment release is caused by intermediate-magnitude events. These events occur due to the growing correlation length of the stress field as the region approaches criticality. This phenomenon can also be observed by monitoring the Gutenberg-Richter frequency magnitude statistics in the region. This model does not predict temporal variations in the b-value during the course of the seismic cycle. Rather, the approach to criticality is characterized by an increase in the maximum magnitude of seismicity with a small corresponding fluctuation of the a-value. In this poster we document these variations before and after several large earthquakes in southern California and western Washington.

PRECARIOUS ROCKS, SHATTERED ROCKS, GROUND MOTION, AND THE HEAT FLOW PARADOX FOR THRUST FAULTS

James N. Brune, University of Nevada, Reno

Recent modeling and field evidence relating to ground motion for thrust faults which break the surface has indicated strong inertial decoupling of the hanging wall from the footwall, resulting in very intense ground motions on the hanging wall and relatively low ground motions

on the footwall. This evidence is of potentially critical importance to estimating hazard from large thrust fault earthquakes in the Los Angeles Basin. Evidence for intense ground motion on the hanging wall of the 1971 San Fernando earthquake, and a Japanese and an Indian earthquake, has been presented by Allen et al.,(1998). Intense shaking on the hanging wall is well documented for the 1952 Kern County earthquake on the White Wolf fault(Oakshott, 1954). Brune (1999) has cited evidence from shattered rock extending several km back from the fault trace on the footwall of thrusts in Southern Calif. Subsequent reconnaissance surveys support the general occurrence of these strong ground motions on all thrust faults in Southern California. On the other hand recently discovered precarious rock evidence on the footwall of the White Wolf and Banning faults has indicated very low accelerations(field work supported by a SCEC grant). This is strong evidence of dynamic inertial decoupling of the hanging wall from the footwall. Further evidence of inertial decoupling is provided by the low teleseismic radiation from thrust faults(low apparent stresses) cited in several recent studies. In particular, Heaton (1982)found no evidence for teleseismic radiation from the shallow part of the San Fernando earthquake rupture, the part of the rupture which evidently experienced intense ground motions and inertial decoupling. If inertial decoupling is a common characteristics of large subduction zone earthquakes it could play a major role in explaining the thrust fault heat flow paradox (Hyndman et al.,1995).

PRECARIOUS ROCKS CONSTRAINTS ON DYNAMIC STRESS-DROP FOR GREAT STRIKE-SLIP EARTHQUAKES

James N. Brune, Rasool Anooshehpour, Yuehua Zeng, Haluk Sucuoglu, Baoping Shi, Anderes Mendez and John G. Anderson
University of Nevada, Reno

Precarious rocks are effectively upper-limit strong motion seismoscopes that have been in place thousands of years, thus providing an upper limit estimate on the ground motion that could have occurred during this time. In the San Gabriel Mountains and the Mojave Desert near Los Angeles testable precarious rocks exist at distances of 15-35 km from the nearby San Andreas Fault, which has likely generated more than 75 great earthquakes during the time the rocks have been in place. Thus the precarious rocks potentially provide an important constraint on the dynamic stress drop of these great earthquakes. The recent large Izmit, Turkey, earthquake is the first large similar strike-slip earthquake recorded on modern instrumentation, and provides critical accelerograms for testing with the precarious rock data. A preliminary estimate of the ground motion that would topple the rocks at a distance of 15 km is about 0.4 g, both in the San Gabriel Mountains and in the Mojave Desert (for a waveform appropriate for a great earthquake). This toppling acceleration estimate decreases to about 0.2 g at a distance of 35 km.

We investigate various waveforms for great earthquakes to test for consistency with our estimates of ground motion. We chose dynamic stress drop (slip rise-time), rupture velocity, source complexity (asperity distribution) for both simple half space models (2-D and 3-D), and layered models with computed Green's functions to produce the waveforms. Preliminary calculations indicate the ground motions for smooth rupture models are generally consistent with the precarious rock constraints for reasonable rupture velocities and dynamic stress drops of less than 100 Mpa. Thus the precarious rocks provide the most useful constraint on the rupture complexity and associated high frequency generation, important to understanding the physics of the rupture process and in estimating earthquake hazard. We plan to present updated estimates of dynamic stress-drop consistent with both the precarious rock data and strong motion data for the recent Izmit, Turkey, earthquake. At the time of writing of this abstract we estimate that the upper-limit constraint on dynamic stress drop and apparent stress for the Zeng, Andersen, and Yu (1994) complex source model will be in the range of 100 bars.

Southern California 3D Velocity Model-Version 2

Rob Clayton and Working Group D

We are in the process of updating the standard 3D velocity model for Southern California. Version 2 of this model will include the following enhancements:

- 1) A Geotechnical layer based on a soil classification map and shallow borehole data (V_p , V_s , and density),
- 2) An Imperial Valley basin,
- 3) A tomographic background velocity for regions outside the basins, and
- 4) A laterally varying Moho depth based on receiver-function estimates.

We are planning to complete Version 2 by the end of 1999. It will be available through the SCEC Data Center early in 2000. [radon:~/3Dvelocity]

Slip Rupture along Bimaterial Interfaces: Ill-posedness, Regularization, and Slip-Pulse Response

Alain Cochard, Ecole Normale Supérieure, Paris
James R. Rice, Harvard University

Faults often separate materials with different elastic properties. Slip then induces a change in normal stress. Weertman [JGR, 1980] suggested this could lead to a self-sustained slip pulse on an interfaces with a constant coefficient of friction f , and Adams [J. Appl. Mech., 1998] fully described such a solution. The pulse propagates steadily at the generalized Rayleigh speed c and the solution exists for all material pairs for which that wave type exists (c corresponds to a localized mode along a freely slipping interface, is a little less than the slower S-wave speed, and exists only for modestly dissimilar materials). That pulse solution can be found for remote driving shear stress that is arbitrarily less than the corresponding frictional strength, but its stability and emergence from generic initial conditions has not been established.

Following Andrews and Ben-Zion [JGR, 1997] and Ben-Zion and Andrews [BSSA, 1998] (ABZ), we study numerically in 2D plane strain the propagation of ruptures along such an interface under remote driving stress that is slightly less than the frictional strength. We use the spectral elastodynamic method, generalized to bimaterials by Breitenfeld and Geubelle [Int. J. Fracture, 1999].

This problem of steady frictional sliding between dissimilar materials is ill-posed for a wide range of elastic material contrasts (including those used by ABZ), in the sense that infinite velocities are reached at arbitrarily short times after a generic perturbation [Renardy, J. Elastic., 1992; Adams, J. Appl. Mech., 1995; Martins et al., J. Vibr. Acoust., 1995]. Ranjith and Rice [to be submitted to J. Mech. Phys. Solids] (RR) showed that when c exists the problem is in fact ill-posed for all values of f and, when it does not, for f greater than a critical value. We illustrate the abovementioned ill-posedness with our model, for ABZ type rupture with remote stress less than the frictional strength, by showing that in the unstable range the numerical solutions do not converge through grid size reduction. By contrast, convergence is achieved in the stable range but, not unexpectedly, only dying pulses are observed in that case.

RR showed that an experimentally based constitutive law of Prakash and Clifton [e.g., Prakash, J. Tribology, 1998] containing a lengthscale L provides a regularization in the Coulomb ill-posed range. In the form of it we use, $d(\tau)/dt = -[(V^* + |V|)/L] [\tau - f \text{ sign}(V)]$, with (small) $V^* \geq 0$ so that the shear strength τ in response to an abrupt change in normal stress

σ evolves gradually with time or slip towards the corresponding Coulomb strength. Here V is slip rate. [Friction laws with an abrupt change in τ , in response to an abrupt change in σ , do not regularize the problem.] We show that convergence through grid refinement is then achieved. For sufficiently small L , compared to the size of the slipping region at nucleation, self-sustained pulses are observed. When c exits, they propagate at that speed but only in the direction which is that of slip in the more compliant medium. When c does not exit, the sustained pulses propagate at the slower S-wave speed, in the same direction.

RR also showed that, for sufficiently high f , another kind of (less unstable) disturbance propagated along steadily sliding interfaces at a speed a little lower than that of the slower P-wave, and in the opposite direction. We have numerically verified that pulses of that type exist, for the ABZ case with applied shear stress slightly below the friction threshold.

Stress Loading From Viscous Flow in the Lower Crust and Triggering of Aftershocks Following the 1994 Northridge, California, Earthquake

Jishu Deng, Kenneth Hudnut*, Michael Gurnis, and Egill Hauksson
California Institute of Technology, Pasadena, California
*US Geological Survey, Pasadena, California

Following the M 6.7 Northridge earthquake, significant postseismic displacements were resolved with GPS. Using a three-dimensional viscoelastic model, we suggest that this deformation is mainly driven by viscous flow in the lower crust. Such flow can transfer stress to the upper crust and load the rupture zone of the main shock at a decaying rate. Most aftershocks within the rupture zone, especially those that occurred after the first several weeks of the main shock, may have been triggered by continuous stress loading from viscous flow. The long-term decay time of aftershocks (about 2 years) approximately matches the decay of viscoelastic loading, and thus is controlled by the viscosity of the lower crust. Our model provides a physical interpretation of the observed correlation between aftershock decay rate and surface heat flow.

Paleoseismic Studies of the San Andreas Fault at Plunge Creek, Near San Bernardino, California

Safaa Dergham, CSU Long Beach
Sally McGill, CSU San Bernardino

A new trench across the San Bernardino segment of the San Andreas fault near Plunge Creek has revealed several fault strands. The fault strands display a normal sense of vertical separation, although the dominant sense of movement is probably right lateral. The trench, located at the edge of an alluvial fan of late Holocene age, was excavated in three stages. In each stage the trench was widened and was deepened by 1.5 meters, reaching a total depth of 4.5 meters. This procedure allowed us to reconstruct a 3-part exposure in a single, vertical plane, even though the sediments are too loose to allow such a tall exposure to be safely exposed all at once. The first stage (0 to 1.5-m deep) exposed well-stratified sand and gravel that was clearly unfaulted. The second stage (1.5- to 3-m deep) unearthed discontinuous sedimentary layers in which no distinct faults were visible, but neither could their presence be ruled out. The third stage (3- to 4.5-m deep) revealed several fault strands in the southern half of the trench. Some of these faults stands may continue upward into the middle tier of the trench. Our work in a previous trench (T7) at the Plunge Creek site (McGill and others, EOS, v. 79, p. F611) suggested that the most recent earthquake on the San Andreas fault at Plunge Creek may have occurred as long ago as A.D. 1440-1640. If this is true, then neither of the two most recent ruptures (A.D. 1812 and A.D. ~1700) at Wrightwood and Pitman Canyon extended as far southeast as Plunge Creek. Unfortunately, a zone lacking clear stratigraphy in trench 7 at Plunge Creek made it

impossible to know for sure whether or not the A.D. 1440-1640 event is the most recent earthquake on this part of the fault. We expect to have radiocarbon dates from the new trench (T8) at Plunge Creek in time for the annual meeting. Because well-defined, unfaulted stratigraphy caps the entire width of the fault zone in trench 8, these dates should unambiguously constrain the age of the most recent earthquake on this portion of the San Andreas Fault.

Estimate of Strain Partitioning across Northern Metropolitan Los Angeles Using Geodesy, Fission Track Thermochronology, and Structural Analysis

Andrea Donnellan, Jet Propulsion Laboratory
Louise Kellogg, University of California, Davis
Ann Blythe University of Southern California
Maggi Glasscoe University of California, Davis

Geodetic data indicate that northern Metropolitan Los Angeles is shortening at a rate of about 6 mm/yr between downtown Los Angeles and the San Gabriel Mountains (Argus et al., 1999). Fission track thermochronology indicates that the San Gabriel Mountains are undergoing bedrock uplift at a rate of 1 mm/yr. If we assume that the shortening crust is isostatically compensated then the thickness of the root is related to the amount of uplift as a function of crustal and lithospheric densities. Using typical density values the total crustal thickening would be 5.5 mm/yr. If the lithosphere is thickening due to a downwelling in the mantle it adds a further dense addition to the root that would need to be compensated and there is a tradeoff between thickening of the lithosphere versus crust. In this case the crustal thickening rate is 4.5 mm/yr. If we assume that all of the uplift of the San Gabriels is due to the major frontal fault system (e.g. the Sierra Madre fault) then the total slip on the system is 5.5 mm/yr based on a dip of 55 degrees. The slip rate accounts for 3.2 mm/yr of the 6 mm/yr of shortening across the belt leaving 2.8 mm/yr of shortening attributable to the faults to the south, near downtown Los Angeles. As a test, we use the Ventura basin to estimate the stress drop per event on the basin bounding faults. Recent trenching indicates 4 m of slip per event on the San Cayetano fault, and recent analysis of geodetic data indicates that nearly all of the basin deformation can be attributed to the San Cayetano Fault. Dividing the slip per event by the observed shortening rate of 7 mm/yr yields an average recurrence interval of 400 year, which is consistent with geologic estimates. Using a strain rate of ~0.7 microstrain/year and basin rigidities of 19-24 Gpa based on P- and S-wave velocities the basin stress loading rate is 0.13-0.17 bar/year. Multiplying the recurrence interval by the stress rate suggests a stress drop of 54-67 bars, which is consistent with stress drops observed for earthquakes in southern California. The compressive strain rate across the Los Angeles shortening belt is about 0.33 microstrain/year which corresponds to a stress rate of 0.06-0.08 bar/year. Using a stress drop of 50-100 bars suggests that earthquakes should occur at intervals of 700-1600 years on fault segments within the belt. Thus the recurrence interval on the frontal, or Sierra Madre, fault system would be about 1300-3000 years. The upper recurrence interval is consistent with estimates based on geologic data. Our inferred rate is higher than estimates based on recent trenching (Rubin et al., 1998), but is within the rate of 4+-2 mm/yr suggested by the Southern California Earthquake Center Phase II report.

Changes in Frequency of Moderate-size Earthquakes and Coulomb Failure Stress before and after the Landers, California, Earthquake of 1992

Du, Wen-Xuan and Lynn R. Sykes, Lamont-Doherty Earth Observatory

Changes in the frequency of moderate-size earthquakes before and after the Landers event are investigated, and their implications are discussed in the context of Coulomb stress

evolution since 1812 in Southern California. We systematically considered circular regions and equal-area annuli centered on the epicenter of the June 28, 1992 Landers earthquake. Frequency-magnitude relationships for two 10-year periods before and two 5-year periods around the Landers event are compared. Only events with magnitude, $M > 4.0$ are included; obvious aftershocks are removed. For the larger circular regions with radii of 140 to 160 km, the rate and slope of the magnitude distribution for moderate-size events just before the main event appear to be anomalous compared to those for either the preceding or subsequent periods. For smaller areas, however, the number of events is few and the differences in the distributions are less obvious. When we examined the seismic activity in annuli of equal area, however, the largest changes occurred about 150 km from the epicenter of the main shock not closer as would be expected for a precursor to the Landers event. We also derive an "Index Value" to better quantify differences in the frequency of occurrence of moderate-size events as a function of time. It and the frequency-magnitude distribution show similar spatial dependence. Since 1812 a large region near Landers has moved closer to failure in terms of changes in Coulomb stress for faults of San Andreas type. These changes, however, are dominated by co-seismic changes associated with the 1812 and 1857 earthquakes and by tectonic stress buildup related to the San Andreas fault, not by stress buildup associated with the Landers faults themselves, which are characterized by very slow long-term displacements. Hence, the most pronounced changes in the frequency of moderate-size earthquakes before 1992 do not appear to be related to stress buildup to the Landers sequence itself. They along with the Landers sequence may be indicative of a broad region that is approaching a self-organized critical state prior to an eventual future great earthquake. Any changes in rates of moderate-size events prior to the Landers earthquake appear to be confined to epicentral distances less than 80 km, not to larger areas as some have proposed. The failure to find a pronounced increase in moderate-size shocks close in to Landers is in accord with the idea that such increases on a time scale of years to decades are associated with the regional buildup of stress to large earthquake along faults of high (not low) long-term slip rates.

Full Waveform Test of the 3D Velocity Model for Southern California

Leo Eisner, California Institute of Technology

The purpose of the Three-Dimensional Velocity Model for Southern California is to provide a unified reference model for the several areas of research that depend on the subsurface velocity structure in their analysis. Several recent studies (Olsen and Archuleta, 1996, 1997, Wald and Graves, 1998) showed the newly developed Three-Dimensional Velocity Model improves fit of the synthetic seismograms to the observed data, if low-passed to periods of 5 seconds and longer. Here we extend this study to earthquakes recorded at a wider span of azimuths and to higher frequencies.

We have simulated some 30 earthquakes in the vicinity of the greater Los Angeles basins recorded on several stations near or inside the basins. The earthquakes were chosen to cover as broad a range of azimuths as possible and to radiate enough energy in the periods of interest (3 seconds and longer).

A set of misfit measurements were developed to characterize the results. In order to conveniently include all three components in the analysis, we use the magnitude of displacement (vector length of all 3 components) as our basic measure. With this measure the time histories of the real and synthetic data are compared in two ways:

- The first is how well do our synthetics cross correlate with data, which can be characterized by maximum correlation and time of the maximum correlation. Time of the maximum correlation is a delay time related to the average velocity deviation along the path.

- The second parameter is rate of coda decay. The time history of the total energy in the synthetics and data is approximated with the best a fitting exponential function peaking at the maximum amplitude. Both the maximum amplitude and decay coefficients for data and synthetics are compared. Here the decay coefficient characterizes coda (and hence the complexity) and maximum amplitude is an important engineering parameter characterizing overall path focusing.

In general, we have found the three dimensional model of the Southern California version to be too fast both inside the basins (2.5%) and outside the basins (6.0%). A simple topographic projection of the time delays shows consistently fast model in all areas crossed by several paths. It should be noted that we are measuring the travel time of the maximum energy waves (generally the shear surface waves) and not the direct P-wave. The analysis of the coda indicates that the southern Los Angeles and San Bernardino Basins lack the complexity necessary to generate the observed coda. The San Fernando Basin appears to generate too much coda which indicates the basin is too complex or the attenuation used in the model (none) is not appropriate.

A detailed study of the individual records from stations or earthquakes in the basin show the effects of relocating of the hypocenter on the coda generated by the 3D model. In general earthquakes relocated to shallower depth show better fit to the data. On several records we observe a strong arrival 20-30 seconds after the main energy that is not explained by the 3D model.

We also show a comparison with a simple one-dimensional model. The results show that the 3D models only improve the fit for stations or events that are near or inside the basins and otherwise it does about as well as the 1D model which in many areas is not very good. This means that the 3D model needs improvement outside the basins as well.

Simulating the Effect of a Shallow Weak Zone on Near-Source Ground Motion

Geoffrey Ely and Steve Day, San Diego State University

Due to the effect of directivity, earthquakes can produce extreme ground motion in the vicinity of faults. Foam rubber scale models have shown that a weak zone in the shallow part of the fault reduces near-source peak accelerations and increases rupture duration (Brune). These controlled experiments provide recordings of rupture propagation unavailable for real earthquakes. We attempt to reproduce the results of the foam rubber experiment using a finite-difference method. The fault is dynamically modeled using a slip-weakening friction law. The code was implemented in parallel using Message Passing Interface (MPI) and achieved near perfect speed up on a three processor machine. This study aims to validate our method of simulating a shallow weak zone so that it may be applied to modeling real seismograms in the future.

Accounting for Site Effects in Probabilistic Seismic Hazard Analysis: Overview of the SCEC Phase III Report

Edward (Ned) Field and the SCEC Phase III Working Group**

** Kim Olsen, John Anderson, William Joyner, Jamison Steidl, Yajie Lee,
Shean-Der Ni, Lisa Wald, Norman Abrahamson, Mark Petersen.

It has been known for over 100 years that neighboring sites can experience significantly different levels of shaking during earthquakes, often referred to as a site effect or site response. Sedimentary deposits usually give rise to the most dramatic site effects, influencing earthquake shaking in the form of sediment amplification, resonances, focussing and defocussing, basin-edge induced surface waves, and nonlinear effects. Although these factors have all been

recognized, it is still not clear how to treat them in hazard analysis. The so-called "Phase III" effort of the Southern California Earthquake Center has focused on how and if site effects can be accounted for in Probabilistic Seismic Hazard Analysis (PSHA). In this context a site effect is defined as the tendency for ground motion to be significantly different at a location, or type of location, when averaged over all potentially damaging earthquakes in the region. The Phase III report, which will soon be published as a collection of papers in the Bulletin of the Seismological Society of America, is summarized here.

In a practical sense the problem amounts to how and if attenuation relationships can be modified to account for site effects. Both theoretical and empirical studies imply that certain site attributes, such as detailed surface geology and/or depth to basement at sediment sites, do indeed correlate with ground-motion amplitudes and can therefore be applied as correction factors. Perhaps an equally important finding is that these site-effect corrections do not appreciably reduce the prediction uncertainty of attenuation relations. This can be understood by the fact that basin-edge induced surface waves, focusing and defocussing, and scattering in general, will be highly sensitive to the source location. These effects produce a high degree of variability from event to event at any given site, making the systematic site effects seem relatively small. However, as will be shown, even small corrections can have a significant impact on hazard analysis.

Working Group on Southern California Earthquake Potential

Edward (Ned) Field and SCEC Working Group 2000**
** David Jackson, John Anderson, William Foxall, Mark Petersen, James Dolan, Steven Ward, Lucile Jones, Egill Hauksson, Julie Nazareth, Kate Hutton, Zheng-kang Shen, and Yan Kagan

SCEC's Phase II report (WGCEP, 1995) represented the first effort to combine seismic, geodetic, and geologic constraints into an integrated seismic-hazard source model using the concept of seismic moment budgeting. The report raised several questions related to a discrepancy between observed and predicted seismicity rates, such as the existence of an historical deficit (or future surplus) of earthquakes compared to the long-term average, as well as the limiting size of events in southern California. Although it has now been shown that a mutually consistent source model can be constructed for southern California, this does not rule out the possibility of an historical deficit or $M \geq 8$ earthquakes, which are indeed predicted by some seismicity models. An important question is the degree to which the different viable source models imply different levels of seismic hazard.

Given these questions, and the fact that many elements used in Phase II have been revised, a SCEC working group (SCEC WG 2000) has been established to revisit the problem. The primary tasks will be to examine the range of earthquake source models consistent with available data and our understanding of earthquake processes, to summarize the implications of these models for seismic hazard, to assess model uncertainty, and to identify important problems for further research.

Rather than providing a "consensus" model as in Phase II, we will present a variety of models based on different data types and assumptions. Such models will include: 1) A basic characteristic earthquake model with segmentation and no cascades (with and without time dependencies); (2) A characteristic earthquake model with strong cascade interactions (with and without time dependencies); (3) A smoothed seismicity model assuming a truncated Gutenberg-Richter magnitude distribution. Other models include one with seismicity proportional to the maximum shear strain rate, and a characteristic model with clock advance based on stress evolution and rate/state friction. Each model will be evaluated for consistency with the moment and seismicity rates implied by geologic, geodetic, and seismic data. Although we will certainly examine hybrid models, and perhaps make strong recommendations on which constraints seem best, the task of constructing "the" model will be left to those who produce the official maps (CDMG/USGS).

Retrospective Test of the 1996 USGS National Seismic Hazard Model

Richard L. Fielding, Dartmouth College
David D. Jackson, University of California, Los Angeles

In 1996, Frankel et al. proposed a model for seismic hazard throughout the contiguous United States. They used both geology and seismicity to estimate the rate of future earthquakes as a function of location and magnitude. Here we report a comparison of the historic earthquake rates with those implied by the model for two regions: the Western U.S. (WUS) and the Central & Eastern U.S. (CEUS).. We used the same earthquake catalogs and fault parameters used to create the model, found on the USGS Hazards website (<http://geohazards.cr.usgs.gov/eq/>). Because the model and the test used the same earthquake data, our retrospective test is not as strict as a prospective one based on future earthquakes. We derived earthquake rates vs. M_w in the range 5.0 to 9.0 for the WUS and 5.0 to 8.0 for the CEUS, assuming the completeness times given by Frankel et al. As a check, we compared our results for California with Petersen (1998), and found good agreement.

The USGS model predicts a higher rate than observed for moment magnitudes less than 7. For the Central and Eastern U.S. the model overestimated rates for magnitudes less than 6.3. We used a likelihood test to determine whether the discrepancies could be due to chance. We estimated the probability of observing a given number of events in each 0.1 unit magnitude bin from 1,000 synthetic catalogs using the theoretical magnitude distribution. We then summed the logs of the probabilities over magnitude for the observed and synthetic catalogs. The WUS catalog had a lower log-likelihood score than >99 percent of the synthetic catalogs, indicating that the discrepancy between observation and model cannot reasonably be ascribed to chance. The excess rate of forecast events there may result from underestimating the size (thus overestimating the rates) of earthquakes on geologically inferred faults. The CEUS relies more on seismicity than faults. There the observed catalog had a higher likelihood score than 99 percent of our synthetic catalogs. Perhaps the earthquake data fit better than expected at random, because the model is based largely on the same earthquake data used to test it.

Collaborative Systems for Research Outreach and Crisis Management

Geoffrey Fox, Syracuse University

We describe/demonstrate the use of web-based collaborative system TangoInteractive in applications of relevance to SCEC. These include:

- 1) Collaborative Research including shared simultaneous access to information systems, computational engines and scientific visualizations
- 2) Interactive outreach where dynamic models and data are shared between teacher and students
- 3) Crisis Management with shared maps, situation reports and sensor data

Alaska: Subduction and Strike-slip Tectonics with Post-Glacial Rebound on the Side

J. T. Freymueller, H. Fletcher, D. Mann, C. Larsen, and C. Zweck
University of Alaska, Fairbanks

This poster presents a brief overview of the active crustal deformation processes observed in Alaska through a series of GPS campaign efforts. Southeastern Alaska is a transform boundary, with most or all of the 46 mm/yr relative plate motion accommodated by the

Fairweather fault. The Fairweather fault separates the Yakutat terrane on the west from North America. Although many workers have assumed that the Yakutat terrane is locked to the Pacific plate, we find that there must be significant relative motion between the Yakutat terrane and the Pacific plate. This region is also uplifting rapidly due to post-glacial rebound, with the maximum uplift reaching approximately 40 mm/yr within Glacier Bay. The Fairweather fault terminates abruptly at the north end of the Yakutat terrane, at which point most of the relative plate motion is accommodated on a series of thrusts within the continental crust. Further west, these thrust systems link up the Aleutian megathrust, a classic subduction margin, which continues west for about 4000 km to the coast of Kamchatka.

Deformation of the overriding plate above the Aleutian megathrust is extremely complex, with substantial spatial variations. We observe regions where the plate coupling is extremely high and the shallow plate boundary appears to be completely locked. We also observe at least two regions where the plate coupling is low and the shallow plate boundary appears to be slipping at or near the plate rate. Preliminary results suggest that the boundary between locked and slipping areas can be very sharp. We also observe a strong postseismic transient 35 years after the Mw 9.2 1964 earthquake. The transient is spatially complex, and full 3D models of the subduction geometry are required to fully explain the observations.

Frictional Aging of Granular Fault Gouge: Humidity Effects

Kevin M. Frye and Chris Marone, Massachusetts Institute of Technology

Friction data from laboratory studies are the basis of constitutive laws used to investigate earthquake source processes and fault mechanics. However, the majority of experiments reported are performed with unsaturated gouge at room temperature. Thus, the question arises: what are the physical mechanisms responsible for friction velocity dependence and time dependent healing under laboratory conditions, and how do these relate to the mechanisms operative at earthquake hypocentral depths? To better understand frictional healing, creep, gouge compaction, and the mechanisms underlying these macroscopic behaviors, we have performed experiments on simulated fault gouge as a function of humidity. We investigate friction behavior during velocity steps and slide-hold-slide tests using the double-direct shear geometry. 3-mm thick layers of quartz-powder gouge were sheared within rough forcing blocks in a controlled-humidity environment. Humidity was varied from less than 5% Relative Humidity (RH) to 100% (water-saturated gouge) RH. We observe a transition from velocity strengthening to velocity weakening as RH is increased. Slide-hold-slide tests exhibit systematically lower healing rates as RH decreases. Tests performed at 5% RH display little time-dependent strengthening, consistent with previous studies conducted on bare quartzite surfaces. These results suggest that a critical amount of water must be present to assist time-dependent growth of contact junction area by cracking or plastic deformation. Gouge layer compaction and dilation measured during aging are similar over the entire range of humidities, even when the observed frictional healing is negligible. This indicates that time-dependent reorganization of the granular fault gouge is independent of the strength of the contact junctions. Future work will focus on separation of chemical and mechanical effects as related to frictional behavior and rate- and state- dependent friction parameters.

The Los Angeles Region Seismic Experiment, Phase II (LARSE II)--A Survey to Identify Major Faults and Seismic Hazards Beneath a Large Metropolitan Area

G.S. Fuis, T.R. Burdette, E.E. Criley, J.M. Murphy, J.T. Perron, Alan Yong
U.S. Geological Survey, Menlo Park

M.L. Benthien, S.A. Baher, R.W. Clayton, P.M. Davis, N.J. Godfrey, T.L. Henyey
M.D. Kohler, J.K. McRaney, D.A. Okaya
Southern California Earthquake Center

G. Simila, California State University, Northridge
G.R. Keller, University of Texas, El Paso
C. Prodehl, Karlsruhe University, Germany
T. Ryberg, GeoForschungsZentrum, Potsdam, Germany
M. Alvarez, IRIS/PASSCAL Instrument Center, New Mexico Tech
I. Asudeh, Geological Survey of Canada, Ottawa
H. Thybo, University of Copenhagen, Copenhagen, DK
U.S. ten Brink, U.S. Geological Survey, Woods Hole

A number of institutions, including the U.S. Geological Survey and the Southern California Earthquake Center, are collaborating in a seismic-imaging survey known as the Los Angeles Region Seismic Experiment, Phase II (LARSE II). This survey includes an active and passive component and is concentrated along a 100-km-long corridor extending from Santa Monica Bay northward to the western Mojave Desert, crossing the Santa Monica Mountains, the San Fernando Valley (through the Northridge epicentral area), the Santa Susana Mountains, and the western Transverse Ranges. LARSE II will complement a 1994 onshore-offshore (airgun) survey along the same corridor. In the active component of LARSE II, 1400 seismographs will be deployed at 100-m spacing along the main corridor, with shotpoints approximately 1000 m apart; in addition, several lines at various angles to the main corridor will be deployed in the San Fernando Valley and Santa Monica areas. All seismographs will record all shots. Chief imaging targets include the Santa Monica, San Gabriel, and San Andreas faults, blind thrust faults (including the Northridge fault), and the depths and shapes of the sedimentary basins in the San Fernando Valley and Santa Monica areas.

Strain Accumulation Across the Eastern California Shear Zone at Latitude 36°30'N

W. Gan, J.L. Svarc, J.C. Savage, and W.H. Prescott
U.S. Geological Survey, Menlo Park

The deformation of a linear array of monuments across the Eastern California shear zone has been measured from 1994 to 1999 with the Global Positioning System (GPS). The linear array is oriented N54°E, roughly perpendicular to the tangent to the local small circle drawn about the Pacific-North American pole of rotation. The velocity field relative to fixed interior North America deduced from GPS measurements has been resolved into components N36°W along the tangent to that local small circle and N54°E perpendicular to it. Plotted as a function of the distance along the linear array the N54°E components shows only a minor systematic trend, whereas the N36°W components show a uniform decrease with distance N54°E across the shear zone but not to the east of it. The horizontal motion within the Eastern California shear zone is approximated by uniform deformation with principal strain rates 53.6±6.9 nanostrain/yr N77.0±2.9°W and -28.7±5.5 nanostrain/yr N13.0±2.9°E, extension reckoned positive, and a clockwise rotation of 37.1±4.1 nanoradians/yr. The strain-rate field rotated into a coordinate system in which the 2 axis is parallel to the strike of the Eastern California shear zone (N23°W)

is $e_{11}=26\pm 7$ nanostrain/yr, $e_{12}=-39\pm 4$ nanostrain/yr, and $e_{22}=0\pm 6$ nanostrain/yr. The observed deformation then suggests that the Eastern California shear zone is a zone of uniform deformation (26 nanostrain/yr extension normal to the zone and 39 nanostrain/yr simple right-lateral shear across it) separating two rigid blocks (the Sierra-Nevada mountains to the west and southern Nevada to the east). That continuous distribution of deformation at the surface could be imposed from below by drag from a viscous shear zone in the upper mantle. Alternatively, it may simply be a superposition of deformation imposed by slip at depth on the individual major fault systems within the zone. The latter explanation would imply (dislocation model with locking depths of 15 km) the following right-slip rates on the principal fault systems: Death Valley-Furnace Creek-Southern Death Valley fault system 3.2 ± 0.9 mm/yr, Hunter Mountain-Panamint Valley fault system 3.3 ± 1.6 mm/yr, and Owens Valley-Little Lake fault system 6.9 ± 1.6 mm/yr.

Paleoseismic Evidence Of A Historic Coastal Earthquake And Uplift Of The San Joaquin Hills, Southern California

Grant, L. B., and Ballenger, L. J., University of California, Irvine

The San Joaquin Hills at the southern margin of the Los Angeles Basin have been rising at a rate of 0.21-0.27 m/ka during the last 122 ka. Grant and others (in press) proposed that the most recent uplift occurred during the Holocene due to seismogenic movement of an underlying active blind thrust fault. Their inference was based primarily on data from a 1954 study of salt marsh in upper Newport Bay, a late Pleistocene erosional gap in the northern San Joaquin Hills. We mapped, measured and sampled remnants of emergent marsh deposits in upper Newport Bay and wave-cut platforms and shorelines along the rocky open coast of the San Joaquin Hills. Paleo-shorelines and marine abrasion platforms are elevated up to 3.6 m above the active shoreline. The elevated deposits and platforms are best explained by co-seismic uplift due to a M 6.7 or larger earthquake beneath the San Joaquin Hills. Radiocarbon dating of marsh deposits demonstrates that the most recent uplift and emergence occurred sometime after deposition of plant material and shells circa 1635 A.D. Historical records suggest that the uplift may have been caused by the first reported earthquake in California in 1769 A.D., or possibly by coastal temblors in 1800 or 1855. Unusual sea waves were reported immediately following the 1855 earthquake at Pt. San Juan along the southern coast of the San Joaquin Hills.

Crustal-Scale Effects of Compressional Tectonics in Southern California: Results From the Los Angeles Regional Seismic Experiment (LARSE)

Nicola J. Godfrey, University of Southern California
Gary S. Fuis, U.S.G.S., Menlo Park
David A. Okaya, University of Southern California

Line 1 of the 1994 LARSE dataset is a 270 km-long, NNE-trending line crossing the Continental Borderland, the Los Angeles and San Gabriel Valley basins, the San Gabriel Mountains, and the Mojave Desert. The San Andreas Fault is located in the northern San Gabriel Mountains. Data include 60 onshore explosion shot gathers, 8 offshore OBS receiver gathers and 29 onshore-offshore receiver gathers.

Our model is derived from a combination of ray tracing through a layered model and travel time calculations through a gridded model (100 by 100m cells). The upper crust is well constrained by the explosion and OBS data, and shows a highly laterally variable velocity structure. Mid- and lower-crustal velocities are less-well constrained, hampering efforts to determine Moho depth. The shape of the Moho, however, is well determined.

Based on our velocity model we divide the crust beneath LARSE Line 1 into 5 regions for interpretation and discussion. Region A is the complex upper crust (above 10 km) including

the 10 km-deep Los Angeles basin, and low velocity zones associated with the major faults. Region B is the middle (6 to 6.6 km/s) and thin (5 km) lower crust (6.6 to 6.8 km/s) beneath the continental borderland above a fairly shallow (22 km) Moho. The crust thickens in Region C beneath the Los Angeles and San Gabriel Valley basins with the Moho at about 27-km depth. The middle crust (6.0 to 6.6 km/s) in Region C overlies a thick (12 km) lower crust (6.6 to 6.8 km/s). Region D has a lower-velocity mid- and lower crust (6.0 to 6.3 km/s), and the Moho deepens to 35 km beneath the central and northern San Gabriel Mountains (centered on the San Andreas Fault). Region E, beneath the Mojave Desert also shows a slow lower crust (about 6.3 km/s), but in this region the Moho shallows again to about 28-km depth.

The low velocity mid-crust of the San Gabriel Mountains reflects the presence of a significant body of Pelona schist. The crust in the Mojave Desert is distinct from crust to the south. The crustal root beneath the San Andreas Fault probably reflects crustal thickening due to compression.

Extraordinary Frictional Weakening at Rapid Subseismic Slip Rates

David L. Goldsby and Terry E. Tullis
Brown University

A series of experiments on quartzite and granite samples in our high pressure rotary shear apparatus at rapid, subseismic slip rates of 0.1 to 3 mm/s, normal stresses relevant to 1-6 km of depth in the earth, and displacements characteristic of seismic slip reveals extraordinary frictional weakening at these conditions. Typically, the friction coefficient decreases from an initial value of 0.6-0.8 to less than 0.35. The magnitude of this reduction increases with normal stress. In one case, at a normal stress equivalent to 6 km of depth in the earth, a decrease in the friction coefficient to less than 0.15 occurred for a quartzite sample in only 1.5 m of displacement. The friction coefficient returns to pre-rapid-sliding values after sliding is resumed at slow rates after rapid sliding.

Temperature measurements made during the experiments coupled with thermal calculations suggest that in most cases the frictionally-generated temperature is not sufficient to melt the entire fault surface. Theoretical considerations demonstrate that the local, so-called 'flash' temperature at contacting asperities, which increases with sliding velocity and normal stress, and decreases with increasing thermal conductivity, is much higher than the average surface temperature. A simple extrapolation of the classic flash temperature measurements of Bowden and Tabor (1958) on metals to the conditions of our experiments suggests that flash temperatures in our experiments are high enough to melt quartz. The degree of weakening we observe therefore likely reflects variations in the degree of melting and hence lubrication of the fault surface. The largest weakening occurred at the highest normal stresses for which the average surface temperature approached that necessary to bring the entire fault surface to a molten state.

Thus, extraordinary frictional weakening can occur over a wide range of conditions relevant to the earth, even when the heat generated is insufficient to melt the entire fault surface. Weakening at seismic slip rates and at higher ambient temperatures in the earth may be even more dramatic than observed at subseismic rates at room temperature. These results therefore likely have important implications for the magnitude of dynamic stress drops and strong ground motions, and can provide a simple explanation for the Heat Flow Paradox on quaking faults.

Strong Ground Motion Validation Studies Using Version 1 of the SCEC 3D Seismic Velocity Model

Robert W. Graves¹, David J. Wald², and Arben Pitarka¹
1 Woodward-Clyde Federal Services
2 United States Geological Survey, Pasadena

We have performed numerical simulations of recent earthquakes occurring in the Los Angeles region to test the performance and adequacy of Version 1 of the SCEC 3D Seismic Velocity Model in matching observed ground motion waveforms. To this point, the analyses have concentrated on data recorded during the Landers and Northridge earthquakes. The numerical simulations utilize 2D and 3D finite difference calculations, and incorporate not only the detailed structural complexity provided by the 3D seismic velocity model, but also employ heterogeneous finite-fault rupture models. For the Landers event, the simulations are limited to frequencies less than 0.5 Hz with a minimum shear velocity of 0.5 km/s. We find that the model predicts the phasing of the motions fairly well in the near source area, but noticeably underpredicts the amplitudes. Adding a sharp gradient in the top 0.6 km of the model to decrease the surface shear velocity from 2.7 km/s to 1.0 km/s provides a significant improvement in the simulated amplitudes. In the San Bernardino basin, the model predicts significant amplification and extended durations of motion, which is consistent with the observed waveforms. For Northridge, the simulations predict large amplification of long period ($T > 1$ sec) motions within the San Fernando and Los Angeles basins. The pattern of amplification is quite consistent with that of the observed motions. In addition, the 3D model predicts large amplitude later phases which are quite similar to the character of the observed waveforms at many of the basin sites, particularly in the northwest LA basin. At higher frequencies (2-6 Hz), the model predicts amplification ratios which are similar to observed spectral amplification factors in the Santa Monica area. However, the spatial pattern of the predicted amplification zone is shifted northward from the observed zone, which lies immediately south of the Santa Monica fault scarp, This suggests that some adjustment of the 3D model structure along the Santa Monica fault zone is required.

Active Tectonics and Earthquake Hazards, Santa Barbara, California

Larry Gurrola and E. A. Keller, University of California, Santa Barbara

The Santa Barbara Fold Belt (SBFB) contains numerous seismic sources on the coastal piedmont of the Western Transverse Ranges and offshore in the Santa Barbara Channel capable of producing large earthquakes that pose a significant seismic hazard to the Santa Barbara area. Seismic sources of the onshore SBFB consist of topographically well-expressed, north-verging anticlines formed on the hanging-wall of (mostly) blind thrust and reverse faults. The principal reverse fault is the 65 km long Mission Ridge Fault System which is subdivided, from west to east, into the More Ranch, the Mission Ridge, and the Arroyo Parida segments. The vertical component of slip on the More Ranch segment has been determined at two sites to be approximately 0.3 mm/yr. Paleoseismic investigation of the More Ranch segment revealed two paleoearthquakes, the oldest of which occurred approximately 36 ka and has approximately 0.4 m of vertical displacement.

Based on segment lengths of 15 to 17 km for the MRFS, a single-segment rupture may produce a maximum moment magnitude of Mw 6.5. If multiple segments were to rupture, then a maximum Mw 6.8 to 7.0 earthquake is possible. Several sources located in the offshore SBFB such as the North Channel Slope, Oak Ridge and Santa Cruz Island faults are capable of producing a Mw 7.1-7.5 event. Estimated earthquakes are consistent with historic seismicity in the SBFB. Assuming a vertical displacement of about 1.0 m per event for a segment of the MRFS, the average return period is approximately 3 ky. The city of Santa Barbara is located on

the hanging-wall of the blind Mission Ridge segment and is subject to amplified seismic shaking as the result of free surface effects and potential for directivity of seismic waves. Parts of downtown Santa Barbara are susceptible to liquefaction where the historic estero (salt marsh) has been filled, in part from debris from the 1925 Santa Barbara earthquake and is susceptible to a tsunami from an earthquake generated in the Santa Barbara Channel.

Recent Changes at the Southern California Earthquake Data Center (SCEDC)

K. Hafner and R. W. Clayton, California Institute of Technology

The Southern California Earthquake Data Center (SCEDC) has undergone a major period of transition during 1999. This transition includes upgrading our archive system, and implementing an ORACLE database to archive parametric earthquake data from the new TriNet system, as well as store pointers to the waveform archive. Specifically we transferred our triggered seismological data archive from a 0.6 Tbyte SONY/AMASS optical mass storage system to a 5 Tbyte DISC/samFS optical jukebox system this past summer. This change means that the SCEDC now uses the same archival software used by the IRIS DMC facility and the NCEDC. In addition to archiving triggered seismic waveform data and GPS data, the SCEDC is now developing the process of archiving continuous waveforms of 20 samples/sec (or less) from the 200-station TriNet digital network.

The new ORACLE database system is currently being run in parallel to the existing SCEDC database. Parametric data for earthquakes located by the TriNet system is being stored in this database, as well as station information, and pointers to the continuous waveform archive. During 2000, the existing SCEDC database will be incorporated into the ORACLE database, thus providing a complete catalog in one location. The goals of implementing the ORACLE database are: 1) to provide rapid user access to real-time parametric and waveform earthquake data, 2) to consolidate and maintain one authoritative database available to the real-time data acquisition systems, the data analysts and users of the SCEDC, and 3) to facilitate a seamless exchange of seismological waveform and parametric earthquake data with the Northern California Earthquake Data Center and the IRIS DMC in the future. This database system design will result in a closer coupling between the SCEDC and the real-time data collection/data analysis systems of the Southern California Seismic Network/TriNet, which will significantly decrease the latency time between the occurrence of an event and data availability.

Crustal Stress Orientations in Southern California

Jeanne L. Hardebeck and Egill Hauksson, California Institute of Technology

A new high-resolution image of southern California crustal stress orientation, determined from inversion of earthquake focal mechanisms, reveals complex patterns of stress. Some of the stress orientation complexity is related to differences between the major tectonic provinces. In the Eastern California Shear Zone (ECSZ), for example, the maximum horizontal compressive stress is oriented N20-45E, compared to the average southern California orientation of N6E. The stress state over much of southern California corresponds to strike-slip faulting, but thrust and normal faulting regimes are also observed. The Los Angeles area exhibits a combination of stress regimes, with strike-slip near the surface and thrust at depth, indicating that 2D models of local tectonics may be inadequate. Stress rotations due to major earthquakes are also observed.

Stress orientations also provide insight into the mechanics and evolution of the San Andreas Fault. For example, the stress state west of Cajon Pass is consistent with thrust faulting, while the stress state to the east is consistent with strike-slip faulting. This implies that little convergence is taking place across the San Bernardino segment of the San Andreas. The San Bernardino Mountains are young, however, indicating significant convergence not long ago. A

recent redistribution of slip on the San Andreas system is therefore implied. The diminished compression across the San Bernardinos could result from a significant amount of slip being transferred to the San Jacinto Fault and the ECSZ. The 1992 Landers ECSZ earthquake relieved enough compressive stress in the San Bernardinos to eliminate the only observed zone of thrust faulting regime, supporting this interpretation.

Paleoseismologic Trenches Across the San Andreas Fault at Elizabeth Lake, California

Ross D. Hartleb, James F. Dolan, Allan Z. Tucker, Shari A. Christofferson, and Jennifer Holsten
University of Southern California

During June 1999 we excavated trenches at several locations along the San Andreas fault along the southern edge of Elizabeth Lake, about halfway between Gorman and Pallett Creek. The fault at Elizabeth Lake is geomorphically well expressed, with a single main active trace that exhibits a nearly continuous south-facing scarp. Trenches at several sites show that the pronounced mountain-facing scarp is a function of the occurrence of resistant bedrock (granodiorite) at the surface along the north side of the fault. We concentrated our efforts at one site ~300 m west-northwest of the residential district of Elizabeth Lake. At that site our trenches exposed a latest Holocene sequence of well-bedded, 5- to 40-cm thick, alternating sand and gravel beds, along with two silty, buried A horizons, which do not appear to record long time periods of soil development.

The 1857 rupture is well expressed in the trenches as a 1-m-wide, near-vertical zone of discrete shears that in general separate the intensely sheared granodiorite north of the fault from unfaulted, gently south-tilted alluvial strata to the south. The shallowest fault strands can be traced to within 70 cm of the ground surface, where they are overlain by undeformed strata. Although the bedrock north of the fault locally forms a groundwater barrier at the site, we were able to use pumps to keep the trench dry enough to map the exposure in detail to 3 m depth. There is possible, but equivocal evidence for a second event horizon stratigraphically about 10 cm below the shallowest level faulted by an 1857 strand. This is an important observation because the location of the northwest end of the December 8, 1812 SAF rupture has not been determined, and it has been suggested that it may have extended northwestward through our trench site. If the 1812 rupture extended through the Elizabeth Lake site, then it must have had a minimum rupture length of at least 90 km (Elizabeth Lake at least as far southeast as Pitman Canyon; Seitz [1999]). No other potential event horizons were observed in the lowest 2 m of our trench. Radiocarbon dates on ^{14}C samples collected from the trenches will help us to determine the length of the pre-1812(?) quiescent interval at the Elizabeth lake site. Furthermore, planned future excavations at a site ~1 km east of the 1999 site, where recent alluvium has buried the fault trace, may allow us to determine unequivocally whether or not the 1812 event extended as far northwest as Elizabeth Lake.

Seismotectonics of the Junction Between the San Andreas, the San Jacinto, and the Cucamonga Faults in Southern California

E. Hauksson and J. Hardebeck, California Institute of Technology

Several major faults appear to influence the tectonics of the south end of the Mojave and north end of the San Bernardino segments of the southern San Andreas fault. The right lateral San Jacinto fault causes movement at an oblique angle to the San Andreas fault resulting in some extensional faulting. The west striking and north dipping Cucamonga fault accommodates extension of the upper block and compression at depth in the vicinity of the San Andreas fault.

The poorly understood Fontana seismicity trend, located to the southwest, is also related to the overall deformation of the region. It is not associated with a mapped surface fault and is characterized by swarm like seismicity.

We analyze the seismicity of the region in the context of new 3-D V_p and V_p/V_s velocity models. For instance, the V_p model and the seismicity show abrupt changes in depth across the San Andreas fault, with higher V_p and deeper seismicity to the west. The south end of the Mojave segment shows mostly thrust faulting while the north end of the San Bernardino segment shows mostly strike slip and normal faulting.

Modern, Digital Multi-Functional Real-time Seismographic Network for Southern California, US: TriNet

E. Hauksson, K. Hafner, T. Heaton, K. Hutton, H. Kanamori, P. Maechling, J. Goltz
California Institute of Technology
L. M. Jones, D. Given, D. Wald
United States Geological Survey, Pasadena

The USGS, Caltech, and CDMG are deploying a new generation of seismographic network in southern California. The purpose of TriNet is to record and analyze earthquake ground motions, and distribute that information quickly, to improve our understanding of earthquakes and their effects, to contribute to improving building codes and structural design, and to facilitate emergency response in cooperation with other agencies. TriNet is to be designed in two elements with the California Department of Conservation element concentrating on engineering applications and the Caltech/USGS element (SCSN/TriNet) concentrating on seismological and emergency response aspects. We report on new technologies, approaches and new products provided by the SCSN/TriNet.

Web Portal for GEM

Tomasz Haupt, Syracuse University

The goal of this effort is to build a Web Portal for the GEM project. In a nutshell, the Web Portal will provide a seamless access to computational resources and data. This in turn will provide an efficient platform for publishing codes and data, and will become a seed for a powerful collaborative workbench for earthquake specialists.

The portal is being implemented as a modern, object-oriented, distributed, three-tier system. The front end is implemented as a collection Java applets. The business logic is encapsulated as distributed components (CORBA based servers) that act as proxies for the back-end services, such as high performance computational resources and distributed data bases.

Challenges of this project include design of a universal, exchangeable data format and tools for instant conversion from a native format of various sources to the standard one enabling using it at input for computational and visualization modules, as well as simplifying data mining. We selected XML to define the standard data representation.

On the Plumbing System at Long Valley Caldera, California

Susan E. Hough, Robert S. Dollar, and Peggy Johnson*
U.S. Geological Survey, Pasadena
*also at Southern California Earthquake Center

A significant episode of seismic and geodetic unrest took place at Long Valley Caldera, California, beginning in the summer of 1997. Activity through late May of 1998 was

concentrated in and around the south moat and the south margin of the resurgent dome. The Sierran Nevada Block (SNB) to the south/southeast remained relatively quiet until a M5.1 event occurred there on 6/9/98 (UT). A second M5.1 event followed on July 15. These later sequences were considered tectonic rather than magmatic; in general the SNB is considered an unlikely location for future eruptions. However, a careful examination of waveforms from the summer, 1998 earthquake sequences reveals a small handful of events whose spectral signature is strikingly harmonic. We investigate the waveforms of these events using spectral, autocorrelation, and empirical Green's function methods and conclude that they were most likely associated with a fluid-controlled source. These events occur at the beginning of a burst of seismicity that began on 8/1/98. The number of events in this subsequence was similar to the aftershock sequence of the 7/15 M5.1 event, but the August sequence was not associated with any events larger than M4.3. This sequence--and "aftershock sequence with a mainshock"--may itself be suggestive of a strain event larger than the cumulative seismotectonic strain release. Our observations suggest there may have been some degree of magmatic involvement in the 1998 SNB sequence, which in turn provides insight into the spatial extent of the so-called plumbing system at Long Valley.

The 1998 Earthquake Sequence South of Long Valley Caldera: Hints of Magmatic Involvement

Susan E. Hough, Robert S. Dollar, and Peggy Johnson*
U.S. Geological Survey, Pasadena
*Southern California Earthquake Center

A significant episode of seismic and geodetic unrest took place at Long Valley Caldera, California, beginning in summer of 1997. Activity through late May of 1998 was concentrated in and around the south moat and the south margin of the resurgent dome. The Sierran Nevada Block (SNB) remained relatively quiet until a M5.1 event occurred there on 6/9/98 (UT). A second M5.1 followed on July 15. These later sequences were considered tectonic rather than magmatic; in general the SNB is considered an unlikely location for future eruptions. However, a careful examination of waveforms from the summer, 1998 sequence reveals a small handful of events whose spectral signatures are strikingly harmonic. We investigate the waveforms using spectral, autocorrelation, and empirical Green's function methods and conclude that they were most likely associated with a fluid-controlled source. These events occur at the beginning of a burst of seismicity than began on 8/1/98. The number of events in this sequence was similar to that following the 7/15 M5.1 event, but the August sequence was not associated with any events larger than M4.3. This sequence--an "aftershock sequence without a mainshock"--is itself suggestive of a strain event larger than the cumulative seismotectonic strain release. Our observations suggest that there was a degree of magmatic involvement in the 1998 SNB sequence, which in turn provides insight into the nature of the "plumbing system" that underlies Long Valley Caldera.

THE SOUTHERN CALIFORNIA INTEGRATED GPS NETWORK (SCIGN)

Kenneth W. Hudnut, United States Geological Survey, Pasadena
Yehuda Bock, University of California, San Diego
Frank Webb, Jet Propulsion Laboratory
Bill Young, SCIGN

SCIGN is an array of Global Positioning System (GPS) stations distributed throughout Southern California with emphasis on the greater Los Angeles metropolitan region. The major objectives of the array are:

- 1) To provide regional coverage for estimating earthquake potential throughout Southern Calif.
- 2) To identify active blind thrust faults and test models of compressional tectonics in Los Angeles
- 3) To measure local variations in strain rate that might reveal the mechanical properties of earthquake faults
- 4) In the event of an earthquake, to measure permanent crustal deformation not detectable by seismographs, as well as the response of major faults to the regional change in strain

These scientific purposes and the network design were developed through several collaborative workshops, as well as by meetings and extensive committee work. Despite the considerable logistical constraints on siting, the design of the network remained driven by the scientific intent.

Data from all SCIGN stations are freely available on-line, as are coordinate solutions, periodic velocity solutions, and other products. Users of data and products are asked to simply acknowledge SCIGN and its sponsors; the W.M. Keck Foundation, NASA, NSF, USGS, and SCEC. These data and additional detailed information on the project are all available at the SCIGN web site - <http://www.scign.org/>

In addition to these scientific purposes, the data will benefit the Surveying, Engineering and Geographic Information System (GIS) communities who are using SCIGN as the basis for their spatial reference system. The new High Precision Geodetic Network for the state of California, which is the fundamental official geodetic control system, will be based upon data from SCIGN stations (and other continuously operating GPS stations in Central and Northern California).

New SCIGN stations are constructed with a 10-meter deep, five-legged monument that is isolated from the uppermost 3.5 meters of soil so that seasonal non-tectonic motions are minimized. For longevity, these monuments are built using stainless steel pipe. All sites employ standard choke ring antennas and SCIGN adapters and radomes, to minimize potential antenna system phase center variations through time (and in the event of equipment changes).

In order to telemeter and process the large quantities of data, SCIGN has developed new programs and automation scripts that are shared with other users and code developers. Site information is being maintained using a relational database, developed with SCIGN support, that is proving useful for other global GPS datasets as well. Furthermore, we employ redundant data processing to obtain the very highest accuracy and precision possible from the data.

Stations are currently being installed by a contractor at an average rate of two sites per week. In addition to the approximately 50 SCIGN stations that were built in a variety of styles earlier in the network's growth, we now have nearly 100 new stations built by the contractor to the new specifications. Over the upcoming year, we intend to construct an additional 70 stations, and to eventually have a total of 250 stations in the network.

Plate Tectonics and Earthquake Potential on the Pacific Rim with Applications to Southern California

Yan Y. Kagan, David D. Jackson, Peter Bird, and Yufang Rong
University of California, Los Angeles

We analyze the plate-tectonic moment rate and earthquake magnitude distribution for circum-Pacific seismic zones (including California), defined by McCann et al. [MNSK, PAGEOPH, 1979] and Nishenko [PAGEOPH, 1991]. We group the zones by categories: for MNSK zones, we follow their red, orange, green, yellow, hatch, and purple classifications; for Nishenko zones, we subdivide the zones either by their characteristic magnitude or by

Nishenko's 10-year probability estimate. We also test classifications based on velocities of relative plate motion and on the ratio of velocities perpendicular to parallel to a plate boundary. We model the magnitude distribution by a gamma law, a modified Gutenberg-Richter relation with three parameters: the total earthquake rate, the b-value, and a corner (maximum) magnitude above which earthquake rate drops rapidly. The results can be summarized as follows:

1. Except for a multiplicative constant, the earthquake frequency distributions are essentially identical in the low, medium, and high MNSK potential zones.
2. The b-value universality ($b = 0.95 \pm 0.03$) is reasonably confirmed for all sets: for the MNSK zones, 7 out of 125 values are outside of 1.96 sigma limits -- for the 95% confidence limit we expect that 6 outliers would be due random fluctuations. For Nishenko zones, 5 out of 98 are out of the 95% limits. The b-values for the categories are also similar.
3. For the corner magnitude we obtain a relatively low correlation coefficient (0.4-0.6) between the number of earthquakes in the zones and plate tectonic deformation. The correlation, however, increases (0.85-0.95) significantly as soon as the zones are combined into categories. The low correlation between earthquake numbers and the tectonic rate in individual zones is probably due to earthquake clustering in time and space. The correlation deteriorates if we compare the sum of earthquake seismic moments to the tectonic rate.
4. In all classifications, earthquake rate is strongly correlated with the plate-tectonic rate. After accounting for this correlation there is no significant effect in color category, plate velocity, the ratio of perpendicular to parallel motion, characteristic magnitude, or 10-year probability. The values of the corner magnitude, using the gamma distribution, are 8.75-9.0 for most categories.

These results confirm [Kagan, JGR, 1997; PAGEOPH, 1999] the universality of the beta-values and the corner moment for shallow earthquakes in plate boundary zones. The results imply that earthquake potential is strongly related to tectonic moment rate, so that geodetic and geologic studies of deformation may be quite effective in long-term earthquake forecasting.

There are some indications (Z. K. Shen), that seismicity levels in southern California correlate with the strain rate estimated from recent GPS survey analysis. In applications to S. California, we interpret these results to mean that the maximum earthquakes rupture length in California may be comparable to that observed in other circum-Pacific zones (500-1000 km), implying that for the S. California we should apply the corner (maximum) magnitude of the order of 8.5. If 8.5 earthquakes are conceivable in California, the seismic hazard may actually be reduced, since to balance the tectonic moment rate, we need to reduce the frequency of magnitude 7-8 events.

Stress Drop and Recurrence Interval for Repetitive Stick-Slip

Stephen L. Karner and Chris Marone
Massachusetts Institute of Technology

Seismic data indicate that stress drop increases logarithmically with earthquake recurrence interval (1-5 MPa per decade time), which has been interpreted as time-dependent fault healing. However, the physical mechanisms that lead to frictional restrengthening are poorly understood. We have performed laboratory experiments to study healing and repetitive stick-slip on bare granite surfaces. Normal stress was 10 MPa and shearing velocity was varied from 0.5 to 300 micron/s. Instabilities occurred quasi-periodically and we study the effect of loading rate on stress drop and recurrence interval.

The frequency of stick-slip instabilities depends on loading rate via a power-law relationship. Stress drops range from 0.1-3.1 MPa (or 4-49% of the failure strength) with larger

stress drops occurring for longer recurrence interval and lower loading rates. Our data indicate that recurrence interval and stress drop vary at two distinct rates: one given by inverse loading rate (such that lower loading rates yield larger stress drop) and a second, higher rate given by the coupling of stochastic variations in frictional yield strength and stored elastic energy. The data highlight the importance of accounting for variations in earthquake recurrence interval in studies of the seismic cycle and earthquake source characteristics.

Evidence for Active Shortening in the Offshore Borderlands and its Implications for Blind Thrust Hazards in Coastal Orange and San Diego Counties

Grant Kier and Karl Mueller, University of Colorado

We combine offshore bathymetric data, seismic reflection profiles and flexural analysis to assess the likely geometry and slip rates on proposed blind thrust faults along the eastern edge of the Gulf of Santa Catalina, along coastal Orange and San Diego Counties. We offer evidence for uplift consistent with slip on the southern extension of the San Joaquin Hills blind thrust. This fault is contained in the upper half of the seismogenic crust and can be modeled as a back thrust on the much larger Oceanside detachment, which is a potential seismic hazard of significant magnitude due to its very low dip. Structural models suggest the high level backthrust is independent of the Newport-Inglewood fault zone and is not a steep splay developed along its western margin. Locally higher uplift rates in coastal Orange County are well documented by marine terraces (Grant et al., 1999). Geodetic results from stations along the coast and offshore islands indicate active shortening between 1-2mm/yr, consistent with proposed blind thrust geometry and rates of uplift defined the terrace deposits. Evidence for slower regional uplift along the Pacific coast in San Diego County and northern Baja California is modeled as a far-field effect of unloading and rift shoulder development associated with lithospheric thinning in the Salton Trough and northern Gulf of California. Besides active rifting, buoyancy is accentuated by the very young age of oceanic crust located offshore southern California and northern Baja California. Although no data exist for testing rates of late Quaternary uplift produced by active rifting, our models suggest the magnitude of uplift at the Pacific coast is consistent with the fraction expected of the total uplift produced by northward propagation of the Gulf of California.

Strong Ground Motion Behavior of the 1994 Northridge Earthquake and Five M>5 Aftershocks

Peg Johnson, Southern California Earthquake Center

The 17 January 1994 Northridge mainshock (Mw 6.7) and five aftershocks (M 5.2 - 5.9) which occurred through March 1994 were recorded on strong motion instruments of four networks in the greater Los Angeles area (USC, CDMG, USGS, and DWP). A total of 200 stations and some 275 aftershock records comprise the database (Todorovska et al., 1999).

I am examining the waveform characteristics of the six earthquakes as observed at these strong motion sites. The pattern of maximum accelerations observed at the stations for the events are in some cases quite different and suggest rather large differences in the peak values of the waveforms as a function of geological site (e.g., basin vs. mountains). For instance, the largest values of acceleration observed for one aftershock are at sites where another aftershock has its smallest values. This is of interest, since the calculated focal mechanisms indicate that the fault planes and sense of displacement are very similar for the two events (thrust). In this report, I focus on the role that geographic factors (such as epicentral distance and site geology) play in contributing to the variability of the waveforms and present results for a subset of the aftershock data.

Upper Mantle Structure Below the Central Transverse Ranges and the SCEC 3D Seismic Velocity Model

Monica D. Kohler
University of California, Los Angeles

High-resolution tomographic images from Los Angeles Region Seismic Experiment (LARSE) array and southern California Seismic Network (SCSN) teleseismic data suggest that the entire lithosphere below the San Gabriel Mountains and San Andreas fault in the Transverse Ranges has thickened in a narrow, vertical sheet. P-wave travel-time inversions of the combined data support the presence of the well-documented upper mantle high-velocity anomaly that extends ~200 km into the mantle under the northernmost Los Angeles basin and Transverse Ranges, and is associated with mantle downwelling due to oblique convergence. We find that the high-velocity, high-density upper mantle anomaly comprises a 60-80 km wide sheet of mantle material that lies directly below a substantial crustal root in the San Gabriel Mountains. The velocity perturbations are as large as 3% in the anomaly, corresponding to a ~2% density increase. The tomographic images suggest that deformation in the ductile lower crust and mantle lithosphere may be partially coupled mechanically and thermally if the thickening is occurring together in response to convergence and that it may be a local compressional feature.

We are in the process of refining the uppermost mantle features of this model by adding travel-time data from several recent dense temporary arrays. Travel-time residuals from approximately 40 teleseismic events recorded by the 18-station, 1997 Los Angeles Basin Passive Seismic Experiment will add new information about shallow structures near the deepest part of the southeastern Los Angeles basin and we estimate that at least 50 events recorded by the 83-station, 1998-1999 Los Angeles Region Seismic Experiment (LARSE) II passive phase will constrain shallow structures below the Santa Monica Mountains, San Fernando Valley, and Western Transverse Ranges. The refined model will be incorporated into Version 3 of the SCEC Seismic Velocity Model.

The Los Angeles Region Seismic Experiment (LARSE) II Passive Array: An Experiment to Elucidate Crustal and Upper Mantle Structures below the Western Transverse Ranges

Monica D. Kohler and Bryan Kerr
University of California, Los Angeles

From October 1998 to May 1999, we managed the deployment, maintenance, and data collection of 83 seismometers comprising the LARSE II passive array. The 100-km long, linear array spanned the Santa Monica Mountains, San Fernando Valley, Western Transverse Ranges, San Andreas fault, and western Mojave Desert. Goals of the experiment are to examine crustal and upper mantle seismic velocity structure, seismic hazard associated with anomalous site amplification, and tectonic evolution of the westernmost Transverse Ranges. Data collection and station maintenance were handled by field assistants Bryan Kerr and Michael Watkins. A consistently large percentage of stations operated continuously without equipment problems or power failure, including remote, buried sites running on battery power only. Each station consisted of a short-period (L22 or L4C, all 3-component) or broadband (Guralp CMG-40T, CMG-3ESP, or CMG-3T) sensor, Reftek 24-bit data recorder (continuous recording at 25 sps, triggered at 50 sps), GPS receiver, and power supplies. The deployment was carried out by volunteer teams from UCLA, Caltech, USGS Pasadena and Menlo Park, and UCSB. Long-term data archival tasks include conversion of data to mseed format, corrections for timing errors, sensor calibrations for correct amplitudes, and creation of teleseismic, regional, and local event waveform files.

Modeling of Absorbing Boundaries and Q for 3-D Numerical Computations

Peng-Cheng Liu and Ralph Archuleta
University of California, Santa Barbara

We have improved the techniques for modeling absorbing boundaries and Q in the numerical time-domain computations of seismic wave fields. Many different techniques have been developed to simulate the absorbing boundaries. A common problem with these computations is that the more accurate they are the most likely they are to induce instabilities in the numerical computations. Following Higdon's (1991) technique, we express the boundary conditions as the composition of two first-order differential operators. However, we combine the first-order operator of Higdon (1991) for the absorption of the outgoing P-wave with the A1 absorbing condition of Clayton and Engquist (1977) for the outgoing S-wave. This new absorbing boundary condition is approximately second-order in accuracy. We implement it in the 3D finite element and finite difference (4th order in space) methods. No instability has been observed in our numerical calculations.

In the time-domain computations the effect of Q is currently simulated by a rational function of frequency. One can adjust the coefficients (weights and relaxation times) of this function to model different Q laws. The more relaxation times that are used the more accurate is the modeling of Q. However, the number of relaxation times is directly proportional to the storage requirements. We optimize both the weights and the relaxation times for the best modeling of a Q law while keeping the storage requirements as small as possible. By using two pairs of weights and relaxation times, we can simulate constant Q within 4 % tolerance over one decade in frequency and within 20 % over two decades. If we use 4 pairs of weights and relaxation times, the misfit is less than 3 % over two decades in frequency. We incorporate the modeling of Q into the numerical computation by using the coarse-grained method of Day (1998). We first optimize four pairs of weights and relaxation times for the minimum Q in the earth model. These relaxation times are then used for all other Q's in the model. Next we optimize the weights for the maximum Q. Linear interpolation of the weights between Q_{\min} and Q_{\max} determine all other weights. This scheme simulates constant Q within 4 % tolerance over two decades in frequency. It adds only a single memory variable, for each stress component, at every other node.

Long Term Tectonic Loading with Earthquake Episodes on Faults with Rate/State Friction: Computational Procedure Allowing Rigorous Elastodynamic Analyses

Nadia Lapusta and James R. Rice, Harvard University
Yehuda Ben-Zion, University of Southern California

We present an efficient and rigorous numerical procedure for calculating the elastodynamic response of planar faults subjected to slow tectonic loading with earthquake episodes. This is done for a general class of rate- and state-dependent friction laws with positive direct velocity effect. The procedure is implemented here for a vertical strike-slip fault model with depth-variable properties (like in Rice, JGR, 1993) in Dieterich-Ruina types of friction laws, considering both the "aging" and "slip" versions of state evolution.

The algorithm allows us to treat accurately, within a single computational procedure, loading intervals of thousands of years and to describe, for each earthquake episode, initially aseismic accelerating slip prior to dynamic rupture, the rupture propagation itself, rapid postseismic deformation which follows, and also ongoing creep slippage throughout the loading period in velocity strengthening fault regions. The work is motivated by earlier but less efficient algorithms with similar aims, described and/or implemented by Zheng et al. (EOS Trans. AGU,

1995), Rice and Ben-Zion (Proc. Nat. Acad. Sci. USA, 1996) and Ben-Zion and Rice (JGR, 1997).

The algorithm separates the elastodynamic stress transfer functional into its long-time static limit and a wave-mediated dynamic part. The latter localizes the effects of the prior deformation history in convolution integrals on slip velocity with rapidly decaying kernels. Truncation of these convolutions allows to simulate long processes without the necessity to deal with all prior deformation history at each time step. Time steps throughout the calculations can vary by several orders of magnitude (as many as 9 in our examples), as dictated by the current values of slip velocities, parameters of the constitutive law and stability considerations. This makes the number of time steps during slow deformation periods numerically manageable while still capturing the details of both the nucleation and dynamic propagation phases as well as of the transitional phase in between. Proper space and time discretization, and a newly developed second-order accurate updating scheme, ensure the reliability of the results which is verified through grid and time-step refinement.

The implementation examples we present adopt the 2-D anti-plane spectral formulation, so that slip varies with depth and time only. The procedures can be readily extended to the 2-D in-plane and 3-D spectral formulations, and, with certain modifications, to the space-time boundary integral formulations as well as to their discretized development using finite-difference or finite-element methods. The nucleation process is studied for a range of nucleation sizes. The size of the zone slipping aseismically just before dynamic breakout is shown to be much larger for the aging than for the slip version of state evolution. Also, the sometimes subtle effects of inadequate discretization in time and space are demonstrated.

Deformation History of a Major Restraining Bend Along a Right-Slip Fault: the San Clemente Fault Offshore Northern Baja California, Mexico

M. R. Legg, Legg Geophysical
D. E. Einstein, Southern California Earthquake Center
H. D. Wang, Northwestern University

Major restraining bends are important features of strike-slip faults that tend to become locked, releasing accumulated tectonic strain during large earthquakes. The deformation history (tectonic evolution) of restraining bends is difficult to study on land where combined tectonic uplift and erosion removes the recent geologic materials that record this history. The offshore depositional environment, however, creates sedimentary sequences that provide a high resolution record of sub-seafloor deformation that is readily imaged by seismic methods. The San Clemente fault zone, located in the California Continental Borderland, is a long (>400 km), N40W-trending right-slip fault that is an active part of the Pacific-North America transform plate boundary. To understand the tectonic evolution of major restraining bends, we examine a 60-km long left bend of the San Clemente fault using a combination of high-resolution (Sea Beam) bathymetry and single-channel seismic reflection profiles. The 15 degree bend in the fault results in a broad asymmetrical seafloor uplift, higher on the shoreward (NE) side, that lies subparallel to the fault, but also appears bent and locally uneven in elevation. Maximum seafloor relief across the uplift ranges from 620 m to 660 m. Individual peaks of the anticlinorium are separated by saddles and represent right-stepping en echelon anticlines typical of dextral wrench faulting. The principal displacement zone of the active San Clemente fault mirrors the complex uplift pattern with an irregular "zig-zag" trace, where right-stepping en echelon fault segments are connected through local pull-apart basins. A beheaded submarine channel on the southeast (offshore) side of the fault may be offset 4-7 km (dextral) from relict submarine fan channels to the northeast. In the area of maximum relief, onlapping sedimentary sequences of the active Shepard submarine fan shows that the uplift began less than 1 Ma. Structural contour and isopach maps of a prominent late Quaternary (200-600 ka) hemipelagic layer combined with the tectonic interpretation of seafloor morphology suggests that the bend is

growing to the southeast into the flat-floored Descanso Plain, joining the transtensional N30W-trending San Isidro fault zone. West-trending fold axes and a north-trending graben on the east flank of the uplift are consistent with a zone of dextral simple shear along a northwest-trending fault. For a locked 60-km bend fault segment, large earthquakes ($M=7$, like 1989 Loma Prieta) may occur; larger ruptures extending beyond the bend (100-400+ km, $M=7.5-8.0$) are conceivable. Assuming an average slip rate of about 5 mm/yr, large earthquakes would have recurrence intervals of 300-800 years. In addition to the expected strong long-period shaking at adjacent coastal cities, coseismic seafloor uplift exceeding one meter along the bend region of the San Clemente fault poses a substantial local tsunami threat.

The 3-D Structure and Healing of the Landers Southern Rupture Zone and Preliminary Seismic Measurements at the Punchbowl Fault

Yong-Gong Li and Keiiti Aki
University of Southern California
John E. Vidale and Fei Xu
University of California, Los Angeles

We have delineated the 3-D internal structure of the Landers southern rupture zone using fault-zone trapped waves generated by aftershocks and near-surface explosions. Trapped waves were recorded at dense linear seismic arrays deployed across and along the surface breaks of the 1992 $M7.5$ Landers earthquake. Group velocities of trapped waves measured from multiple band-pass filtered seismograms for aftershocks occurring at different depths between 1.8 km and 8.2 km show an increase in velocity with depth. Group velocities range from 1.9 km/s at 4 Hz to 2.6 km/s at 1 Hz for shallow events while for deep events group velocities range from 2.3 km/s at 4 Hz to 3.1 km/s at 1 Hz. Coda-normalized spectral amplitudes of trapped waves decreased with distance between the source and receiver along the fault, giving an apparent Q of 30 for shallow events and 50 for deep events. We evaluated depth-dependent fault zone structure and its uncertainty from these measurements plus our previous results from explosion-excited trapped waves [Li et al., 1999] in a systematic model parameter-searching procedure using a 3-D finite difference computer code [Graves, 1996]. Our best model of the Landers fault zone is 250 m wide at the surface, tapering to 100-150 m at 8.2 km depth. The shear velocity within the fault zone increases from 1.0 km/s to 2.5 km/s and Q increases from 20 to 60 in this depth range. These values vary slightly along the fault. Fault zone shear velocities are reduced by 35-45% from those of surrounding rocks. Repeated seismic surveys at the Landers rupture zone showed an increase of velocities by 1.5-2.5% within the zone from 1994 to 1998, indicating that the Landers fault is strengthening, most likely because of closure of cracks that opened by the 1992 earthquake. We also found that the healing rate decreased in the later stage and was relatively high at the ends of the rupture zone.

Recently, we carried out a pilot seismic survey at the Punchbowl fault in the San Gabriel Mountains to measure seismic velocities around the fault process zone for comparison with the crack density distribution measured by Chester [1998]. The reverse seismic profiles across the fault show a velocity contrast between the granite rock on the SW side and the Punchbowl formation on the NE side of the fault. Seismic profiles also show that high frequency energy attenuated rapidly as waves pass the fault. We also notice a coherent phase likely reflected from the granite-sandstone contact. We will do more extensive seismic profiling at the Punchbowl fault in Fall of this year.

Analysis of the Spatial Distribution of Earthquake Locations With Point Correlation Functions

Shoshana Levin and Yehuda Ben-Zion, University of Southern California
Yan Kagan, University of California, Los Angeles

We analyze the quality of observed earthquake catalogs and calculate spatial point correlation functions of hypocenters in the catalogs. The primary goal is to find out whether the hypocenter locations reside on a branching fractal structure as suggested by Kagan [GJRAS, 1982], or whether the locations can be explained by a collection of more-or-less planar structures as is commonly assumed. A second goal is to attempt to characterize the evolution of fault structure (as manifested by the associated hypocenter locations) with cumulative slip and/or other variables. The work done so far is preliminary and involves calculating 2-point correlation functions in space of seismic activity in southern California. We analyze one catalog for the region as a whole and two sub catalogues focusing on the San Jacinto fault zone and the portion of the San Andreas fault stretching from San Bernardino to the junction with the Garlock fault. The calculated 2-point correlation functions for the three catalogs are compared to corresponding calculations for a synthetic catalog with a uniform random spatial event distribution. Our preliminary investigation of the quality of the southern California catalog acquired from CNSS suggests significant changes in the rate of activity recorded at various times over the last few decades. Many of these changes are probably related to alterations of the local network and we intend to examine the matter further. Continued research will include conducting 3-point and 4-point correlation studies of the data sets as well as catalogs for other regions. We will also calculate the point correlation function of synthetic catalogs representing a variety of fault structure models.

Paleoseismic Studies of the San Andreas Fault at Frazier Mountain

Scott Lindvall, William Lettis & Associates, Valencia
Timothy E. Dawson and Tom Rockwell, San Diego State University
J. Helms, William Lettis & Associates, Valencia

We continued in 1999 to develop the Mesa Valley Farm paleoseismic site located on the northeast flank of Frazier Mountain between the towns of Gorman and Frazier Park. The fundamental purpose of this study is to develop an event chronology for the Big Bend reach of the San Andreas fault (SAF). Comparing the timing of past large earthquakes at Frazier Mountain with other paleoseismic records northwest in the Carrizo Plain and southeast at Pallet Creek will allow us to critically test and better develop models of earthquake recurrence, fault segmentation, and behavior on the SAF, as well as provide much-needed physical constraints for models involving earthquake physics (Group F).

Following the 1998 El Nino winter season, the closed depression was inundated with up to 4 feet of standing water even as late as June of 1998. The resulting pond and saturated ground conditions prevented our opening fault trenches last year, and therefore our 1998 effort at this site concentrated on (1) dewatering activities, (2) site mapping, (3) radiocarbon dating, and (4) interpretation/analysis of our 1997 exploratory trench. This year, we were successful in dewatering the site and have now opened a trench across a principle strand of the fault that bisects the central portion of the pond. As we are now entering the driest part of the year, this field effort will continue through the fall.

Our 1997 exploratory trench exposed a ~2.5 meter section of well-stratified, distal fan and pond deposits, interrupted by two discontinuous, weakly developed buried A horizons. Two fault strands cut up section to the same paleosurface, located approximately 1.3 meters below the present ground surface. Six radiocarbon samples from units above, below, and within the event horizon share similar dates, with calendar ages between 1480-1650 AD (2s), thus these minor faults appear to have ruptured during this interval. An event during this period is also observed

at both the Bidart Site in the Carrizo Plain and at Pallet Creek and may correlate to the event at Frazier Mountain.

This year, our trench extends from the 1997 trench and has crossed a principle fault strand which bisects the sag pond and forms a subtle 30 cm high, north-facing scarp. In the trench, we observe evidence of fault displacement of units nearly to the surface: we attribute this faulting to the 1857 Fort Tejon earthquake. We do not observe evidence of an event between the 1857 event horizon and the ~1480-1650 AD event horizon. We believe that the 1812 AD earthquake probably did not rupture as far north as the Big Bend region: this is consistent with a Jeffery pine at Mill Potrero, which shows no disturbance of tree rings around 1812 AD, but were disturbed following the 1857 earthquake (Jacoby, 1998).

These new data support the idea that the San Andreas fault may have failed in prior 1857 type earthquakes. However, event dating at Frazier Mountain remains problematic since the penultimate event falls within a period of the 14C calibration curve with multiple intercepts. We believe that a combination of additional dates and statistical methods such as those employed by Biasi and Weldon (1994) will help further constrain the event chronology at the Frazier Mountain site. Furthermore, as the water table continues to fall, we plan to deepen the trench to explore for additional events. Dating of deeper units will clarify the chronology of this important site.

Modeling of Absorbing Boundaries and Q for 3-D Numerical Computations

Peng-Cheng Liu and Ralph Archuleta, University of California, Santa Barbara

We have improved the techniques for modeling absorbing boundaries and Q in the numerical time-domain computations of seismic wave fields. Many different techniques have been developed to simulate the absorbing boundaries. A common problem with these computations is that the more accurate they are the most likely they are to induce instabilities in the numerical computations. Following Higdon's (1991) technique, we express the boundary conditions as the composition of two first-order differential operators. However, we combine the first-order operator of Higdon (1991) for the absorption of the outgoing P-wave with the A1 absorbing condition of Clayton and Engquist (1977) for the outgoing S-wave. This new absorbing boundary condition is approximately second-order in accuracy. We implement it in the 3D finite element and finite difference (4th order in space) methods. No instability has been observed in our numerical calculations.

In the time-domain computations the effect of Q is currently simulated by a rational function of frequency. One can adjust the coefficients (weights and relaxation times) of this function to model different Q laws. The more relaxation times that are used the more accurate is the modeling of Q. However, the number of relaxation times is directly proportional to the storage requirements. We optimize both the weights and the relaxation times for the best modeling of a Q law while keeping the storage requirements as small as possible. By using two pairs of weights and relaxation times, we can simulate constant Q within 4 % tolerance over one decade in frequency and within 20% over two decades. If we use 4 pairs of weights and relaxation times, the misfit is less than 3% over two decades in frequency. We incorporate the modeling of Q into the numerical computation by using the coarse-grained method of Day (1998). We first optimize four pairs of weights and relaxation times for the minimum Q in the earth model. These relaxation times are then used for all other Q's in the model. Next we optimize the weights for the maximum Q. Linear interpolation of the weights between Q_{\min} and Q_{\max} determine all other weights. This scheme simulates constant Q within 4 % tolerance over two decades in frequency. It adds only a single memory variable, for each stress component, at every other node.

Analysis of Acoustic Emission and Stress-Strain Lab Data with a Damage Rheology Model

Yunfeng Liu, University of Southern California
Vladimir Lyakhovskiy, The Hebrew University, Jerusalem
Yehuda Ben-Zion, University of Southern California
Dave Lockner, United States Geological Survey, Menlo Park

Lyakhovskiy et al. [JGR, 1997] developed a damage rheology model to describe evolving non-linear properties of rocks under conditions of irreversible deformation. The model adds to the parameters of linear Hookean elasticity λ and μ a third parameter γ to account for the asymmetry of the response of rocks under loading or unloading conditions, and makes all three parameters a function of an evolving damage state variable α . Conceptually, damage evolution in rock deformation leading to brittle failure can be divided into the following three stages: frozen initial damage, distributed material degradation, and localization of damage culminating with macroscopic failure. In the first stage, the elastic moduli λ , μ and γ are all constant and γ equals to zero for damage-free rocks. During the second stage with distributed damage, effective moduli of stress-strain can be used to describe evolution of average elastic properties in the deforming solid. In the third localized stage, the heterogeneity of the material must be taken into account. The acoustic emission (AE) and stress-strain data of Lockner et al. [Academic Press, 1992] provide direct records for these three stages of rock deformation.

In this report we try to relate the damage rheology model of Lyakhovskiy et al. [1997] to the lab data of Lockner et al. [1992] for the first two stages of deformation. The results show a good agreement between model predictions and observations for the granite experiment G3. The curve of stress-strain deviates from linearity near the observed onset of AE. The lower limit of the faulting angle estimated from the damage rheology model using the onset of AE is 17.9° , which is slightly below the observed value $22 \pm 3^\circ$. Assuming that the actual onset of material degradation (damage increase) starts before the observed occurrence of AE events (weak events are probably missed) the predicted faulting angle is compatible with the observed value. The calculated stress-strain curve using evolving damage rheology moduli matches the observations well in most of the range between the onset of AE and observed localization of AE events.

Inversion of Teleseismic Receiver Functions via Evolutionary Programming

Chris Lynch, San Diego State University

Through the inversion of teleseismic receiver functions, we are able to make rough estimates of crustal velocity structure. In this study, I explored the use of evolutionary programming techniques to generate an evolving population of crustal velocity depth models. The goal is to produce a population of models that have converged upon an optimal solution for the structure of a given locality. By repeated application of this technique it is hoped to obtain a family of possible solutions that can then be analyzed by comparison with other data for a particular source region to determine the probable velocity depth structure of the region under investigation.

Enhancements to the Southern California Seismic Velocity Model

Harold Magistrale, San Diego State University

I am engaged in activities to enhance the SCEC southern California 3D seismic velocity model. These are: (1) adding geotechnical borehole constraints to the shallow portion of the model, (2) extending the model to include the Imperial Valley, and (3) refining and adding a variable depth Moho.

Geotechnical Constraints.

It is desirable to have well-constrained shallow properties in the southern California velocity model because near-surface seismic velocities can have a strong influence on earthquake ground motions, and it will greatly increase the utility of the model to the geotechnical community as a convenient and unique reference for near-surface properties. The data are S- and P-wave velocities and densities measured in boreholes by various organizations and compiled by W. Silva. The boreholes are tens to hundreds of meters deep and provide reasonable coverage over much of the heavily populated areas of the model. We are using a soil classification map developed by the CDMG and developing generic velocity-depth profiles for each soil type. The velocity-depth profile at a particular point will be a weighted combination of profiles from boreholes that are located nearby and within the same soil classification; a generic profile will be provided in cases when no nearby borehole data is available. We are developing separate V_p - V_s -density relations for each soil type. The geotechnical constraints will be cleverly blended with the deeper portion of the model to avoid artificial interfaces.

Imperial Valley

Extending the southern California velocity model to include the Imperial Valley is useful because it contains many potential earthquake sources and it influences regional wave propagation. I constructed a model of the Imperial Valley to include in Version 2 of the southern California velocity model. I digitized P-wave seismic velocity cross sections based on seismic refraction lines, and converted the cross section information into isovelocity surfaces. The model is generated by a code that reads the isovelocity surfaces and interpolates the velocity at any point of interest within the Imperial Valley; outside the Valley, the code assigns velocities interpolated from the tomographic results of E. Hauksson. This technique of blending basin models with tomographic velocities of basement rocks is to be used around all the basins in the Version 2 model. I've used the Imperial Valley model as a starting model for a local tomographic inversion.

Moho Configuration.

A well characterized, variable depth Moho is a desirable element of the southern California velocity model not only to accurately model the regional distribution of seismic velocities, but also to constrain models of the tectonic evolution of the region. We are defining Moho depths from existing receiver functions of teleseismic events (determined by L. Zhu) recorded on the Terrascope, Trinet, Anza, and temporary networks. Existing Moho models disagree, likely due to uncertainties in the crustal V_p and V_p/V_s values used. We are evaluating V_p/V_s found from (1) the timing of multiples found on the existing receiver functions, (2) regional tomographic studies, and (3) directly from Wadati diagrams of P- and S-wave arrival times recorded on the SCSN, which show V_p/V_s varying as a function of depth and geologic province. With the best crustal velocities, we will redetermine the Moho depths from the existing receiver functions, and produce a Moho surface to include in the Version 2 of the southern California velocity model.

Modeling Surface Wave Propagation: a Spherical Coordinate Finite-Difference Approach

Carey Marcinkovich and Toshiro Tanimoto, University of California, Santa Barbara

Short-period (<30s) surface waves are strongly influenced by the heterogeneous structure of the crust and upper-mantle, which results in complex propagation characteristics, such as refraction and contributions from diffractions. However, most surface wave analyses attribute waveform characteristics to vertical and lateral structural variations along great-circle paths between sources and receivers. Considering the sensitivity of short-period surface waves to shallow 3D structure, this is not an accurate description of their propagation. To begin addressing the problem of modeling complex features in surface waves we invoke the use of a finite-difference (FD) scheme. The FD method does not restrict propagation to invariant paths and naturally accommodates complexity in propagation due to heterogeneous velocity structure.

Propagation over regional to teleseismic distances requires consideration of sphericity; thus, we solve a spherical coordinate system of velocity-stress equations. We use a mixed order, staggered grid development and incorporate a planar free-surface, sponge style absorbing boundaries and a 6-component moment tensor source. Preliminary empirical dispersion analysis, for the spherical coordinate scheme, suggests a minimum of 10 grids per wavelength for the highest frequency is necessary to accurately reproduce waveforms. Test results between our FD scheme and Axitra, a robust spectral method, for basic faults in homogenous and layered media, are satisfactory. In addition, FD propagation in a PREM style velocity structure, with long-period (>100s) energy, yields excellent results.

Release of Version 2.0 of "Investigating Earthquakes through Regional Seismicity": <http://www.scecdc.scec.org/Module/module.html>

J. Marquis, K. Hafner and E. Hauksson, California Institute of Technology

We present the completed web-based module (version 2.0) on earthquakes for high school and undergraduate level earth science educational levels. This module has been designed for use in classrooms as part of an earth-science curriculum, with a storyline of concepts organized under the unifying concept of "The Earth is constantly changing." Version 2.0 of the module consists of the following three sections: "What is an Earthquake?" released in version 1.0 last year, "The Distribution of Earthquakes," which has been greatly expanded since last year's release, and the newly released third section, "Measuring Earthquakes." This final section focuses on the methods used to record and calculate the properties (location, magnitude, etc.) of earthquakes. Scientists and educators alike have reviewed the content and format of this module, and portions of the module have been field tested in high school and community college settings.

The module's setup also allows it to stand alone as a user-friendly WWW-based resource for basic seismological information. This resource can be used by students working on independent research projects, by science teachers wanting to increase their knowledge about earthquakes, and by the interested public. Each main section topic consists of a sequence of pages -- explanatory text and inline images -- hyperlinked to activities that explore concepts in greater depth, and in a graphical, interactive manner. Many of these activities themselves are linked to separate, related on-line resources (e.g. fault maps) and interfaces that provide access to seismological data archived at the SCEC Data Center. This interconnection, combined with the module's accessibility on the World Wide Web, ensures that this educational module contains more than just static information about earthquakes. The "real-time" accessibility to earthquake data provides an educational experience for all "students" that relates earthquakes to the world around them.

Geodetic Constraints on Deformation in the Southern Walker Lane Belt, California

S. McClusky (1), S. Bjornstad (2), B. Hager (1), E. Hearn (1), R. King (1),
B. Meade (1), M. Miller (3), F. Monastero (2), B. Souter (1)

(1) Massachusetts Institute of Technology
(2) Geothermal Program Office, Naval Air Weapons Center, China Lake
(3) Dept. of Geology, Central Washington University

Recent modeling [Hearn and Humphreys, 1999] has addressed the consistency between geological slip-rate estimates for active faults and geodetic constraints on crustal motions in the southern Walker Lane Belt (WLB). Because the deformation in the WLB in this model is constrained mainly by the VLBI velocities at Goldstone and Owens Valley, questions remain regarding the distribution of strain on structures within the region, particularly south of Owens Valley. To obtain a more detailed map of deformation, we have analyzed GPS data from 35 stations surveyed by the Navy Geothermal Program at China Lake and the National Imaging and Mapping Agency detachment at Edwards AFB between 1994 and 1999, and 20 stations surveyed by Central Washington University between 1991 and 1998.

To compare geologic slip rates and geodetic velocities, we constructed a block model for the Walker Lane belt and adjacent regions. This model includes the effects of elastic strain accumulation on the faults that bound the blocks while satisfying the path-integral constraint. We find 11 mm/yr of dextral shear between the southern Great Basin and the Sierra Block, in the north, slip partitions 3, 1, and 7 mm/yr on the Furnace Creek, Hunter Mountain, and Owens Valley faults, respectively. Just north of the Garlock fault, the dominant shear, 5 mm/yr, occurs through the Indian Wells Valley, with 3, 1, and 2 mm/yr on the Death Valley fault, Panamint Valley fault, and through the Argus Range. Our model places less than 2 mm/yr sinistral shear on the Garlock fault along all segments east of the southeast terminus of the Sierra Block. The most notable misfits to the model occur for the Coso geothermal field, for a zone of unmodeled extension immediately to its north, and for four stations in the eastern and central Mojave, whose motions suggest block rotations and/or post-Landers deformation.

Thickness of the Seismogenic Crust in Southern California: Constraints from Seismicity

Julie J. Nazareth and Egill Hauksson, California Institute of Technology

We seek to provide a detailed quantitative constraint for the thickness of the seismogenic crust for moderate to large earthquakes in southern California. Although the thickness of the seismogenic crust is an important parameter in seismic hazard analysis, it has never been determined systematically for southern California. For example, the SCEC Working Group on California Earthquake Probabilities (1995) assumed a value of 11 km for the seismogenic crust because it predicted an acceptable total seismic moment rate for the region. If the seismogenic thickness is correctly determined, other aspects of hazards models can be improved and possibly the overall uncertainty reduced.

We propose to use the distribution of the moment release with depth of the background seismicity to estimate the upper and lower depth limits for rupture during moderate to large earthquakes. We plan to produce detailed regional maps and along strike measurements of seismogenic crustal thickness for SCEC class A and B earthquake sources. To show that this approach is reasonable, we compare the moment release distribution of the pre-mainshock seismicity to that of the mainshock for a number of earthquakes in southern California. Preliminary results for the 1992 Landers earthquake show that the 11 years of seismicity prior to the mainshock has approximately the same proportion of moment release at depth as the

mainshock, with little pre-mainshock moment release below the bottom of the finite source model at 15 km.

Site Amplification in the Los Angeles Basin from 3D Modeling of Ground Motion

Kim Olsen, University of California, Santa Barbara

We have used 0-0.5 Hz finite-difference, finite-fault simulations to estimate the three-dimensional (3D) response of the Los Angeles basin to nine different earthquake scenarios. Amplification is quantified as the peak velocity obtained from the 3D simulation divided by that predicted using a regional one-dimensional (1D) crustal model. Average amplification factors are up to a factor of 4, with the values from individual scenarios typically differing by as much as a factor of 2.5. The average amplification correlates with basin depth, with values near unity at sites above sediments with thickness less than 2 km, and up to factors near 6 above the deepest and steepest-dipping parts of the basin. There is also some indication that amplification factors are greater for events located farther from the basin edge. If the 3D amplification factors are divided by the 1D vertical SH-wave amplification below each site, they are lowered by up to a factor of 1.7. The duration of shaking in the 3D model is found to be longer, by more than 60 seconds in some areas for some scenarios, relative to the 1D basin response. The simulation of the 1994 Northridge earthquake reproduces recorded 0-0.5 Hz particle velocities relatively well, in particular at near-source stations. The synthetic and observed peak velocities agree within a factor of two and the log standard deviation of the residuals is 0.37. This is a reduction of 45% compared to the overall regression value for pseudoacceleration response spectra obtained by Boore et al. (1997) at 0.5 Hz. This result suggests that long-period ground motion estimation can be improved considerably by including the 3D basin structure.

Criticality of Earthquake Rupture Dynamics

Kim Olsen, University of California, Santa Barbara
Raul Madariaga, Ecole Normale Supérieure, Paris

We study the propagation of seismic ruptures along a fault surface subject to a heterogeneous stress distribution and/or inhomogeneous frictional parameters. When prestress is uniform, rupture propagation is simple but presents some non-trivial differences with the circular shear crack models of Kostrov. The best known difference is that rupture can start only from a finite initial patch (or asperity). The other difference is that rupture is asymmetric with the rupture front elongated in the inplane direction. If the initial stress is sufficiently high, the rupture front makes a transition to super-shear speeds. For simple rectangular faults or asperities rupture propagation is clearly controlled by the width of the fault or asperity. When stress or strength are heterogeneous rupture propagation changes completely and is controlled by local length scales in the initial stress distribution as well as rupture resistance. Thus short rise times (Heaton pulses), rupture arrest, stopping phases, etc reflect the length scales of the stress and strength distributions. Through a number of numerical experiments we have identified a non-dimensional parameter that controls rupture. This parameter measures the ratio of local available strain energy to fracture energy derived from the friction law. A bifurcation occurs when this parameter is greater than a certain critical value that depends mildly on the geometry of the stress distribution on the fault. We have verified that the non-dimensional parameter, computed using frictional parameters determined by different studies for several recent earthquakes (e.g., the 1992 Landers event) are near the critical value. Our results suggest that earthquakes are critical phenomena controlled by a single local non-dimensional number.

CRUST AND MANTLE STRUCTURE BENEATH THE LOS ANGELES BASIN AND VICINITY: CONSTRAINTS FROM GRAVITY AND SEISMIC VELOCITIES

Mousumi Roy, University of New Mexico
Robert Clayton, California Institute of Technology

We use Bouguer gravity data to provide an independent constraint on the regional 3-D seismic velocity structure of the crust in the Los Angeles basin and surrounding areas. The regional 3-D seismic velocity model, which was developed as part of the efforts of the Southern California Earthquake Center (SCEC) in 1997-99, is used to construct a 3-D density model of the crust using empirical scaling relations. The regional Moho structure is based on teleseismic studies by Zhu and Helmberger. The resulting density structure is used in a forward model to predict the regional gravity field. By comparing the predicted and observed gravity fields, we test the consistency of the seismic velocity model with the gravity data, and thus provide an independent geophysical constraint on crustal tomography and on the empirical scaling relations between velocity and density.

We find that the SCEC 3-D velocity model adequately represents first-order variations in the crustal density structure, including the Los Angeles and San Fernando basins and the Transverse Ranges. The short-wavelength (shallow crustal) features of the gravity are well matched by the velocity-based density model, although we detect systematic deviations in the predicted and observed gravity fields. This is particularly obvious in the Los Angeles basin, where the predicted and observed gravity minima over the basin are rotated with respect to each other. In addition, the predicted gravity anomaly over the San Fernando basin is shifted northwards with respect to the observed anomaly. We investigate the implications of such misfits on both the density model (particularly in the shallow sub-surface) and on the empirical scaling relations between velocity and density.

ULTRA STRONG ASPERITIES AT PARKFIELD? MAYBE NOT.

Charles G. Sammis, Youlin Chen, Yehuda Ben-Zion
University of Southern California

By combining the seismic moments of repeating earthquakes on the San Andreas Fault in central California with geodetic data, Nadeau and Johnson (1998) were able to calculate the area and displacement of the individual events. They analyzed 53 repeating sequences at Parkfield having magnitudes in the range -0.7 to 1.4 as well as 8 similar but larger sequences from the Stone Canyon section of the fault and the main sequence at Parkfield. The smallest events were found to have occurred on patches having a linear dimension on the order of 0.5 m and displacement of about 1 cm. Using these parameters in an elastic crack model yields stress-drops on the order of 2000 MPa, roughly ten times larger than rock strengths measured in the laboratory. Stress-drops calculated in this way decrease as a power law of the seismic moment reaching the commonly observed value of 10 MPa at about magnitude 6 . The inferred decrease of stress-drop with increasing magnitude follows from the scaling observed by Nadeau and Johnson in which the displacement d varies with area as $A^{0.20}$. In order to have constant stress drop, the crack model requires that d vary as $A^{0.5}$. Although Sammis et al. (1999) argued that the large strengths required by the small events can not be ruled out on physical grounds, we now suggest that they may be an artifact of using a crack in an elastic medium to model an elastic asperity in an otherwise creeping fault zone. We show here that when the repeating patches are modeled as asperities that are loaded by creep on the surrounding fault, d is predicted to vary as $A^{0.25}$ and high stress drops are no longer inferred for the small events. This result is obtained using analytic stress intensity factors and also by numerical simulation using a 3-D elastic fault model.

4D Fault-Zone Properties on the Duzce Branch of the North Anatolian Fault System Ruptured in the August 1999 Izmit, Turkey, Earthquake

Leonardo Seeber and John G. Armbruster, Lamont-Doherty Earth Observatory
Yehuda Ben-Zion, David Okaya and Ned Field, University of Southern California
Andrew J. Michael, United States Geological Survey/Menlo Park
Mustafa Aktar, Kandilli Institute of Bogazici University, Istanbul
Naside Ozer, Istanbul University, Istanbul

The August 17, 1999, Izmit Mw7.4 earthquake rupture is traced for about 100km at the surface and may continue westward under the Marmara Sea for as much as 70 km. Two distinct contiguous strands of the North Anatolian fault system are involved. Rupture nucleation and maximum observed slip (4.5m) are on the longer segment which is mostly westward of the 1967 rupture along the main northern branch of the system. The shorter (≈ 30 km) segment is along a minor strand of the system, the Düzce fault, which overlaps with the 1967 rupture. The North Anatolian and San Andreas continental transforms in western Turkey and in southern and central California, respectively, are similarly multi-stranded. The overlapping and intersecting 1967 and 1999 ruptures in western Anatolia resemble in geometry and scale the San Andreas and San Jacinto faults in southern California and the San Andreas and San Gregorio faults west of San Francisco in central California.

In the days following the Mw7.4 earthquake we deployed a 10-station PASSCAL seismic network along and around the Düzce fault. That segment of the rupture cuts through exposed pre-Quaternary rocks and had 1.3-1.5 m of right lateral surface slip. The deployment aims to record seismic fault zone guided waves and split S waves and to provide accurate locations of the aftershock sources. The goals are: (1) To correlate segmentation and other structural complexities at the surface with structure at depth as inferred from propagation pattern and waveform modeling of fault zone guided waves, and high quality aftershock locations. (2) To examine non-linear wave propagation effects in the damaged fault zone rock by comparing seismograms from small and large aftershocks. (3) To examine ground motion amplification in and around the fault zone. (4) To examine post seismic temporal evolution of fault zone properties by comparing measurements over the first two months of the postseismic period. Preliminary analysis shows an abundance of high quality waveforms, candidate fault zone guided waves and shear waves splitting at sites on the rupture. Results will be discussed at the meeting.

We acknowledge the remarkable hospitality and cooperation by Turkish scientists and people amidst great tragedy. We especially thank A. M. Isikara, Serif Baris, Mustafa Erdik, and Cemil Gürbüz for highly efficient help with facilities, logistics, and field work.

Constructing More Accurate Chronologies by C-14 Dating of Different Peat Fractions

Gordon G. Seitz¹, John R. Southon¹, Ray J. Weldon² and, Tom E. Fumal³
1 Lawrence Livermore National Laboratory
2 University of Oregon
3 U.S. Geological Survey, Menlo Park

Peat-bearing site chronologies provide the highest resolution chronologies not only due to the abundance of datable material, but perhaps more importantly because the context uncertainty is low due to in situ formed organic matter. This is observed by the relatively high degree of stratigraphic consistency of C-14 dated peat chronologies compared to detrital charcoal chronologies, and typically results in refined layer date estimates with precision of 20 to 60 years. While most of the C-14 dates at the 3 best-dated San Andreas Fault paleoseismic sites, Pallett Creek (75 dates; Sieh et al., 1989), Wrightwood (92 dates; Fumal et al., 1993), and Pitman

Canyon (42 dates; Seitz, 1999) are stratigraphically consistent, about one third of the dates are temporally and stratigraphically inconsistent. Since no clear criteria have been identified to select the "true" dates the scatter in dates has resulted in less certain chronologies. We anticipate that the results of this investigation will ultimately lead to more accurate chronologies by identifying the most reliable fractions for C-14 dating.

We have previously recognized the effect of C-14 laboratory pretreatments resulting in significantly different ages (Seitz et al., 1998), and are now investigating this in greater detail. In general we have discovered that the "acid only" (AO) pretreated dates show greater stratigraphic consistency. We attribute this to the majority of the carbon fraction, which is dated being derived from in situ formed organic matter. The acid only pretreated sample may well include a minor possibly different age humin fraction. A typical dated carbon mass balance in these peats is 85% in the humic acid and 15% in the residual humin. Thus the all too often recommended more aggressive "full" pretreatment (AAA-acid-alkali-acid), consisting of varying cycles of acid and base washes can concentrate an older carbon fraction by effectively removing the in situ formed organic matter. We will present results, which will include AMS C-14 dated AO, AAA, humic acid precipitate, and macro fossil fractions from the Pitman Canyon and Wrightwood sites.

Considering that this pretreatment related age effect may only be recognized at sites with multiple closely-spaced dated samples, we make the following recommendations: 1) For new sites date the various isolated peat fractions, and determine the existence, extent and nature of contamination. The humic acid precipitate and the residual humin dates should be compared; 2) Report C-14 pretreatments, and consider them when evaluating existing chronologies.

Work was performed in part under the auspices of the Department of Energy at Lawrence Livermore National Laboratory under contract W-7405-ENG-48.

Structural and Seismologic Investigations of Concealed Earthquake Sources in the Los Angeles Metropolitan Area

John H. Shaw, M. Peter Seuss, and Carlos Rivero, Harvard University

We report on progress of three related efforts to define concealed earthquake sources in southern California:

Regional Seismic Transect

Using 2 and 3D reflection data acquired by the petroleum industry, we have assembled a nearly contiguous seismic transect across the central Los Angeles basin and San Pedro Bay. This transect images several potential earthquake sources, including the Palos Verdes, THUMS-Huntington Beach, Compton-Los Alamitos, Newport-Inglewood, Puente Hills, Elysian Park, and Whittier faults. This profile is depth converted using borehole sonic and stacking velocity data, and will be combined with well data and relocated seismicity (E. Hauksson) to characterize active fault systems. The transect provides important insights into the nature of blind-thrust faults and their interactions with active strike-slip systems.

Oceanside Thrust

We define the Oceanside blind thrust as a massive, east-dipping fault system that extends offshore from Los Angeles to San Diego using industry reflection data, precisely relocated seismicity, and 3D structural models. The Oceanside structure originated as a low-angle normal fault, and has been reactivated with thrust motions in the Pliocene. Forward- and back-thrust splays above this fault produce folds and localized deformations offshore and along the coast in the San Joaquin Hills (L. Grant, K. Mueller). The fault may extend beneath the Peninsular Ranges and produce uplift of the California coast south of Los Angeles that is recorded by marine terraces. We also map the San Diego thrust, which is akin to the Oceanside fault. Using new 3D velocity models and precisely relocated seismicity (L. Astiz & P. Shearer), we associate

the San Diego thrust with the 1986 Oceanside (M_L=5.3) earthquake. This establishes the activity of these offshore thrust systems, which may pose substantial earthquake hazards to metropolitan areas of southern California.

Contributions to SCEC 3D Velocity Modeling Effort

We present comparisons of the SCEC 3D Velocity model with borehole sonic and industry stacking velocity data in the Los Angeles basin. In addition, we provide four new velocity functions for the northern San Fernando basin that correspond to SCSN station locations. These functions and data from 10 sonic logs will be added to the Data Repository that is currently available to the SCEC community through our webpage (<http://structure.harvard.edu>).

Improving Southern California Geodetic Velocity Map 2.0

Zheng-kang Shen, University of California, Los Angeles

A major goal of the Southern California Earthquake Center (SCEC) is to map the crustal deformation field and relate it to regional seismic potential. The deformation field has been released and then revised (http://www.scecdc.scec.org/group_e/release.v2), and another update is underway. In the current update we plan to include all the important geodetic measurements collected in southern California during the past 30 years and available to us, including electronic distance meter (EDM), very long interferometry baseline (VLBI), and global positioning system (GPS) data. Although the EDM and VLBI data have longer observational histories, the largest contribution, in terms of the spatial coverage and the precision of the derived station velocities, comes from GPS measurements. SCEC is conducting surveys to remeasure about 150 GPS stations in southern California this year. Inclusion of these data enhances resolution, particularly in the Los Angeles basin region. Data from both the survey mode and permanent (SCIGN) GPS networks are processed together uniformly, and station velocities and coseismic displacements are derived in a global reference frame. Stations whose post-seismic velocities may have been perturbed by the Landers earthquake are allowed to have different secular velocities before and after the earthquake. All together the network has about 400 stations covering most of the major faults in southern California, with their horizontal station velocity uncertainties < 4 mm/yr. About 2/3 of the sites have their uncertainties < 2 mm/yr. Although a complete update of the solution will not be completed until the end of this fiscal year, we will show some intermediate results at this annual meeting. Data sets first time to be included in the solution are the Landers 1997-1998, Ventura Basin 1993, Cholame 1989, Caltrans District 7 1992, and post-Northridge joint survey 1994. The last two data sets will be useful for a complete update of the Northridge co-seismic solution.

Rapid Subsidence, the Offshore Santa Monica (Dume) Fault, and the Santa Monica Mountains Blind Thrust

Christopher C. Sorlien, University of California, Santa Barbara
Nicholas Pinter, Southern Illinois University
Leonardo Seeber, Lamont-Doherty Earth Observatory of Columbia University

The surface trace of the Santa Monica fault splits near the coastline into the Malibu Coast fault and the Dume fault. We used a grid of industry seismic reflection data to map the Malibu Coast fault directly into the Santa Cruz Island fault. The combined fault is 200 km-long, is left-lateral with a reverse component, and does not have any known kilometer-scale breaks in continuity. The Dume fault west of its intersection with the Palos Verdes fault near Pt. Dume has a 700 m-high sea-floor fault/fold scarp and ~2 km vertical separation of the youngest pre-fold horizon. South of Port Hueneme, the sea-floor scarp height decreases from 700 m to zero within

a 4 km distance, where the Dume fault bends sharply southwest. This bend is associated with a 10 km south advance of the thrust front that is in turn associated with the structural saddle between the Santa Monica Mountains and northern Channel Islands. Minor subsurface folding along the NE-SW segment of the Dume fault and the major shortening across the E-W segment indicates relative south-southwest displacement of the hanging wall. Identification of the age of the map horizon at wells near Pt. Dume, completion of a structure-contour map, and use of the software Unfold on the resulting digital map will allow the rate of displacement to be quantified. A very gently N-dipping fault, the Santa Monica Mountains "thrust", is imaged south of and beneath the Dume fault. This fault preserves normal separation of presumed Miocene strata, and is probably a major strand of the extensional detachment fault system responsible for rotation of the western Transverse Ranges. Subtle folding south of the Dume scarp indicates reactivation of this fault. Seismicity east of Point Dume through northern Los Angeles basin illuminates an active mid-crustal blind thrust that is aligned with or beneath the fault imaged on the seismic reflection data (Geiser and Seeber, 1996). Evidently, much of the slip on the deep Santa Monica Mountains thrust comes to the surface along the Dume fault.

Our work along the flanks of the northern Channel Islands anticline indicates large scale regional subsidence unrelated to sediment compaction. Cliniform rollovers ("paleo-shelf breaks") of low stand deltas north of the islands, correlated to be less than 1 Ma, have subsided between 150 and 400 m (from presumed low-strand eustatic sea levels of -100 m). This subsidence and uplift of the islands indicates a progressive north tilt. Projecting this tilt to the north edge of the fold indicates subsidence in the range 0.5 to 1 mm/yr. Evidence for subsidence is also seen south, west, and east of the northern Channel Islands. For example, the northwest part of the Santa Cruz-Catalina Ridge appears wave-eroded and is now at 700-800 m depth, and an unconformity along the crest of the anticline between the Santa Monica Mountains and Anacapa Island is now at 400 m depth. We interpret this regional subsidence to be an isostatic response to surface uplift of the Islands and the Santa Monica Mountains. Vertical motion of the hanging wall north of the Dume fault is the sum of this isostatic subsidence plus uplift due to thrust motion. This sum is near zero on the shelf southwest of Pt. Dume. Uplift of coastal terraces of the Malibu coastline needs to be measured with respect to an isostatically-subsiding base level, and not with respect to sea level, when evaluating activity on the Dume fault and on the Santa Monica Mountains thrust.

Reference: Geiser, P., and Seeber, L, 1996, Three-Dimensional Seismo-Tectonic imaging in the Transverse Ranges: the Santa Monica Seismic Zone (SMSZ) and evidence for a critical wedge, EOS, (Trans. AGU), v. 77, no. 46, p.F738

GROUND MOTION MODELING USING SCEC BOREHOLE INSTRUMENTATION

Jamison H. Steidl, L. Fabian Bonilla, and Ralph J. Archuleta
University of California at Santa Barbara

In March of 1997 a workshop was held to discuss the initiation of a borehole instrumentation program within SCEC to be coordinated with other ongoing drilling programs in Southern California. Shortly after the workshop the first year of the program was approved with three borehole sites planned for the first year, and three per year proposed for the following three years. The long term scientific objectives of this program are: to estimate the degree of nonlinearity for strong ground shaking on typical Southern California soils; to improve our capabilities in predicting the effects of near-surface soil conditions on ground motions; and to examine the details of the earthquake source process.

This marks the third year of the borehole instrumentation program. To date, seven boreholes have been drilled, logged and sampled for near-surface soil properties, and cased for deployment of the permanent borehole instrumentation. Four of the seven boreholes have been instrumented and are providing data real-time to the Caltech/USGS Southern California Seismic Network (SCSN). This data is available via the SCEC data center archive. These four boreholes

are located on the exterior of the Los Angeles basin, three to the north within the Santa Monica Mtns. in a linear array with about 7 km spacing, and the fourth to the south-west on the Palos Verdes Peninsula. A fifth borehole located at the CDMG California strong motion instrumentation program (CSMIP) Obregon Park site in the LA Basin should be instrumented this fall and data will be streamed real-time to both the SCSN and CDMG in Sacramento. A 350 meter deep borehole has been drilled and cased in the LA Basin at the Long Beach water reclamation plant, and along with a shallow 30 meter borehole at the same location, will be instrumented this fall/winter. This vertical array will provide critical data on the soil behavior of a "typical" LA Basin site in both the small and large strain regimes as the waves propagate up through the soil column.

Borehole and surface observations from this project, and a second SCEC funded project using portable borehole instrumentation at the Van Norman Dam site in the San Fernando Valley, are used to calibrate the current numerical wave-propagation methods for predicting soil response. This data is also being used for development of new nonlinear modeling techniques for the behavior of soils under large strains. Using the borehole data as the input to our linear models, and the geotechnical site characterization data provided under collaboration with the ROSRINE project, we are able to reproduce the surface observations in the time, frequency, and response spectral domains for frequencies up to 10 Hz. The degree of non-linear behavior in California soils at large strain levels is a critical issue for determining the maximum plausible ground motions from large earthquakes. However, the lack of observed large-strain data from these new borehole sites in Southern California forces us to calibrate our nonlinear models with data from other regions. We will show results using the Port Island vertical array observations from the Hyogo-ken Nambu (Kobe) earthquake to test our newly developed nonlinear soil behavior models.

Recent Rupture History of the San Andreas Fault Southeast of Cholame in the Northern Carrizo Plain, California

Elizabeth Stone and J. Ramon Arrowsmith, Arizona State University
Lisa B. Grant, University of California, Irvine

We conducted a paleoseismic study on the San Andreas fault southeast of Cholame, CA to investigate the record of earthquakes within an 80 km data gap between Parkfield and the Carrizo Plain. The only data previously available for this area were ambiguous geomorphic offsets. The site excavated is the LY4 site, located approximately 37.5 km southeast of Cholame. This site is on an alluvial fan that emanates from the Temblor Mountains and crosses the fault trace at the distal end of the fan. We excavated a 20-m-long and 3-m-deep trench perpendicular to the fault. We found evidence of four ruptures within the past 931-715 yrs. The oldest event, C4, caused apparent normal offset that is only present in the lower half of the trench. Event C3 is based on fracturing which is truncated above event C4 and had no apparent vertical displacement. The units ruptured by events C3 and C4 are not continuous across the fault zone. Event C2 is inferred because lower units that cross the fault are offset with an apparent normal sense of slip while those above are not. The event horizon C1 does not have an apparent vertical sense of offset and is defined by fractures that terminate above C2. Because of limitations in the production and preservation of datable material, the only age constraint is on a paleosol two units below the fourth event horizon. Two samples from this layer have a summary 2 sigma age range of 881-665 cal BP.

Paleoseismic sites in the Carrizo Plain contain five ruptures during the last 900 years. The geomorphic offsets in the Carrizo Plain were larger than the offsets southeast of Cholame during the 1857 Fort Tejon earthquake. The characteristic earthquake model, a model often used to consider earthquake recurrence, states that ruptures along a particular fault segment recur at similar magnitudes and with similar offsets. If there is a uniform slip rate on these segments, then this model suggests that there should be more frequent earthquakes on the Cholame segment

with smaller offsets. However, our findings imply that the San Andreas fault in the Carrizo may have actually ruptured more frequently than along the Cholame. Rupture scenarios that link the Cholame ruptures with Carrizo earthquakes fail to maintain a uniform slip rate if the offsets are characteristic, given this result. Scenarios that link Cholame ruptures with Parkfield earthquakes do not conform to a characteristic rupture length of the Carrizo events such as experienced in 1857. This abstract was also submitted to the Fall AGU meeting.

Evidence for the Most Recent Rupture of the San Bernardino Strand, San Andreas Fault in the 13th to 15th Century AD, Burro Flats near Banning, California

Ashley Streig, Occidental College

The San Bernardino strand of the San Andreas fault has not ruptured in historic time. A trenchsite at Burro Flats near Banning, CA shows convincing structural and stratigraphic relationships that constrain the most recent event on this fault to have occurred in the 13th to 15th century AD. There was no evidence for younger events. Structural evidence includes truncation, and apparent offset of units. Stratigraphic evidence includes a north-facing fault scarp, and an onlap sequence of silt and fine layered (1mm) peat layers. Samples that loosely bracket the event horizon include two samples of peaty soil, and one sample of horizontal plant fibers in peat. Calibrated calendar ages constrain the event to have occurred between ~A.D. 1225 - 1460. This timing overlaps in age with the two most recent events described from the same fault strand at Plunge Creek near San Bernardino, CA (Dergham and McGill, 1998 SCEC Annual Meeting). One of the two events described from Plunge Creek may be eliminated with a more precise age determination of the event at Burro Flats. No evidence exists at Burro Flats for younger ruptures that correspond to either the A.D. 1700 or 1812 events found in the Wrightwood, Pitman Canyon and Pallett Creek areas. Furthermore, evidence of the A.D. 1680 event at Indio does not appear at Burro Flats. The behavior of the San Andreas fault at Burro Flats therefore appears to be in striking contrast to the fault's behavior to the northwest and southeast, at Wrightwood and Indio, respectively. Assuming a conservative slip rate of 10mm/year for the San Bernardino strand, the amount of strain accumulated on the fault could exceed 5m since the last event.

MODELING AND OBSERVATION OF WEAK AND STRONG GROUND MOTION INCLUDING NONLINEARITY

Feng Su, Yuehua Zeng, John G. Anderson
University of Nevada-Reno

Recent studies of the Northridge earthquake sequence at co-located weak and strong motion sites (Field et al, 1997, Su et al, 1998) have found strong evidence of nonlinear site response during the Northridge mainshock at stations near the epicentral area. In this study, we compared these observations with the model prediction of EPRI (1993) for nonlinear soil response. Our previous observation finds significant nonlinear soil response in the near epicentral area at the frequency band of 0.5 to 14 Hz. The model matches the observation well for the frequency range from 1.5 to 10 Hz. However, it diverged from the observation in frequencies below 1.5 Hz and above 10 Hz. At frequencies below 1.5 Hz, the data show continuous nonlinear deamplification in contrast to the model prediction. At frequencies above 10 Hz, the model generated additional high frequency energy which is actually an artifact of the nonlinear stress-strain relationship used. Nevertheless, it improves synthetic predictions. For peak ground motion parameters, the error between the synthetic prediction and the observation is significantly smaller than that of the regression prediction.

We also estimated the spectral attenuation parameter Kappa at these co-located weak and strong motion sites. The result suggests significant source effects on kappa estimates in addition to the path and site effects. After-shocks recorded at two closely spaced stations in Tarzana show about 20-30 msec of highly correlated variability in measurements of kappa after an adjustment for the attenuation between the source and receiver. The correlation is most easily explained if the cause of the variability is in the source region. For sites exhibit strong nonlinear site response, i.e., their peak ground accelerations exceeds 0.3g (Su et al., 1998), their kappa estimates from the weak motions are much greater than the corresponding values measured from the strong motion records, suggesting that kappa measurements may also be a function of nonlinear site response.

TECTONIC GEOMORPHOLOGY OF THE SANTA YNEZ MOUNTAINS, CALIFORNIA

Timothy Tierney, University of California, Santa Barbara

The Santa Ynez Mountains comprise the westernmost extremity of the Transverse Ranges. Rigorous tectonic geomorphic analysis utilizes a suite of geomorphic indicators of active tectonics. With the aid of a digital elevation model (DEM), topographic, geologic and geomorphic analyses including: mountainfront sinuosity, stream-length indices, and valley width/height ratios are being applied along the lateral extent of the range in order to identify relative tectonic activity within the range. Research questions include : 1) Is the range deformed by shortening and folding in the Holocene and late Pleistocene? 2) What are the relationships between rock resistance and topography and tectonics? 3) What is the drainage history of the range, and has the range propagated laterally during its evolution?

The State of Strain Accumulation in the Western US

B. Shen-Tu and W. E. Holt

State University of New York, Stony Brook

Quantifying the distribution of strain accumulation within a plate boundary zone is an essential step towards the estimation of the location and size of future large earthquakes. In this study we present a simple approach to quantify the distribution of current strain accumulation in the western United States plate boundary zone. We first inferred the minimal strain accumulation at the beginning of the historic earthquake catalog (1850). The strain accumulation since 1850 is then determined by integrating the velocity gradient tensor field [Shen-Tu et al., 1998, 1999] for the western US over time, while satisfying the spatial and temporal distribution of seismic strain release within the plate boundary zone over the past 148 years. The initial and final state of strain accumulation is determined iteratively. The highest current strain accumulation lies in the area containing the southern San Andreas fault, which is consistent with the area that has the highest Coulomb stress change since 1812 estimated based on a Coulomb stress model [Deng and Sykes, 1997a, 1997b]. The equivalent seismic moment accumulation within a 11-km seismogenic layer in this area is large enough to generate an $M_w = 7.6$ or 3 $M_w = 7.2$ events. Strain accumulation in the areas containing the Carrizo - Big Bend - Mojave segment of the San Andreas fault, and the Western Transverse Ranges are also large enough to generate an $M_w = 7.0$ event along each 50-km long fault segment. The accumulated strain along major active faults in the San Francisco Bay area (the San Andreas fault, Calaveras fault, Hayward fault, Rogers Creek fault), along the San Gregorio-Hosgri fault zone, in Santa Barbara Channel, and in the Salton Sea areas are capable of generating 6 -7.0 events. The total current moment accumulation in the plate boundary zone is 2.5×10^{28} dyne cm, which exceeds the moment accumulation in 1850 by about 6.7×10^{27} dyne cm, and is mainly concentrated along the San Andreas fault zone and its vicinity.

PALEOSEISMIC RESULTS FROM THE EASTERN SIERRA MADRE FAULT, SAN DIMAS, CA: AN EARLY TO MID-HOLOCENE AGE FOR MOST RECENT SURFACE RUPTURE

Allan Z. Tucker and James F. Dolan, University of Southern California

One of the most important questions facing seismic hazard planners in metropolitan southern California concerns the hazard associated with large reverse-fault earthquakes. During June, 1998, we excavated a 60-m-long trench and a transect of seven 11-25 m deep bucket auger holes across one of the largest of these reverse faults, the Sierra Madre fault, in San Dimas, CA, near the east end of the fault. The trench revealed a 25-north-dipping fault that is traceable as a planar feature to >20 m depth in the bucket-auger transect. Miocene Puente Formation mudstone crops out above the fault, which is characterized by a 30-cm-thick clay gouge zone. The faulted strata are truncated and overlain by a 4-m-thick section of gently south dipping alluvial sands and gravels. Three detrital charcoal samples from the lowest meter of the unfaulted strata yielded ¹⁴C dates of 5.1 ka to 7.3 ka, in correct stratigraphic sequence. A fourth detrital charcoal sample obtained from a bed that has experienced at least 10 m of reverse slip yielded a ¹⁴C date of 20 ka. The very long current quiescent interval at this site (7000 years), coupled with the minimum 10 m of displacement that occurred at this site between 20 ka and 7 ka, is consistent with the occurrence of very large, but infrequent earthquakes. The San Dimas site data are thus consistent with trench results with the central Sierra Madre fault in Altadena, 40 km west of our site, where Rubin et al. (1998) interpret only two surface ruptures during the last 15 ka, which together resulted in ~10 m of reverse slip. The San Dimas site data indicate that if the Sierra Madre fault ever breaks together with the San Andreas fault in very large events, as has been suggested previously, that such events must be extremely rare, insofar as dozens of San Andreas fault Big Ones (Mw7.5-8.0 events) have probably occurred since the most recent surface rupture on the eastern Sierra Madre fault.

The Application of Fast Multipole Methods to Increase the Efficiency of a Single-Fault Numerical Earthquake Model

Terry E. Tullis, Brown University
John Salmon, Sandpiper Networks, Thousand Oaks, CA
Naoyuki Kato, Brown University and Geological Survey of Japan
Michael Warren, Los Alamos National Laboratory

Many types of numerical earthquake models involve computations in which a very large number of fault elements would be desirable. In some cases these elements may each represent one fault, whereas in others they may each represent small portions of a single fault. In most computation schemes the computer time required is proportional to n^2 , where n is the number of elements. Thus for a single-fault model, if the linear cell dimension is reduced by a factor of 2 the computation time increases by a factor of 16. In other areas of physics fast multipole methods have been developed for which the compute time only increases as $n \log n$, a much more favorable situation as n becomes large. We are exploring the application of such methods to a single fault problem and it shows promise for overcoming the previous limitations on the cell size.

The fault problem chosen to test this method is a computationally intense numerical instability model of Parkfield earthquakes that uses non-linear rate- and state-friction as the constitutive law on the fault plane. Small cells are needed for two reasons: 1) only small cells can adequately represent a continuum and 2) only small cells can represent the fine-scale spatial variability in properties needed to produce a wide range in earthquake sizes. In contrast to previous versions of this model, we use a radiation damping approach to determine the fault behavior during the earthquake instability.

In the numerical model as previously implemented, the boundary element method was used to calculate stress changes on each observation-point cell due to slip on every other (source) cell, resulting in the n -squared compute-time dependence. The essence of the fast multipole method is that source cells remote from the observation-point cell are grouped together in a hierarchical manner and so fewer Green's functions need to be evaluated. A systematic scheme involving a hierarchical tree structure is employed to automate the decision-making involved in grouping the remote cells. We employ a scheme so that Green's functions are computed as needed and stored in a lookup table so they do not have to be computed again.

The methods used in this study and the efficiencies gained by their use could be adapted to other classes of earthquake model.

Ground Shaking Maps for Scenario Earthquakes

Alexei Tumarkin, University of California, Santa Barbara

We have produced maps of peak ground accelerations and velocities for the Los Angeles Basin region using a stochastic ground motion prediction approach. The algorithm is based on an extended kinematic fault rupture modeling with moment and energy constraints (Tumarkin, 1999). We have used three types of generic site response transfer functions based on (Steidl et al, 1996; Bonilla et al, 1997) to account for differences in site amplification for hard rock, stiff soil and soft soil conditions.

Pressure Solution in the San Cayetano Fault Zone: Implications for Strain Accommodation and Seismic Risk

J. M. Vermilye, Whittier College

Leonardo Seeber, Lamont-Doherty Earth Observatory, Columbia University

The evaluation of seismic hazard requires reconciliation of measured strain and observed seismicity. Although most of the strain accumulated during interseismic periods is thought to be stored elastically (until released by seismic slip) a poorly known but possibly significant portion of the total strain may be accounted for by permanent aseismic deformation. This permanent deformation may be temporally and spatially related to large earthquakes.

The San Cayetano is a seismically active fault located in the western Transverse Ranges, CA. It is one of the fastest moving thrust faults in southern California. We examined pressure-solution structures along six transects across the fault in order to evaluate the role that pressure solution plays in accommodating aseismic deformation. Pressure-solution controlled deformation includes distinct components that can be classified as 1) aseismic slip on faults 2) shortening along cleavage planes, and 3) diffuse grain-scale deformation within the rock masses between faults and cleavage planes. These classes of pressure solution structures may represent differences in depth dependency and/or distinct phases of aseismic deformation within the earthquake cycle. Distributed grain-scale shortening fabrics and solution cleavage accommodate shortening in the earliest stages of compression in the most external portions of the orogenic belt, at the leading edge of the deforming wedge. Within several hundred meters of the major fault surface, there is an increase in the density of small faults characterized by mineral fiber growth. Pressure-solution slip on these faults may result from a combination of enhanced fluid flow, pore pressures, and shear stress near the San Cayetano fault, possibly associated with large ruptures. This form of pressure solution accommodates shortening in the later stages of deformation.

Finite grain-scale dissolution strain accommodates from 9-23% shortening while slip on the small faults accommodates 2-8% shortening. These values represent a minimum for aseismic strain because additional strain is taken up by removal of material on cleavage planes. The orientations for spaced solution cleavage planes as well as the orientations for the grain-scale

pressure solution fabrics and slip lineations on the small faults generally indicate N-S to NE-SW shortening directions. These orientations are consistent with the present day compressional tectonic setting.

Pressure-solution strain detracts from the elastic strain energy budget and decreases the hazard from earthquakes. In addition to this first-order effect, pressure-solution strain is probably coupled with other deformation processes such as fault-related folding, fault growth, and the stress/strain cycle along large seismogenic faults. Understanding this coupling may shed new light on the evaluation of seismic hazard as well as crustal deformation processes in general.

Post-Landers Slip Events in the Salton Trough Region, Southern California, Revealed by Radar Interferometry.

Paul Vincent, University of Colorado and Lawrence Livermore National Laboratory
John B. Rundle, Roger Bilham, and Rick Ryerson, University of Colorado

Post-Landers slip events along the southern San Andreas, Superstition Hills and Coyote Creek faults are captured by four interferograms covering different epochs and centered over the Salton Sea in southernmost California. In addition, post-Landers slip events are seen across the Burnt Mountain and Eureka Peak Faults in interferograms centered over the Coachella Valley (the next contiguous ERS frame to the northwest) beginning one month after the June 29, 1992 Landers Mw7.3 earthquake. These events appear in some interferometric pairs covering specific epochs and time periods but not in others. This suggests that the observed signals are short-term slip events rather than ongoing interseismic creep. Rates determined from profiles done across the slip signals in various interferograms show similar magnitudes but different rates between interferograms covering different time spans, also suggesting slip events rather than ongoing deformation. Synthetic interferograms were calculated to match the observed signals and the best-fit model parameters show similar magnitudes and depths as those determined from inverting GPS and creepmeter data collected one month after the Landers earthquake.

Evaluation of Methods for Estimating Linear Site Response Amplifications in the Los Angeles Region

Lisa A. Wald, United States Geological Survey
Jim Mori, Disaster Prevention Research Institute, Kyoto

We have evaluated two methods of estimating linear site response amplifications and the standard index for classifying sites by comparing the results of each technique to observed ground motions at 33 sites in the Los Angeles region. Using velocity and density profiles from 33 boreholes, we evaluated the use of the average 30-meter shear-wave velocity and associated site classifications, the quarter-wavelength method, and the Haskell propagator matrix method. We correlated the average 30-meter shear-wave velocity and NEHRP site classification at the borehole sites co-located within 290 m of a site with observed ground motion. The observed data follow the expected trend of higher ground motion amplifications for lower average shear-wave velocities, but there is a significant degree of variability. Also, there is a great deal of scatter in the observed amplifications within each NEHRP class. We used the velocity and density information in the database to calculate the average frequency-dependent site response in the frequency ranges 1-3 Hz, 3-5 Hz and 5-7 Hz for a one-dimensional flat-layered structure using the Haskell propagator matrix method and the quarter-wavelength method. There is a general correlation with the ground motion data, however, once again there is a great degree of scatter, although slightly less for the quarter-wavelength method. We note that both the observed and predicted amplifications can change dramatically over a distance as small as one kilometer or less. Even though all techniques considered give results that follow the expected trend of

higher amplifications for softer sediments, the "predicted" site response at any particular site with the current level of information may not be representative of the shaking that will actually occur during an earthquake. The disparity between observed and predicted amplifications appears to be a result of oversimplification inherent in the amplification estimation methods, such as the use of average or assumed values for the site conditions in the absence of measured values, the "smoothing" effect of using an average velocity, limiting the properties considered to the uppermost 30 m of material, and complexities in the wave propagation that are not addressed by these methods.

Asteroid Impact Tsunami: A Probabilistic Hazard Assessment

Steven N. Ward and Erik Asphaug
University of California, Santa Cruz

Part of SCEC's legacy are the effects it had on other fields of science. I suggest that the work below that applies seismic hazard theory to asteroid tsunami hazard is a good example.

We investigate the generation, propagation, and probabilistic hazard of tsunami spawned by oceanic asteroid impacts based on the same guiding principles as are used in seismic hazard analysis. The process first links the depth and diameter of parabolic impact craters to asteroid density, radius, and impact velocity by means of elementary energy arguments and crater scaling rules. Then, linear tsunami theory illustrates how these transient craters evolve into vertical sea surface waveforms at distant positions and times. By measuring maximum wave amplitude at many distances from a variety of impactor sizes, we derive simplified attenuation relations that account both for geometrical spreading and frequency dispersion of tsunami on uniform depth oceans. In general, the tsunami wavelengths contributing to the peak amplitude coincide closely with the diameter of the transient impact crater. For the moderate size impactors of interest here (those smaller than a few hundred meters radius), crater widths are less than or comparable to mid-ocean depths. As a consequence, dispersion increases the $1/\sqrt{r}$ long-wave decay rate to nearly $1/r$ for tsunami from these sources. In the final step, linear shoaling theory applied at the frequency associated with peak tsunami amplitude corrects for amplifications as the waves near land. By coupling this tsunami amplitude/distance information with the statistics of asteroid falls, the probabilistic hazard of impact tsunami is assessed in much the same way as probabilistic seismic hazard, by integrating contributions over all admissible impactor sizes and impact locations. In particular, tsunami hazard, expressed as the Poissonian probability of being inundated by waves from 2 to 50 meter height in a 1000 year interval, is computed at both generic (generalized geography) and specific (real geography) sites. For example, a typical generic site with 180 degrees of ocean exposure and a reach of 6,000 km, admits a 1-in-12 chance of an impact tsunami of 2 meter height or greater in 1000 years. The likelihood drops to 1-in-35 for a 5 meter wave, and to 1-in-385 for a 25 meter wave. Specific sites of Tokyo and New York have 1-in-24 and 1-in-46 chances of suffering an impact tsunami greater than 5 m in the next millennium. We believe that investigations of this style that merge proper tsunami theory with rigorous probabilistic hazard analysis advance considerably the science of impact tsunami forecasting.

Tectonic Geomorphology and Earthquake Hazard Analysis of the Rincon Creek Anticline and Associated Rincon Creek Fault, Carpinteria, Santa Barbara County, California

Adam C. Webber, Edward A. Keller, and Larry Gurrola
University of California, Santa Barbara

The Rincon Creek anticline (RCA) is a prominent east-west trending topographic high, located approximately 1.5 km east of the city of Carpinteria. The fold is approximately 2.5 km long, 1 km wide tapering off to the west, and has a maximum topographic high of approximately 40 m. The RCA is developing on the oxygen isotope stage 3a marine terrace of approximately 45 ka (Gurrola, per. comm., 1999), suggesting an uplift rate for the terrace of 1.1 mm/yr. The fold is a surface expression of the Rincon Creek fault (RCF), a blind reverse fault dipping between 35° and 60° to the south (Jackson and Yeats, 1982). Geomorphic mapping has identified three wind gaps along the axis of the fold, suggesting that it is propagating west, presumably along with the RCF. Using the age of the Casitas Formation (~100 ka) as an upper limit and the marine terrace age (~45 ka) as a lower limit and based upon the length of the fold (2.5 km), the anticline has been propagating between 2.5 and 5.5 cm/yr. Based upon the length of the RCF (~20 km) and other factors such as the average shear modulus of the rock and the presumed slip rate, the maximum potential earthquake magnitude of the RCF is 6.6 (Keller, pers. comm., 1999), presenting a serious seismic hazard to Carpinteria. Research and previous work has shown that the Rincon Creek anticline is a fault-propagation fold, as well as the surface expression of a subsurface bend in the Rincon Creek fault known as a fault-bend fold. Based upon stratigraphic evidence, the Casitas formation was tilted, possibly due to the Carpinteria fault, prior to the initiation of the folding due to the Rincon Creek fault.

An Undergraduate Course in Earthquakes for Non-Majors Robert S. Yeats, Oregon State University

With SCEC support, I am writing *Living with Earthquakes in California*, a follow-up to *Living with Earthquakes in the Pacific Northwest* (1998, Oregon State University Press, 304 p., order from orders@uapress.arizona.edu). The Northwest book was written for an OSU course meeting a baccalaureate core curriculum requirement for a 3-hour synthesis course relating science, technology, and society. No previous science course is required other than that required of all students. The course requires a short term paper using earthquake-related websites which are listed in the references. The book is suitable for decision-makers and disaster-response professionals as well as the general public.

An introduction reviews 3 centuries of earthquake awareness in California. Chapters follow on geologic time, plate tectonics, faults including blind thrusts, crustal strain, and earthquakes. 4 chapters summarize earthquake environments: San Andreas system, Transverse Range convergent zone, eastern California, and Cascadia subduction zone. Earthquake prediction and forecasting are discussed, and separate chapters deal with secondary effects (strong ground motion, liquefaction, and landsliding) and tsunamis.

A chapter covers insurance (including the CEA experience), retrofits of homes and large structures, and the role of the federal, state, and local government, including building codes, zoning, and grading ordinances. Finally, individual preparedness is discussed: what can we do to make our home, school, and office more earthquake resistant, and how should we prepare ourselves?

California is a world leader at the state and local level in preparing for earthquakes. But islands of ignorance remain, and public education is necessary. The book is upbeat: we can't predict earthquakes, but we can predict site response, and we can build structures that won't kill people during an earthquake, and maybe we can figure out how to insure ourselves at a reasonable cost.

FAULT SEGMENTATION IN THE NORTHERN LOS ANGELES BASIN, CALIFORNIA

Robert S. Yeats, Oregon State University
Gary J. Huftile, Queensland University of Technology, Brisbane
Hiroyuki Tsutsumi, Kyoto University, Kyoto
Tom Bjorklund, University of Houston
Pierfrancesco Burrato, Istituto Nazionale di Geofisica, Rome
Daniel J. Myers, Oregon State University

We identify potential earthquake sources in the northern Los Angeles (LA) basin. The steeply north-dipping North Strand of the Santa Monica fault merges downward with the gently-dipping South Strand and may connect at depth with the range-front fault, which is inactive at the surface. The Santa Monica North Strand connects with the Hollywood fault via a left stepover at the West Beverly Hills lineament, a continuation of the Newport-Inglewood fault (NIF). The Santa Monica Mountains are uplifted along a blind reverse fault with a slip rate < 1 mm/yr. The blind Las Cienegas fault, bounded on the west by the NIF and on the south by the LA trough, has a late Quaternary slip rate of 0.5 mm/yr, losing separation eastward and dying out. The Elysian Park anticlinorium is expressed in tectonic topography; the fold hinge at its southern edge is the Coyote Pass Escarpment. The anticlinorium is bounded on the east by the East Montebello fault; on the west, it may bifurcate into the MacArthur Park lineament extending to the Hollywood fault and the San Vicente fault which extends to the NIF. The Montebello and Santa Fe Springs anticlines overlie a blind thrust that ruptured in the 1 October 1987 Whittier Narrows earthquake (M 5.9). The folds die out westward toward the LA trough, and the Montebello anticline terminates eastward against the East Montebello fault. The Whittier fault in the western Puente Hills forms the range front and is variable in strike, connecting with the East Montebello fault. Farther east, the Whittier right-slip fault occurs within the southern foothills of the Puente Hills and is relatively straight in map view. South of the Santa Ana River, the Whittier fault changes to south side up. A series of east-west anticlines forming the Coyote Hills are formed by a blind thrust which may comprise a separate earthquake source or connect at depth with the Whittier fault.

PALEOSEISMIC RECORD OF THE SAN BERNARDINO STRAND, SAN ANDREAS FAULT AT BURRO FLATS

Doug Yule and Kerry Sieh, California Institute of Technology
Ashley Streig, Occidental College
Cameron Kennedy and Tammy Surko, California State University

We report preliminary results from this summer's excavation across the San Bernardino strand, San Andreas fault at Burro Flats near Banning California. Burro Flats is an intermontane basin filled by south-dipping, coalesced alluvial fans and bounded on the southwest by the San Andreas fault. The fault shows north-facing scarps and a vegetation lineament at the surface, and forms a barrier to ground water. The site occurs in a marsh at a right step in the fault where modern alluvium has buried two parallel scarps.

Two intersecting trenches, 40 and 60 meters long, expose an ~7.5 meter section of well-stratified distal fan, pond, peat, and peaty soil deposits. With one exception, thirteen samples from peat and peaty soil yield stratigraphically consistent radiocarbon ages that range in age from AD 1900 near the top to BC 1600 1.0 meter above the base of the exposed section. The trenches expose two fault zones, correlatives of the two scarps seen at the surface away from the modern fan deposits. Faulting and associated folding provides convincing evidence for four rupture events and less clear evidence for three additional events. Calibrated calendar radiocarbon ages from peat layers that loosely bracket each event constrain the timing of the

events to between: 1465-1225 AD (two events), 1300-695 AD, 605-30 AD, 225 AD-960 BC, 920-1685 BC, and pre-BC 1685. The most recent event is described in more detail by Streig, this volume. All ages are from AMS analyses of residue after acid/alkali/acid pre treatment. We expect to obtain a more precise chronology with further dating of peats closer to each event horizon and by dating both solute and residue fractions (see Seitz et.al., 1998 SCEC Annual Meeting).

Our work this summer suggests that the San Bernardino segment, San Andreas fault has a longer average recurrence interval for events than the Mojave and Coachella Valley segments. Less frequent events on the San Bernardino segment requires larger slip per event or strain partitioning onto other faults in the region.

Source Modeling and Directivity study of Several Important Large Earthquakes

Yuehua Zeng, University of Nevada

In this paper, I studied the earthquake source rupture processes of several important earthquakes using the composite source model (Zeng et al., 1994). Near field strong motion seismograms from those events within about 40 km of the fault planes were selected. The Genetic Algorithm was used to find the locations and rake angles of the composite subevents to best match the synthetic waveforms with the observation. The resulting composite source slip models agree in general with other modeling studies of earthquake source rupture processes using the near field strong motion waveforms for the Loma Prieta, Imperial Valley, Northridge and Kobe earthquake events. For Landers earthquake, the inversion solution differs from Wald et al. (1994) and shows large slip zones near the centers of the three fault segments. Locations of minimum fault slips coincide well with the ends or stepping sections of the fault, suggesting that fault stepovers act like barriers to the source dynamic rupture. I used those composite source models to examine the effect of near fault rupture directivity. The results indicate that the composite source model generates consistent rupture directivity effect as that from the observation.

High Resolution Crustal Structure Across the San Andreas Fault from the LARSE-93 Passive Seismic Recording Experiment

Lupei Zhu

Southern California Earthquake Center, University of Southern California

During the 1993 LARSE passive recording experiment, a 180 km-long profile, starting from the Los Angeles Basins through the San Gabriel Mountains, the San Andreas Fault (SAF), and into the Mojave Desert, was occupied by 89 short-period instruments, including 60 three-component instruments. We analyzed about 5000 short-period records from 30 teleseismic events using multi-channel cross-correlation and teleseismic receiver function techniques. We found that when the teleseismic earthquakes are large enough there is still sufficient signal energy at 1 s and longer for receiver function analysis. Crustal structure along the profile was imaged by stacking teleseismic P-to-S converted phases in receiver functions using a Common Conversion Point (CCP) stacking algorithm. The crust/mantle discontinuity (Moho) is visible as a continuous feature at a depth around 30 km under the Mojave segment of the profile, but is offset 6 to 10 km beneath SAF. A small Moho disruption can also be seen under the Eastern California Shear Zone (ECSZ). These results suggest that SAF and ECSZ extend through the entire crust. The Moho upwarp under the San Gabriel Mountains indicates that the mountain ranges were lifted en masse as a result of crustal buckling under horizontal compression.

US/China GPS Workshop Abstracts

NEW CONSTRAINTS ON ASIAN DEFORMATION FROM GEODESY ACROSS THE ALTYN TAGH FAULT

R. Bendick, R. Bilham, K. Larson, University of Colorado
J. Freymueller, University of Alaska
G. Peltzer, Jet Propulsion Laboratory
Guanghua Yin

The collision between India and Asia has attracted a diversity of mathematical models that describe or predict the motions of the major faults of east Asia. The slip rate of the largest of these faults, the 2000-km-long Altyn Tagh fault on the northern edge of the Tibetan Plateau, is central to these models, yet geological estimates of its rate vary from 3-9 mm/yr to 20-30 mm/yr. We report here geodetic data that indicate a 9 ± 5 mm/yr slip rate on the Altyn Tagh fault. This result, combined with the observation that convergence across the Altyn Tagh system is a factor of three lower than north/south contraction of Tibet, is consistent with the predictions of dynamic models, but requires many kinematic models of the collisional process to be revised. Additional GPS sites installed in the Altyn Tagh array in 1998 may afford a more complete picture of fault kinematics, as well as investigate the effect of variations in crustal block rheology on deformation partitioning.

CRUSTAL MOVEMENT OBSERVATION NETWORK OF CHINA

Chen Xinlian, Center for Analysis and Prediction, CSB, Beijing
Niu Zhijun and Sun Jianzhong, China Seismological Bureau, Beijing

It is the main aim of the Crustal Movement Observation Network of China (CMONOC) to monitor the crustal deformation in China mainland and in area around it for the prediction of intraplate earthquakes in China mainland. The network also serves for the geodetic survey and national construction. GPS is the main observation technique of the network which combines existing space techniques of VLBI and SLR, and precise leveling and precise gravimetry. There are 25 fiducial stations with continuous GPS observation, 56 basic stations which will be repeatedly observed at regular time intervals and 1000 regional stations which will be observed at irregular intervals and 700 of them are setup in areas of high seismic activity. There is a data center for data transfer and data analysis for the network. In this paper the role and significance of CMONOC in monitoring crustal deformation is described with emphasis on the general design, structure of the network and major technical specifications of the network. The result of the first observation of the fiducial and basic stations is analyzed.

GPS MEASUREMENT OF CRUSTAL MOTION IN SOUTHWEST CHINA

Chen Ziliang, Liu Yuping, Tang Wen-qing, Zhao Ji-Xiang, and Zhang Xuan-yang
Chengdu Institute of Geology and Mineral Resources, Ministry of Geology, Chengdu

B. C. Burchfiel, R. King, L. Royden, F. Shen, and E. Wang
Massachusetts Institute of Technology

We present and interpret GPS measurements of crustal motions for the period 1991-1998 for a network encompassing the eastern part of the Tibetan plateau and its foreland. Viewed relative to South China, stations of the northeast plateau, bounded by the Qilian Shan and the Altyn Tagh fault, move NNE to NE with velocities ranging from 19 mm/yr within the plateau to

4-10 mm/yr in its foreland. The Altyn Tagh fault shows left-lateral slip of ~10 mm/yr at 95 deg E and shortening across the fault of less than 5 mm/yr. Stations south and west of the Xianshuihe/Xiaojiang fault system define a crustal fragment rotating clockwise at ~10 mm/yr relative to South China around the eastern Himalayan syntaxis. The GPS measurements indicate no significant shortening (< 3mm/yr) within the Longmen Shan of the central eastern plateau and its adjacent foreland. Geological studies indicate that the deformational field was established diachronously in Late Miocene to Pliocene time, was characterized by no east-west shortening of the Tibetan crust, and has an inhomogeneous style of deformation resulting from a balance of different tectonic processes. Viewed relative to Eurasia, stations within all parts of the plateau foreland in South China move 8-10 mm/yr SE, indicating that the eastward movement within the plateau is part of a broader eastward movement that involves the plateau and its eastern and northern foreland. North of the plateau, foreland stations move eastward at ~8 mm/yr, indicating that the northern boundary of the deformation zone lies north of the plateau.

CRUSTAL DEFORMATION MONITORING SYSTEM IN NORTHEASTERN BORDER OF TIBET PLATEAU

Ding Ping, Second Center for Crustal Deformation Monitoring, CSB, Xi'an

With tectonic block Qingzang, Alashan, Erdossi, Xinjiang and Nahua conjunct and interact here, the northeastern border of Tibet plateau is a strong deforming and seismically active region. Since 1900, there have been 6 strong earthquakes with magnitude great than 7 occurred here, the biggest event is the Haiyuan Ms8.5 earthquake on Dec. 16, 1920. In order to strengthen earthquake prediction work of the region, the Second Center for Crustal Deformation Monitoring, China Seismological Bureau, has gradually established a comprehensive crustal deformation monitoring system here since 1970. The main monitoring approaches include:

1. Leveling network. There are many first-class leveling lines distributed in northeastern border area of Tibet plateau. Since 1970, all the leveling lines have been resurveyed at least four times. The leveling repetitions have played an important role in vertical crustal deformation investigation and in intermediate earthquake predication.
2. GPS network. GPS network of northeastern border of Tibet plateau mainly consists two parts: Hexi-C GPS network consisting of 32 sites and CMNOC GPS network. Established in 1991, the first measurement of Hexi-C GPS network has been carried out in 1993 with WM102 receivers, the second reoccupation will be carried out in September 1999. As part of the whole CMNOC project, there are nearly 200 GPS sites established in the region, and the first measurement of CMNOC sites have completed in August 1999. GPS observations will play an important role in investigating how the Tibet sub-plate interacts with other blocks in this area.
3. Fault deformation monitoring sites. In northeastern border area of Tibet plateau, there have gradually established nearly 70 sites for fault deformation monitoring since 1970s, the measuring approaches include short leveling, baseline and laser ranging. Measured three times a year, the fault deformations have played an important role in short-term earthquake prediction. At present, We are also trying to introduce GPS technique into fault deformation monitoring, the relevant experiments for short side GPS network had been completed.
4. Gravity measurement. Apart from the above-mentioned geodetic approaches, we also carry out gravity measurement in northeastern border area of Tibet plateau. Starting from 1989 and being measured once a year, the gravity repetitions have well served the intermediate earthquake prediction and study of geodynamics together with other deformation observations.

We are looking forward to international cooperation in this region.

EXTRACTING TECTONIC INFORMATION FROM THE QUASI-OBSERVATION APPROACH

D. Dong, Jet Propulsion Laboratory

Quasi-observations provide an efficient mechanism for combining daily and campaign GPS solutions or combining different types of geodetic data to estimate tectonically induced secular motion and episodic site motion in a region of active deformation. The primary observations are analyzed separately to produce loosely constrained estimates of station positions and network parameters. These loosely constrained estimates are then combined as quasi-observations to estimate a velocity field and coseismic and/or postseismic displacements.

We will present the principles, the requirements and the procedures of the quasi-observation approach. More details will be provided during the discussion session.

PRESENT-DAY KINEMATICS OF THE INDIA-EURASIA PLATE COLLISION ZONE

Jeffrey T. Freymueller (1), Chen Qizhi (1), Wang Qi (2), Yang Zhiqiang (3), Wang Wenying (3), Kristine Larson (4), Roger Bilham (4), Rebecca Bendick (4), Yin Guanghua (5), and Liu Benpei (6)

(1) Geophysical Institute, University of Alaska, Fairbanks

(2) Institute of Seismology, State Seismological Bureau, Wuhan, CHINA

(3) Xi'an Engineering University, CHINA

(4) University of Colorado

(5) Xinjiang Seismological Bureau, Urumqi, CHINA

(6) Wuhan Technical University of Surveying and Mapping, Wuhan, CHINA

Many GPS sites have been established on and around the Tibetan plateau in order to study the active deformation processes of the India-Eurasia plate collision zone. We have integrated results from many of these sites into a velocity field in a common reference frame, sampling the deformation field along a north-south transect at approximately 80E to 90E longitude. We use these data to constrain the rates of several important deformation processes: underthrusting of India beneath southern Tibet, east-west extension of southern Tibet, north-south shortening across the Tibetan plateau, shortening and strike slip motion at the northern edge of the plateau, and shortening across the Tian Shan.

In a Eurasian plate reference frame, the eastward velocity of sites in southern Tibet increases eastward toward the Eastern Syntaxis, a result of east-west extension across the southern plateau. The extension is not confined to the southernmost part of the plateau, where large normal fault systems are found, but extends across nearly the entire plateau. In a transect along the Golmud-Lhasa road we do not see significant left-lateral strike slip motion until we reach the latitude of the Kunlun fault system. We find about 10 mm/year of north-south shortening across the plateau, about half of which appears to be concentrated in the central plateau near the Tanggula Shan. We find only about 10 mm/year left-lateral strike slip motion on the Altyn Tagh fault, much less than expected from previous work that had suggested a slip rate of as much as 30 mm/year. Significant deformation must occur in the Altay or within Mongolia, since Urumqi on the northern foothills of the eastern Tian Shan moves roughly 10 mm/year relative to Eurasia.

DATA PROCESSING OF THE FIRST OBSERVATION IN THE CRUSTAL MOVEMENT OBSERVATION NETWORK OF CHINA

Gu Guohua and Niu Hongye

Center for Analysis and Prediction, China Seismological Bureau, Beijing
Zhao Chengkun

First Center for Crustal Deformation Monitoring, Tianjin

In the Crustal Movement Observation Network of China (CMONOC), 25 fiducial stations and 56 basic stations were first observed from August 28 to September 7, 1998. The observed data of the 81 stations and the data of an IGS station at Xian were processed with the GAMIT/GLOBK and Bernese GPS data processing software at the Data Center of CMONOC. Both results are of high accuracy and in good agreement. In this paper, the Data Center is briefly introduced and the data processing and the result for the first observation in the network are described. With repeated observations at 23 fiducial stations, significant northward displacements were detected in the western part of China and southward displacements were detected in Yunnan in reference to stations in the eastern part of China. The crustal deformation in the network shows that China mainland is being pushed by the Indian plate.

COMPARISON OF GEOLOGIC, GEODETIC, AND SEISMIC RATES OF SHORTENING ACROSS THE TIEN SHAN OF KYRGYZSTAN, CENTRAL ASIA

B. H. Hager, B. Meade, T. A. Herring, P. Molnar, MIT
S. C. Thompson, University of Washington
C. M. Rubin, M. M. Miller, Central Washington University

The Tien Shan of central Asia constitute the world's outstanding laboratory for the study of intracontinental mountain building. Half or more of the present-day convergence between India and Asia is occurring across the Tien Shan. The combination of outstanding structural and stratigraphic exposure and a high level of seismotectonic activity make the Tien Shan an ideal environment to address basic questions of continental dynamics by integrating a wide variety of observations of kinematics and structure. We make detailed comparisons of geologically constrained rates of active faulting to GPS velocities along a N-S transect across the Kyrgyz Tien Shan at a longitude of $\sim 75^\circ$ E. On the basis of geologic reconnaissance mapping, we identified 6 faults as the most active across the N-S transect. Slip rates and fault geometries are based upon detailed geologic mapping, paleoseismologic studies, and river terrace profiling. Preliminary slip rates, from north to south, are 3 ± 2 , $2.5 \pm 2.5/-1.5$, $7 \pm 6/-3$, 0.8 ± 0.1 , $1.0 \pm 2.0/-0.5$, and 10 ± 5 mm/a on the most active thrust faults that bound the individual ranges. The GPS profile yields 12 mm/a across the same region and is consistent with deformation on the discrete mapped structures. Extrapolating this over the range into China, we estimate a total shortening rate of 20 mm/a, consistent with the rate of seismic moment release in this region in the past century. We compare GPS observations to predictions using conventional elastic dislocation models that integrate the geologically constrained fault geometry and slip rates. The comparison of observations and predictions is excellent. Viscoelastic models with a stiff lower crust mimic these elastic dislocation models, suggesting strong coupling between mantle and crustal deformation. The excellent match between geodetic and geologic rates suggests that GPS geodesy provides a powerful tool for estimating seismic hazard.

JOINT MODELING OF THE KINEMATICS AND DYNAMICS OF ASIA

William Holt (1), Lucy Flesch (1), A.J. Haines (2), Nicolas Chamot-Rooke (3), Xavier LePichon (3), Jinwei Ren (4), Bingming Shen-Tu (1)

- (4) Department of Geosciences, SUNY at Stony Brook
- (5) Bullard Laboratories, University of Cambridge
- (3) Laboratoire de Géologie, Ecole Normale Supérieure, Paris
- (4) Institute of Geology, China Seismological Bureau

We have developed methods to quantify the kinematics of the active deformation using information from both Quaternary fault slip rates and GPS observations. These kinematic constraints are then used to help define the dynamics (distribution of stresses and effective rheology) of the lithosphere in Asia. Strain rates inferred within areas using the Kostrov summation are interpolated with continuous spline functions in order to recover a self-consistent estimate of the horizontal velocity gradient tensor field. GPS vectors, within a defined frame of reference, are matched during the interpolation process by the model velocity field. In the joint inversion solution India moves relative to Eurasia about a pole of rotation at (30.8 N, 5.2 E, 0.38 deg./M yr), which yields total relative motions that are about 78% to 84% of the expected NUVEL-1A IN-EU model velocity magnitude along the Himalaya; the eastward component of velocity relative to Eurasia is about 3.5 to 6.5 mm/yr greater than that predicted by the NUVEL-1A India-Eurasia model. South China moves at an almost uniform velocity E-SE (azimuths of 110 +/- 15 degrees) relative to Eurasia at 14 +/- 3 mm/yr (95% confidence). We compare predicted seismic moment rates with those observed in this century in Asia. Significant moment deficits exist within W. Tibet-Karakorum, Altyn Tagh, Quidam Basin, Indo-Burman Ranges, Northern Pamir, western Tien Shan, the southern Kazakh Platform, Qinling Shan-Dabie Shan, and eastern China. On the other hand, many areas that have experienced great earthquakes in this century show moment release rates that are a factor of 2 - 8 times the long-term moment release rate inferred from GPS and Quaternary fault slip rates. Examples are Mongolia (factor of 8) and Haiyuan region (factor of 5).

Our dynamic approach involves the determination of the vertically averaged deviatoric stress field associated with gravitational potential energy differences plus stress boundary conditions. The stress boundary conditions are associated with the accommodation of India-Eurasia relative motion. Absolute magnitudes of vertically averaged deviatoric stress vary between 50 - 400 bars. Using the strain rates defined by the Quaternary slip rate and GPS observations and the absolute values of stress, we determine the vertically averaged effective viscosity for Asia. The effective viscosity for Tibet is relatively uniform with average values around $0.5-5 \times 10^{22}$ Pa-s, compared with $1-5 \times 10^{23}$ Pa-s in more rigid areas elsewhere in the region. Forward modeling demonstrates our method of directly solving the force-balance equations for the absolute values of stress is valid for cases in which there are spatial variations in the effective viscosity of several orders of magnitude. The method we present is also appropriate for non-linear, or power-law rheologies. Results for the total stress field and effective viscosity are consistent with a weak lower crust in Tibet, they confirm that the deforming continental lithosphere there is behaving like a fluid, they predict considerable eastward extrusion of lithosphere relative to Eurasia, and they show that potential energy differences have a profound influence on the style and magnitude of strain around the Tibetan Plateau. Furthermore, the results in this study show that it is the vertical average of rheology that controls large-scale deformation, while local vertical variations are expected to affect only short-wavelength features. Thus lower crustal flow different from surface flow is not required to explain the broad-scale present-day kinematics inferred from GPS observations, Quaternary fault slip rates, and earthquake mechanisms. With refined GPS coverage the kinematics of the large-scale deformation field within deforming Asia will become better resolved. With better resolved rates of strain we will be able to distinguish more accurately the relative role of gravitational potential energy differences, boundary conditions of stress, and shear tractions.

RECENT CRUSTAL HORIZONTAL MOVEMENT IN MAINLAND CHINA

Li-ren Huang and Min Wang
First Center for Crustal Deformation Monitoring, CSB, Tianjin

At 22 GPS stations distributed on main tectonic blocks in mainland China, two GPS measurement campaigns with high precision were made respectively in 1994 and 1996 in order to research recent horizontal movement in mainland China. Some information about the two campaigns are introduced in detail in this paper. The observed data are carefully pre-processed. Results show that the relative accuracy of baseline between any two GPS stations is as high as $Mb(94)=2.14\text{mm}+0.95\text{ppb}\cdot B$ or $Mb(96)=2.16\text{mm}+1.19\text{ppb}\cdot B$ (B = baseline length) respectively. A model, which describes relative motion on a spherical surface among rigid blocks and strain deformation in blocks, is established to study relative movements among 5 major tectonic blocks in mainland China and strains at each GPS station. Based on the model, relative movement parameters and strain parameters are derived. And then recent relative motion velocities on the boundary zones between blocks are also estimated. Based on the obtained results, the major characters of recent crustal horizontal movement in mainland China and their meanings in site-prediction of strong earthquake are discussed.

THE SOUTHERN CALIFORNIA INTEGRATED GPS NETWORK (SCIGN)

Kenneth W. Hudnut, United States Geological Survey, Pasadena
Yehuda Bock, University of California San Diego
Frank Webb, Jet Propulsion Laboratory
Bill Young, SCIGN

SCIGN is an array of Global Positioning System (GPS) stations distributed throughout Southern California with emphasis on the greater Los Angeles metropolitan region. The major objectives of the array are:

- 1) To provide regional coverage for estimating earthquake potential throughout Southern California
- 2) To identify active blind thrust faults and test models of compressional tectonics in Los Angeles
- 3) To measure local variations in strain rate that might reveal the mechanical properties of earthquake faults
- 4) In the event of an earthquake, to measure permanent crustal deformation not detectable by seismographs, as well as the response of major faults to the regional change in strain

These scientific purposes and the network design were developed through several collaborative workshops, as well as by meetings and extensive committee work. Despite the considerable logistical constraints on siting, the design of the network remained driven by the scientific intent.

Data from all SCIGN stations are freely available on-line, as are coordinate solutions, periodic velocity solutions, and other products. Users of data and products are asked to simply acknowledge SCIGN and its sponsors; the W.M. Keck Foundation, NASA, NSF, USGS, and SCEC. These data and additional detailed information on the project are all available at the SCIGN web site - <http://www.scign.org/>

In addition to these scientific purposes, the data will benefit the Surveying, Engineering and Geographic Information System (GIS) communities who are using SCIGN as the basis for their spatial reference system. The new High Precision Geodetic Network for the state of California, which is the fundamental official geodetic control system, will be based upon data from SCIGN stations (and other continuously operating GPS stations in Central and Northern California).

New SCIGN stations are constructed with a 10-meter deep, five-legged monument that is isolated from the uppermost 3.5 meters of soil so that seasonal non-tectonic motions are minimized. For longevity, these monuments are built using stainless steel pipe. All sites employ standard choke ring antennas and SCIGN adapters and radomes, to minimize potential antenna system phase center variations through time (and in the event of equipment changes).

In order to telemeter and process the large quantities of data, SCIGN has developed new programs and automation scripts that are shared with other users and code developers. Site information is being maintained using a relational database, developed with SCIGN support, that is proving useful for other global GPS data sets as well. Furthermore, we employ redundant data processing to obtain the very highest accuracy and precision possible from the data.

Stations are currently being installed by a contractor at an average rate of two sites per week. In addition to the approximately 50 SCIGN stations that were built in a variety of styles earlier in the network's growth, we now have nearly 100 new stations built by the contractor to the new specifications. Over the upcoming year, we intend to construct an additional 70 stations, and to eventually have a total of 250 stations in the network.

REFERENCE FRAMES FOR EAST ASIAN STUDIES

R. King, B. C. Burchfiel, T. Herring, S. McClusky, L. Royden
Massachusetts Institute of Technology
Chen Ziliang and Zhang Xuanyang, Chengdu Institute of Geology and Mineral
Resources, Ministry of Geology, Chengdu

The interpretation of large-scale tectonic processes from GPS measurements often depends strongly on the frame of reference in which the estimated velocities are viewed. With the current network of global space-geodetic stations, a robust and conventionally unambiguous approach is to realize the frame by constraining the a priori velocities of 20-50 global stations to the values empirically determined in the ITRF no-net-rotation (NNR) frame. Motion relative to a major plate can then be inferred by applying the rotation prescribed by the NUVEL-1A plate motion to relate the plate to the NUVEL-1A NNR frame. The potential weakness in this approach is that errors in NUVEL-1A or in the ITRF realization of the NUVEL-1A NNR frame will map into the representation of the velocities with respect to the chosen plate. The first of these problems can be alleviated by constraining the global stations to their NUVEL-1A velocities [Shen et al., 1999]; the second will require refinement of the NUVEL-1A model itself. A more direct approach to frame realization is to perform the GPS analysis while constraining (to zero) only the velocities of stations on the plate of interest. The potential weakness of this approach is that the much smaller number of stations available makes definition of the frame more susceptible to errors in the velocities of individual stations. For current studies of the tectonics of China, the two approaches to realization of a Eurasian frame produce velocities which differ by 3-9 mm/yr in magnitude and 25-60 degrees in direction. In our analysis, using stations only within Eurasia to define the frame yields an rms misfit of ~1 mm/yr, whereas a global realization of Eurasia using ITRF96 and NUVEL-1A yields a misfit of 1 mm/yr globally but 3 mm/yr within Eurasia itself.

Fault-Block Deformation Model in North China

Lanbo Liu, University of Connecticut

The Discontinuous Deformation Analysis (DDA) method is used to simulate the long term cross-fault short baseline and other terrene-based geodetic data related to aseismic tectonic deformation in north China region. By this simulation we have found that: (1). Slips on faults with different orientation are generally in agreement with the ENE-WSW tectonic stress field. However, the maximum shear strain with respect to the faults can vary from nearly orthogonal, to pure shear along the strike of the faults, this pattern cannot be explained by simple geometric relation between the strike of the fault and the direction of the tectonic shortening. This phenomenon has been observed at many sites of cross-fault geodetic surveys, and might be caused by the interactions between different blocks and faults. (2). According to the DDA model, the average aseismic slip rate along major active faults is at the order of several tenth of millimeter per year, which is in agreement with the cross-fault geodetic surveys. Meanwhile, according to the model, the typical strain rate inside a block is at the order of 10⁻⁸ year⁻¹ or less. Thus, the block deformation rate of 10⁻⁶ year⁻¹, as reported by some observations in certain sub-areas, is controversial to the fault slipping rate and cannot be the representative deformation rate in this region. (3). Between the slips caused by regional compression and block rotation, there is a possibility that the sense of slip caused by rigid body rotation in two adjacent blocks is opposite to the slip caused by the tectonic compression. But the magnitude of slip resulted from the tectonic compression is much larger than that due to the block rotation. In general, the slip pattern on faults as a whole agrees with the sense of tectonic compression in this region. That is to say, the slip caused by regional compression dominates the whole slip budget. (4). Based on (3), some observed slips in contradiction to ENE tectonic stress field may be caused by some more localized sources. Data from recently built and densified GPS network in this region appears to be the leading factor to reduce the discrepancies between the observation and the model and eventually lead to a more rigorous deformation model in this region.

A METHOD ON THE ESTABLISHMENT OF THE ATMOSPHERIC DISTRIBUTION MODEL AND ITS APPLICATION IN GPS DATA PROCESSING

Luo Zhiguang, Engineering Center of Crustal Movement Observation Network of China

In order to eliminate the effects caused by tropospheric delay, standard meteorological parameters on the sea-level are generally used in GPS data processing, and tropospheric correction parameters in the zenith direction at observation stations are introduced in the adjustment model. But the tropospheric delay is still one of the main errors influencing the precision of GPS crustal deformation network. In the paper, a method is proposed to establish atmospheric distribution with meteorological measurement data. The application of the method is discussed in the GPS data processing.

THE OBSERVATION AND RESULT ANALYSIS FOR THE GEODYNAMICAL GPSNETWORKING IN XINJIANG

Linbo Ma, No. 2 Surveying Team of State Bureau of Surveying and Mapping
Peng Zhang and Zhihao Jiang, National Geography Center of China

Located in the hinterland of Eurasia, Xinjiang is an assimilating area of several large tectonic bands in Eurasia. according to intercontinental tectonic, there are many key parts of the earth structure in the form of "three mountains & two basins" as Xinjiang extends across. Consequently, the study in plate conformation of Xinjiang is significant to resolve continental

plate conformation, moreover to develop tectonic study of the whole world. State Bureau of Surveying and Mapping makes observation once per year since 1995. By GPS technology, studies plate conformation and movement of Xinjiang combining geologist's arguments. The authors introduced the GPS network of Xinjiang, the site choice, observation plan, data processing and give the analysis result.

THE USE OF GPS MEASUREMENTS IN QUANTIFYING THE KINEMATICS OF ASIAN DEFORMATION FOR STUDY OF ITS DYNAMICS, AND THE DYNAMICS OF CONTINENTAL DEFORMATION IN GENERAL

Peter Molnar, Massachusetts Institute of Technology
Philip England, Oxford University

We seek an accurate velocity field for Asia in order to construct an internally compatible, laterally varying strain-rate field from which we can infer a laterally varying effective viscosity field for the lithosphere. We use two types of data, estimates of average slip rates on faults during Quaternary time and GPS measurements of baseline length changes between benchmarks. Both are used to estimate average strain rates within triangular elements. In addition, we use long baseline length changes as direct constraints on the velocity field. Because of lingering questions about reference frames and the demonstrable errors in NUVEL-1a for the relative velocity of India and Eurasia, we do not (yet) use both components of relative velocities between benchmarks. Because in obtaining a velocity field, we seek a minimum in estimated strain rates within elements, weighted by their uncertainties, we obtain an internally consistent strain-rate field. Previous work demonstrating the robustness of this approach include the prediction that slip rates on some faults (such as the Altyn Tagh) had been grossly overestimated, and if less impressive, a lower convergence rate between India and Eurasia than that given by NUVEL-1a. A preliminary examination of the dynamic balance between gradients in potential energy and gradients in surrogates of stresses justifies the assumption that on large scales the lithosphere can be treated viscous fluid.

CONTINENTAL EVOLUTION: IDEAS FROM SEISMOLOGY AND GPS DATA

Walter D. Mooney, USGS-Menlo Park

Modern GPS measurements of crustal deformation, together with related geophysical, geochemical and geologic data provide important insights into the evolution of continental crust and the sub-crustal lithosphere. In China it is possible to investigate crustal evolution for ages ranging from ancient (Precambrian) blocks to the young, actively deforming region of Western China. I discuss the process of crustal and lithospheric evolution in three epochs (I-III): Archean, Proterozoic, and Phanerozoic.

(I) There is only a limited amount of Archean crust in China.

Globally, isotopic data (Sm-Nd and Re-Os systematics) from diamond inclusions indicate that the Archean lithosphere formed at approximately the same time as overlying crust. However, petrologic evidence indicates that the Archean mantle was 100-150°C hotter than the present day. The evidence appears to favor very early lithospheric formation as a remnant (restitute) of mantle plumes that produced thick oceanic crust (plateaux) and ultramafic extrusions (komatites). However, this early Archean model is speculative. Deep seismic reflections from the Archean sub-crustal lithosphere remain elusive, perhaps due to a relatively homogeneous structure.

(II) The Proterozoic Era is found mainly in Northern China.

Evidence from crustal seismology, laboratory seismic velocity measurements, xenolith compositions, isotopic data, and field mapping favor an evolution from accreted oceanic island arcs in an environment similar to modern plate tectonics. Anorogenic magmatism (possibly associated with a superswell that formed beneath the thermal blanket of a Mid-Proterozoic supercontinent) thickened the Proterozoic crust with felsic and anorthositic upper crustal intrusions and basal crustal mafic underplate. Strong near-horizontal mantle reflections at depths of 60-200 km have been imaged on several deep seismic reflection profiles across Proterozoic lithosphere (e.g. Great Bear Province, Canada). These observations suggest that Proterozoic lithospheric may have formed by horizontal thrusting and stacking of oceanic lithosphere (lithospheric shingling), in contrast to the hypothesized formation of primitive Archean lithosphere in situ as a magmatic remnant.

(III) Phanerozoic crust is abundant in China.

Some Phanerozoic crust may evolve from the accretion of oceanic plateaux and island arcs, but evidence from crustal seismology indicates a significantly more felsic whole crustal composition for Phanerozoic crust as compared with Precambrian crust. Guided by recent seismic results, I cite two key processes that produce a felsic Phanerozoic crust. (1) Eclogite transformation/lower crustal delamination: recent seismic refraction and xenolith data (Sierra Nevada, California) indicate that the middle and lower crust of this Mesozoic magmatic arc is not preserved within the crust. The granulite-to-eclogite transformation and/or delamination of the middle and lower crust can explain the remarkably low average seismic velocity (6.0-6.2 km/s) for the whole crust of the Andes and the southern Tibetan Plateau. (2) Stacking of subduction/ accretion complexes: field observations indicate that Phanerozoic crust commonly grows by the stacking of accretionary prisms that are quartz rich because their source rocks are the upper crust of adjacent cratons.

Modern GPS measurements in China will provide important constraints on crustal deformation in both young, active regions, and the more stable, but still seismogenic, intra-plate regions.

Benefits of Cooperation with the International GPS Service

Ruth Neilan, Director, IGS Central Bureau, Jet Propulsion Laboratory

Cooperation in international and regional ground networks is recognized as a being one of the true successes in leveraging national resources. Within the International GPS Service, over 80 institutions contribute to the daily operations and generation of the IGS products. Each organization then benefits from the combined effort and natural evolution of the technology. China has contributed to this global effort for many years most notably by the operation some key IGS stations through partnership with other organizations. It is timely through this US/China Workshop that China could consider a larger role in this global activity by engaging in the broader efforts of the IGS.

The IGS now produces GPS ephemerides on the order of <5 cm 3-d wrms. Station positions and velocities are being determined with uncertainties at the sub-centimeter level. The impact of this for research and understanding of crustal deformation is significant, particularly when this is achieved within a homogeneous and robust terrestrial reference frame. This talk will focus on the current status of GPS network densification and potential benefits for GPS analyses and solutions in China.

Over the last two years the IGS has also formed projects for various applications using GPS and dependent on continuous networks, or subnetworks of the IGS: precise time transfer, ground based tropospheric research through recovery of precipitable water vapor, planning ground support for high-rate and low-latency stations for Low Earth orbiter missions (CHAMP, GRACE, SAC-C, COSMIC, etc.), global ionospheric monitoring, an initiative for sea-level monitoring through observations of tide gauges and their benchmarks, and most recently the highly successful GLONASS tracking experiment (IGEX). These projects will be described very briefly.

A summary of potential points for cooperation based on the IGS model will be developed.

THE INITIAL STUDY ON PRESENT-DAY TECTONIC ACTIVITY AND CRUSTAL DEFORMATION MONITORED BY GPS IN THE AREA OF JIASHI AND NORTH-EAST PAMIR REGION

Qiao Xuejun (1), Ding Guoyu (2), Wang Qi (1), Wang Xiaoqiang (3), You Xinzhao (1)

1) Institute of Seismology, CSB, Wuhan

2) Center of Analysis and Prediction, CSB, Beijing

3) Xinjiang Seismological Bureau, CSB

The research group deployed GPS stations and carried out repeated GPS survey in the area of Jiashi and the north-east of Pamir region. The results computed from high-accuracy data processing GPS software GAMIT show that the baseline precision is improved by 3-5 mm than before. Initially, the present-day velocity map of crustal deformation and time series of baseline vector are also solved. The result indicates: 1) all stations of this district have an ideal environment for geology and survey. Each site was constructed with high quality and stability. The points are evenly distributed within whole region with an average length of 60~100km. Therefore, crustal deformation and earthquake activities in this area can be effectively monitored. 2). In 1994, the baseline repeatability for the N-S components and E-W components were 7mm and 12mm. It has been improved to the level of 4mm and 7mm in 1998. That indicates the scheme and design for the GPS net is available. It can meet the needs of detecting crustal movement with high resolution and precision in the dimension of time and space. 3). the tendency of baseline change in horizontal direction between Kashi and Biskek within more than two month is completely identical with the tendency in terms of 4 years. 4). Jiashi district suffers compression from Tianshan mountain block, Pamir block (Qinghai and Tibet plateau) and Tarim basin. Thus, it causes complicated tectonic movement and frequent strong earthquakes. On the other hand, if we make Biskek the fixed station when analyzing horizontal deformation velocity, the Jiashi district will slide to Tianshan mountain by the level of ~19mm/a along the N-S direction. That is basically identical with the result 20mm/a which is inferred from geophysics model consisting of various geological data.

THE ANTICLOCKWISE ROTATION OF SOUTHEAST ASIA

Ren Jinwei, CSB, Beijing

William E. Holt and Bingming Shen-Tu, SUNY, Stony Brook

The velocity field of the active deformation in central and southeast Asia, within a Eurasian reference frame, is determined by modeling the complete horizontal strain rate field with the velocity boundary constraints from plate motions, GPS, and VLBI data. The strain rate solutions are analogous to the response of a generally anisotropic Newtonian thin viscous sheet. In the model, we specify the India-Eurasia, the Australia-Eurasia, and the Arabia-Eurasia

velocities, defined by the NUVEL-1A Euler vectors, as constraints. In each grid area, constraints are also placed on the model strain rate tensor using information from both earthquake moment tensors and Quaternary fault slip rates. Southeast Asia, including south China, rotates anticlockwise relative to Siberia about a rotation pole at (62N, 146E, 0.14 deg/Myr). This gives an eastward motion to the south China block at a rate of about 9 mm/yr relative to Siberia. Borneo moves east-southeast relative to Siberia at a rate of about 14 mm/yr. The result of an anticlockwise rotation of southeast Asia relative to Siberia about a pole in the vicinity of (65N, 145E) appears quite stable and is consistent with the velocity fields obtained from inversion of earthquake and Quaternary strain rates alone. Robust features in the model are 18-25 mm/yr of compression across the Himalayas, 1-4 mm/yr of extension across the Baikal rift, 11-14 mm/yr of compression across the Tien Shan, and only 7-10 mm/yr of left-lateral strike-slip motion on the Altyn Tagh fault zone. The compression across the Himalayas absorbs almost half of the relative motion between India and Eurasia, the Tien Shan takes up about one fourth, and less than one fourth is absorbed across the Altyn Tagh. This means that more than 75% of the north-south shortening between India and Eurasia is absorbed by crustal thickening strains. Many of the deformational features in Asia, such as strike-slip motion on the Altyn Tagh fault, east Kunlun fault, Xianshuihe fault, and extension in Shanxi graben, Baikal rift, appear to be more a consequence of the anticlockwise rotation of southeast Asia relative to Siberia than that of the collision between India and Asia. The anticlockwise rotation of southeast Asia is likely a result of a eastern margins of southeast Asia as well as the collision between India and Asia.

COLLABORATIVE RESEARCH: GPS CRUSTAL DEFORMATION MONITORING IN CHINA

Zheng-kang Shen and David Jackson, University of California, Los Angeles
Peng Fang and Yehuda Bock, University of California, San Diego
Danan Dong and Ruth Neilan, Jet Propulsion Laboratory
Bradford Hager and Thomas Herring, Massachusetts Institute of Technology
Roger Bilham, University of Colorado
Jeffrey Freymueller, University of Alaska,
William Prescott, US Geological Survey, Menlo Park

We plan to measure and interpret crustal deformation in China using GPS. We will collaborate with Chinese scientists on their project "Crustal Motion Observation Network of China", sharing our expertise in network design, data processing, analysis, and geophysical interpretation. In the upcoming year we will jointly analyze and interpret the initial phase of the Chinese data collected recently, to assess the network monument stability, data quality, and approaches to best analyze the data. We will visit the participant institutions in China to discuss and coordinate specific future research efforts to strengthen the Crustal Motion Observation Network of China project at both the regional and national levels. We anticipate a full discussion with our Chinese colleagues at this US-China Geodynamics Workshop about an integrated plan for GPS data collection and analysis in China for the next several years.

GPS-DERIVED DEFORMATION ALONG THE NORTHERN RIM OF THE TIBETAN PLATEAU AND THE SOUTHERN TARIM BASIN

Zheng-Kang Shen 1, Min Wang 1, 2, David D. Jackson 1, An Yin 1, Yanxing Li 2, Chengkun Zhao 2, Danan Dong 3, and Peng Fang 4

1 University of California, Los Angeles

2 First Crustal Deformation Monitoring Center, China Seismological Bureau, Tianjin

3 Jet Propulsion Laboratory

4 University of California, San Diego

We analyzed GPS data collected from 1993 to 1998 along the northern rim of the Tibetan plateau spanning the western Kunlun, Karakaxi, Altyn Tagh, and Qilian Shan faults. Station velocities at 30 sites have been estimated with horizontal uncertainties of 2-3 mm/yr. Preliminary result indicates about 3-6 mm/yr left-lateral shear motion along the Karakaxi and western Kunlun faults, striking west-northwest and north-northwest respectively. Convergence rate across the faults increases from Karakaxi to western Kunlun, from a couple of mm/yr at longitude 79.5E to about 10 mm/yr at longitude 75.5E. The station velocities along the southern rim of the Tarim basin show a systematic increase from east to west relative to Siberia, suggesting a clockwise rotation of the basin with respect to the Tien Shan at a rate of about 9.0 nano-radian/yr around a pole of 35.4N, 78.0W. Assuming all of the Tarim-Siberia relative motion is absorbed within the Tien Shan Range, our result suggests about 20 mm/yr convergence across the western Tien Shan and about 10 mm/yr across the eastern Tien Shan.

We estimate about 6-8 mm/yr left lateral shear along the central Altyn Tagh at longitude 90E. The northeast Tibetan plateau is dominated by east-northeastward motion with respect to Siberia. This motion tapers off gradually toward the plateau borderland, accommodated by convergence across strands of thrust faults in the Qadam basin striking east-southeast. Up to 10 mm/yr convergence is detected across the Qilian Shan fault. East of the Qilian Shan fault we find about 7 mm/yr eastward motion relative to Siberia, which must be driven by the eastward motion of the Tibetan plateau. We infer about 7 mm/yr east-west extension north of the Altyn Tagh fault between longitude 86E and 99E, believed to be influenced by the strong east-west extension of the Tibetan plateau south of the fault.

DYNAMIC CORRELATION BETWEEN LOD VARIATION AND SITE DEFORMATIONS: IMPLICATION TO GEODYNAMICS

Wang Qing-Liang, Cui Du-Xin, Wang Wen-Ping and Liang Wei-feng
Second Center for Crustal Deformation Monitoring, CSB, Xi'an

Plate tectonic theory is one of the greatest scientific achievements in the 20th century. Although the plate framework has been widely accepted by geologists, the driving force of plate and crustal movement is still unsolved. In present paper, we first put forward some surprising evidences on dynamic correlation between excess LOD (length of day) variation and site deformations as well as site stress observations, and then discuss its implications to geodynamics.

1. LOD Variations

Precise astronomical observations reveal that the Earth does not rotate at a constant rate. The LOD variations of the Earth can mainly classified into three types: secular deceleration induced by friction of ocean tides, periodic variations induced by global atmospheric circulation and solar tide, irregular fluctuations induced by inner disturbance of the Earth. Among irregular

fluctuations, the typical decade variation, as generally regarded, is related to outer-core perturbation and core-mantle coupling of the Earth.

2. Correlation between LOD and Site Deformation as well as Stress

In order to detect possible earthquake precursors, there are nearly 300 fault deformation monitoring sites, 40 tilt observation sites and 30 stress observation sites distributed all over China. By comparing the observations with the excess LOD data downloaded from IERS, we found a lot of surprising dynamic correlation between excess LOD and site deformations as well as stresses. The correlation appears most typically in the decade variation of LOD, and the maximum correlated stress can reach several hundreds kpa.

3. Implications

The find of correlation between LOD and site deformation as well as stress provides a new important clue to driving force of plate and crustal movement. As theoretically calculated, the Earth rotation variation induced stress is too small to drive the crust, so the most possible mechanism for the dynamic correlation is that, both decade LOD variation, correlated site deformation and site stress are all dominated by the same process of deep perturbation of the Earth. Which implies that deep dynamic perturbation of the Earth is an important driving force of the undulated plate and crust movement. LOD variation dependent correlation should be an universal phenomenon, namely, the correlation should be found in other areas of the world and in other time series of observation data such as long leveling, GPS, VLBI and gravity.

We are looking forward to international collaborations in this filed.

INTRODUCTION OF THE PRESENT CRUSTAL HORIZONTAL MOVEMENT IN SHANXI FAULT BELT SHOWN BY GPS

Yang Guohua, Wang Min and Han Yueping
First Center for Crustal Deformation Monitoring, CSB, Tianjin

By use of existing GPS re-observation data (1996-1997-1998), the present state of crustal horizontal movement in Shanxi fault belt was shown that: (1) The activity of Shanxi fault belt has been controlled by the north-west-orientated or north-west-west-orientated compressive stress possibly and there has not been strike-slip movement; (2) The strength of motion in the north is larger than that in the south; (3) The motion for 1997-1998 is stronger than one for 1996-1997.

ARRANGEMENT AND OBSERVATION OF REGIONAL NET OF CRUSTAL MOVEMENT OBSERVATION NETWORK OF CHINA

Zhang Zusheng
First Center for Crustal Deformation Monitoring, CSB, Tianjin

The principles and methods for the arrangement of regional net of Crustal Movement Observation Network of China and the first overall joint observation have been introduced in the paper. Used directly for earthquake prediction, the regional net is mainly distributed in the major seismic monitoring defensive areas and the areas with strong tectonic activities in order to monitor the movements of active blocks and main active tectonic zones. The 1081 stations (including the datum stations and basic stations) of the whole net have formed the monitoring network covering the whole continent of China. In the first joint observation of the regional net,

the observation scheme of the complete and continuous network is adopted, which ensures the accuracy, uniformity and net-shape continuity of the whole net, and has provided a good and unified datum for the data analysis of local re-measurements in the future.

CRUSTAL MOTION OF CHINESE MAINLAND MONITORED BY GPS

Wenyao Zhu, Xiaoya Wang, Zongyi Cheng, Yongqin Xiong, Qiang Zhang, Shuhua Ye, Zongjin Ma (1), Junyong Chen (2), Houtze Hsu (3), Ziqing Wei (4), Xi'an Lai (5), Jinnan Liu (6), Biaoren Jin (6), Jinwei Ren (1) and Ji Wang (5)

Shanghai Astronomical Observatory, Chinese Academy of Sciences, Shanghai

1 Institute of Geology, China Seismological Bureau, Beijing

2 National Bureau of Surveying and Mapping, Beijing

3 Wuhan Institute of Geodesy and Geophysics, CAS, Wuhan

4 Xi'an Institute of Surveying and Mapping, Xi'an

5 Institute of Seismology, China Seismological Bureau, Wuhan

6 Wuhan Technical University of Surveying and Mapping, Wuhan

To measure and monitor the crustal motion in China, a GPS network has been established with an average side length of 1000 km and with more than 20 points on the margins of each major tectonic block and fault zones in China. Three campaigns were carried out in 1992, 1994 and 1996, respectively by this network. Here we present, for the first time, the horizontal displacement rates of 22 GPS monitoring stations distributed over the whole China and global IGS stations surrounding China, based on these GPS repeated measurements. From these results by GPS, we have obtained the sketch of crustal motion in China.

1. The first part of the document discusses the importance of maintaining accurate records of all transactions and activities. It emphasizes that this is crucial for ensuring transparency and accountability in the organization's operations.

2. The second part of the document outlines the various methods and tools used to collect and analyze data. It highlights the need for consistent and reliable data collection processes to support effective decision-making.

3. The third part of the document focuses on the role of technology in data management and analysis. It discusses how modern software solutions can streamline data collection, storage, and reporting, thereby improving efficiency and accuracy.

4. The fourth part of the document addresses the challenges associated with data management, such as data quality, security, and privacy. It provides strategies to mitigate these risks and ensure that data is used responsibly and ethically.

5. The fifth part of the document concludes by summarizing the key findings and recommendations. It stresses the importance of ongoing monitoring and evaluation to ensure that data management practices remain effective and aligned with the organization's goals.

6. The sixth part of the document provides a detailed overview of the data collection process, including the identification of data sources, the design of data collection instruments, and the implementation of data collection procedures.

7. The seventh part of the document discusses the importance of data quality and the various factors that can affect data quality, such as measurement error, non-response, and data entry errors.

8. The eighth part of the document explores the different methods of data collection, including surveys, interviews, focus groups, and observational studies, and discusses their respective strengths and limitations.

9. The ninth part of the document focuses on the analysis of data, including the selection of appropriate statistical methods, the interpretation of results, and the communication of findings to stakeholders.

10. The tenth part of the document discusses the ethical considerations surrounding data collection and analysis, such as informed consent, confidentiality, and the potential for bias and discrimination.

11. The eleventh part of the document provides a comprehensive overview of the data management process, from data collection to data storage, backup, and recovery.

12. The twelfth part of the document discusses the importance of data security and the various measures that can be taken to protect data from unauthorized access, loss, or destruction.

13. The thirteenth part of the document focuses on the role of data in decision-making and the various ways in which data can be used to inform strategic and operational decisions.

14. The fourteenth part of the document discusses the importance of data governance and the various policies and procedures that can be implemented to ensure the effective and ethical use of data.

15. The fifteenth part of the document concludes by summarizing the key findings and recommendations and providing a final overview of the data management process.

16. The sixteenth part of the document provides a detailed overview of the data collection process, including the identification of data sources, the design of data collection instruments, and the implementation of data collection procedures.

17. The seventeenth part of the document discusses the importance of data quality and the various factors that can affect data quality, such as measurement error, non-response, and data entry errors.